

SIMULATION OF A SUDDEN EXPANSION USING AXIS SYMMETRIC MODELING FOR
NEWTONIAN BLOOD FLOW

A Paper
Submitted to the Graduate Faculty
of the
North Dakota State University
of Agriculture and Applied Science

By

Christopher James Schmit

In Partial Fulfillment
for the Degree of
MASTER OF SCIENCE

Major Department:
Mechanical Engineering

April 2014

Fargo, North Dakota

North Dakota State University
Graduate School

Title

SIMULATION OF A SUDDEN EXPANSION USING AXIS SYMMETRIC
MODELING FOR NEWTONIAN BLOOD FLOW

By

Christopher James Schmit

The Supervisory Committee certifies that this *disquisition* complies
with North Dakota State University's regulations and meets the
accepted standards for the degree of

MASTER OF SCIENCE

SUPERVISORY COMMITTEE:

Dr. Yildirim B. Suzen
Chair

Dr. Ghodrat Karami

Dr. Om Prakash Yadav

Dr. Yechun Wang

Approved:

7/11/2014
Date

Dr. Alan Kallmeyer
Department Chair

ABSTRACT

This paper examines the flow of a Newtonian modeled blood through axisymmetric sudden expansion geometry. Reynolds number of 500, 2000, 3500, 5000, and 6500 are examined using laminar, shear stress transport, and base line analysis solvers using ANSYS 14.0. Simulation data sets are then examined against experimental data sets provided by the FDA.

Results of the solution sets indicate that the laminar case set ($Re = 500$) is well predicted by the laminar solution set, while the fully turbulent flow ($Re = 6500$) is well predicted by the shear stress transport solver. Simulation and comparison of transitional cases lead to moderate discrepancies from the experimental data.

ACKNOWLEDGMENTS

The author of this paper would like to express his gratitude to the staff and faculty members of the Department of Mechanical Engineering as well as the Department of Industrial Engineering. The author would like to give a sincere thanks to the author's major advisor Dr. Yildirim Bora Suzen, for the guidance and encouragement throughout the research work. The author would also like to thank the contributions of Sandy Steward, PhD at the Food and Drug Administration for the support of the experimental data and guidance of the study. Finally the author would like to thank his family, friends, and work place members for the continued support through the completion of this degree.

TABLE OF CONTENTS

ABSTRACT.....	iii
ACKNOWLEDGMENTS	iv
LIST OF TABLES	vii
LIST OF FIGURES	viii
LIST OF SYMBOLS	xxiv
1. INTRODUCTION	1
2. METHODS.....	8
2.1. Model	8
2.2. Boundary Conditions	10
2.3. Computational Method	14
2.4. Mesh Study	14
2.5. Fluid Properties	26
2.6. Simulation Convergence and Solver Method	27
2.7. HI% Calculations	28
3. DATA MANAGEMENT	29
4. RESULTS AND DISCUSSION	30
5. CONCLUSION.....	109
6. REFERANCES	111
APPENDIX A. AXIAL CENTERLINE VELOCITY	115

APPENDIX B. RADIAL VELOCITY & SHEAR STRESS SECTIONAL PROFILES	120
APPENDIX C. AXIAL WALL SHEAR STRESS.....	128
APPENDIX D. WALL PRESSURE.....	133
APPENDIX E. HI SECTIONAL % & TOTAL PRECENTAGE	138

LIST OF TABLES

<u>Table</u>	<u>Page</u>
1. Reynolds number cases and entrance velocities.....	12
2. Wall boundary conditions for simulations	14
3. Boundary layer thickness, traditional methods	15
4. Boundary layer thickness, seventh root law	18
5. Mesh control parameters, entrance/exit	19
6. Mesh control parameters, converging/diverging section.....	20
7. Mesh metrics, all simulation runs.....	21
8. Fluid properties for the experimental data from the FDA.....	26

LIST OF FIGURES

<u>Figure</u>	<u>Page</u>
1. Flow direction and model of center model geometry	8
2. Geometry sizing of the convergence/divergence section	8
3. Geometry boundary conditions and divisions.....	10
4. Cross sectional markers for geometry	11
5. Entrance development length to converging/diverging mesh interface.....	16
6.A. Mesh of convergence/divergence section	21
6.B. Mesh of convergence/development section, zoom out	22
6.C. Mesh of convergence/development section, zoom in	22
6.D. Mesh of convergence section	23
6.E. Mesh of expansion section	23
6.F. Mesh of expansion/reattachment section	24
6.G. Mesh of development to convergence, first layer	24
6.H. Mesh of converging section, first layer	25
6.I. Mesh of sudden expansion, zoom in.....	25
7.A. Axial velocity, laminar, Re 500, station -0.088m.....	31
7.B. Axial velocity, laminar, Re 500, station -0.064m.....	31
7.C. Axial velocity, laminar, Re 500, station -0.048m.....	31
7.D. Axial velocity, laminar, Re 500, station -0.02m	31

7.E. Axial velocity, laminar, Re 500, station -0.008m.....	31
7.F. Axial velocity, laminar, Re 500, station 0.0m.....	31
7.G. Axial velocity, laminar, Re 500, station 0.008m.....	32
7.H. Axial velocity, laminar, Re 500, station 0.016m	32
7.I. Axial velocity, laminar, Re 500, station 0.024m.....	32
7.J. Axial velocity, laminar, Re 500, station 0.032m	32
7.K. Axial velocity, laminar, Re 500, station 0.06m.....	32
7.L. Axial velocity, laminar, Re 500, station 0.08m	32
7.M. Legend for figures 7.A-7.L.....	33
8.A. Axial shear stress, laminar, Re 500, station -0.088m	34
8.B. Axial shear stress, laminar, Re 500, station -0.064m	34
8.C. Axial shear stress, laminar, Re 500, station -0.048m	34
8.D. Axial shear stress, laminar, Re 500, station -0.02m.....	34
8.E. Axial shear stress, laminar, Re 500, station -0.008m	34
8.F. Axial shear stress, laminar, Re 500, station 0.0m	34
8.G. Axial shear stress, laminar, Re 500, station 0.008m	35
8.H. Axial shear stress, laminar, Re 500, station 0.016m	35
8.I. Axial shear stress, laminar, Re 500, station 0.024m	35
8.J. Axial shear stress, laminar, Re 500, station 0.032m	35
8.K. Axial shear stress, laminar, Re 500, station 0.06m	35

8.L Axial shear stress, laminar, Re 500, station 0.08m.....	35
8.M. Legend for figures 8.A-8.L.....	36
9.A. Axial velocity, laminar, Re 2000, station -0.088m.....	37
9.B. Axial velocity, laminar, Re 2000, station -0.064m.....	37
9.C. Axial velocity, laminar, Re 2000, station -0.048m.....	37
9.D. Axial velocity, laminar, Re 2000, station -0.02m	37
9.E. Axial velocity, laminar, Re 2000, station -0.008m	37
9.F. Axial velocity, laminar, Re 2000, station 0.0m	37
9.G. Axial velocity, laminar, Re 2000, station 0.008m.....	38
9.H. Axial velocity, laminar, Re 2000, station 0.016m.....	38
9.I. Axial velocity, laminar, Re 2000, station 0.024m.....	38
9.J. Axial velocity, laminar, Re 2000, station 0.032m.....	38
9.K. Axial velocity, laminar, Re 2000, station 0.06m.....	38
9.L. Axial velocity, laminar, Re 2000, station 0.08m	38
9.M. Legend for figures 9.A-9.L.....	39
10.A. Axial shear stress, laminar, Re 2000, station -0.088m.....	40
10.B. Axial shear stress, laminar, Re 2000, station -0.064m.....	40
10.C. Axial shear stress, laminar, Re 2000, station -0.048m.....	40
10.D. Axial shear stress, laminar, Re 2000, station -0.02m	40
10.E. Axial shear stress, laminar, Re 2000, station -0.008m	40

10.F. Axial shear stress, laminar, Re 2000, station 0.0m	40
10.G. Axial shear stress, laminar, Re 2000, station 0.008m.....	41
10.H. Axial shear stress, laminar, Re 2000, station 0.016m	41
10.I. Axial shear stress, laminar, Re 2000, station 0.024m.....	41
10.J. Axial shear stress, laminar, Re 2000, station 0.032m.....	41
10.K. Axial shear stress, laminar, Re 2000, station 0.06m.....	41
10.L. Axial shear stress, laminar, Re 2000, station 0.08m	41
10.M. Legend for figures 10.A-10.L.....	42
11.A. Axial velocity, BSL, Re 2000, station -0.088m	43
11.B. Axial velocity, BSL, Re 2000, station -0.064m	43
11.C. Axial velocity, BSL, Re 2000, station -0.048m	43
11.D. Axial velocity, BSL, Re 2000, station -0.02m.....	43
11.E. Axial velocity, BSL, Re 2000, station -0.008m	43
11.F. Axial velocity, BSL, Re 2000, station 0.0m	43
11.G. Axial velocity, BSL, Re 2000, station 0.008m	44
11.H. Axial velocity, BSL, Re 2000, station 0.016m	44
11.I. Axial velocity, BSL, Re 2000, station 0.024m	44
11.J. Axial velocity, BSL, Re 2000, station 0.032m	44
11.K. Axial velocity, BSL, Re 2000, station 0.06m	44
11.L. Axial velocity, BSL, Re 2000, station 0.08m.....	44

11.M. Legend for figures 11.A-11.L.....	45
12.A. Axial shear stress, BSL, Re 2000, station -0.088m	46
12.B. Axial shear stress, BSL, Re 2000, station -0.064m	46
12.C. Axial shear stress, BSL, Re 2000, station -0.048m	46
12.D. Axial shear stress, BSL, Re 2000, station -0.02m	46
12.E. Axial shear stress, BSL, Re 2000, station -0.008m	46
12.F. Axial shear stress, BSL, Re 2000, station 0.0m	46
12.G. Axial shear stress, BSL, Re 2000, station 0.008m	47
12.H. Axial shear stress, BSL, Re 2000, station 0.016m	47
12.I. Axial shear stress, BSL, Re 2000, station 0.024m	47
12.J. Axial shear stress, BSL, Re 2000, station 0.032m	47
12.K. Axial shear stress, BSL, Re 2000, station 0.06m	47
12.L. Axial shear stress, BSL, Re 2000, station 0.08m	47
12.M. Legend for figures 12.A-12.L.....	48
13.A. Axial velocity, SST, Re 2000, station -0.088m	49
13.B. Axial velocity, SST, Re 2000, station -0.064m	49
13.C. Axial velocity, SST, Re 2000, station -0.048m	49
13.D. Axial velocity, SST, Re 2000, station -0.02m.....	49
13.E. Axial velocity, SST, Re 2000, station -0.008m	49
13.F. Axial velocity, SST, Re 2000, station 0.0m	49

13.G. Axial velocity, SST, Re 2000, station 0.008m	50
13.H. Axial velocity, SST, Re 2000, station 0.016m	50
13.I. Axial velocity, SST, Re 2000, station 0.024m	50
13.J. Axial velocity, SST, Re 2000, station 0.032m	50
13.K. Axial velocity, SST, Re 2000, station 0.06m	50
13.L. Axial velocity, SST, Re 2000, station 0.08m	50
13.M. Legend for figures 13.A-13.L.....	51
14.A. Axial shear stress, SST, Re 2000, station -0.088m.....	52
14.B. Axial shear stress, SST, Re 2000, station -0.064m.....	52
14.C. Axial shear stress, SST, Re 2000, station -0.048m.....	52
14.D. Axial shear stress, SST, Re 2000, station -0.02m	52
14.E. Axial shear stress, SST, Re 2000, station -0.008m	52
14.F. Axial shear stress, SST, Re 2000, station 0.0m.....	52
14.G. Axial shear stress, SST, Re 2000, station 0.008m.....	53
14.H. Axial shear stress, SST, Re 2000, station 0.016m.....	53
14.I. Axial shear stress, SST, Re 2000, station 0.024m.....	53
14.J. Axial shear stress, SST, Re 2000, station 0.032m.....	53
14.K. Axial shear stress, SST, Re 2000, station 0.06m.....	53
14.L. Axial shear stress, SST, Re 2000, station 0.08m	53
14.M. Legend for figures 14.A-14.L.....	54

15.A. Axial velocity, BSL Re 3500, station -0.088m	55
15.B. Axial velocity, BSL Re 3500, station -0.064m	55
15.C. Axial velocity, BSL Re 3500, station -0.048m	55
15.D. Axial velocity, BSL Re 3500, station -0.02m.....	55
15.E. Axial velocity, BSL Re 3500, station -0.008m	55
15.F. Axial velocity, BSL Re 3500, station 0.0m	55
15.G. Axial velocity, BSL Re 3500, station 0.008m	56
15.H. Axial velocity, BSL Re 3500, station 0.016m	56
15.I. Axial velocity, BSL Re 3500, station 0.024m	56
15.J. Axial velocity, BSL Re 3500, station 0.032m	56
15.K. Axial velocity, BSL Re 3500, station 0.06m	56
15.L. Axial velocity, BSL Re 3500, station 0.08m.....	56
15.M. Legend for figures 15.A-15.L.....	57
16.A. Axial shear stress, BSL, Re 3500, station -0.088m	58
16.B. Axial shear stress, BSL, Re 3500, station -0.064m	58
16.C. Axial shear stress, BSL, Re 3500, station -0.048m	58
16.D. Axial shear stress, BSL, Re 3500, station -0.02m	58
16.E. Axial shear stress, BSL, Re 3500, station -0.008m	58
16.F. Axial shear stress, BSL, Re 3500, station 0.0m	58
16.G. Axial shear stress, BSL, Re 3500, station 0.008m	59

16.H. Axial shear stress, BSL, Re 3500, station 0.016m	59
16.I. Axial shear stress, BSL, Re 3500, station 0.024m	59
16.J. Axial shear stress, BSL, Re 3500, station 0.032m	59
16.K. Axial shear stress, BSL, Re 3500, station 0.06m	59
16.L. Axial shear stress, BSL, Re 3500, station 0.08m	59
16.M. Legend for figures 16.A-16.L.....	60
17.A. Axial velocity, SST, Re 3500, station -0.088m	61
17.B. Axial velocity, SST, Re 3500, station -0.064m	61
17.C. Axial velocity, SST, Re 3500, station -0.048m	61
17.D. Axial velocity, SST, Re 3500, station -0.02m.....	61
17.E. Axial velocity, SST, Re 3500, station -0.008m	61
17.F. Axial velocity, SST, Re 3500, station 0.0m	61
17.G. Axial velocity, SST, Re 3500, station 0.008m	62
17.H. Axial velocity, SST, Re 3500, station 0.016m	62
17.I. Axial velocity, SST, Re 3500, station 0.024m	62
17.J. Axial velocity, SST, Re 3500, station 0.032m	62
17.K. Axial velocity, SST, Re 3500, station 0.06m	62
17.L. Axial velocity, SST, Re 3500, station 0.08m	62
17.M. Legend for figures 17.A-17.L.....	63
18.A. Axial shear stress, SST, Re 3500, station -0.088m.....	64

18.B. Axial shear stress, SST, Re 3500, station -0.064m.....	64
18.C. Axial shear stress, SST, Re 3500, station -0.048m.....	64
18.D. Axial shear stress, SST, Re 3500, station -0.02m	64
18.E. Axial shear stress, SST, Re 3500, station -0.008m	64
18.F. Axial shear stress, SST, Re 3500, station 0.0m.....	64
18.G. Axial shear stress, SST, Re 3500, station 0.008m.....	65
18.H. Axial shear stress, SST, Re 3500, station 0.016m.....	65
18.I. Axial shear stress, SST, Re 3500, station 0.024m.....	65
18.J. Axial shear stress, SST, Re 3500, station 0.032m.....	65
18.K. Axial shear stress, SST, Re 3500, station 0.06m.....	65
18.L. Axial shear stress, SST, Re 3500, station 0.08m	65
18.M. Legend for figures 18.A-18.L.....	66
19.A. Axial velocity, BSL, Re 5000, station -0.088m	67
19.B. Axial velocity, BSL, Re 5000, station -0.064m	67
19.C. Axial velocity, BSL, Re 5000, station -0.048m	67
19.D. Axial velocity, BSL, Re 5000, station -0.02m.....	67
19.E. Axial velocity, BSL, Re 5000, station -0.008m	67
19.F. Axial velocity, BSL, Re 5000, station 0.0m	67
19.G. Axial velocity, BSL, Re 5000, station 0.008m	68
19.H. Axial velocity, BSL, Re 5000, station 0.016m	68

19.I. Axial velocity, BSL, Re 5000, station 0.024m	68
19.J. Axial velocity, BSL, Re 5000, station 0.032m	68
19.K. Axial velocity, BSL, Re 5000, station 0.06m	68
19.L. Axial velocity, BSL, Re 5000, station 0.08m.....	68
19.M. Legend for figures 19.A-19.L.....	69
20.A. Axial shear stress, BSL, Re 5000, station -0.088m	71
20.B. Axial shear stress, BSL, Re 5000, station -0.064m	71
20.C. Axial shear stress, BSL, Re 5000, station -0.048m	71
20.D. Axial shear stress, BSL, Re 5000, station -0.02m	71
20.E. Axial shear stress, BSL, Re 5000, station -0.008m	71
20.F. Axial shear stress, BSL, Re 5000, station 0.0m	71
20.G. Axial shear stress, BSL, Re 5000, station 0.008m	72
20.H. Axial shear stress, BSL, Re 5000, station 0.016m	72
20.I. Axial shear stress, BSL, Re 5000, station 0.024m.....	72
20.J. Axial shear stress, BSL, Re 5000, station 0.032m.....	72
20.K. Axial shear stress, BSL, Re 5000, station 0.06m	72
20.L. Axial shear stress, BSL, Re 5000, station 0.08m	72
20.M. Legend for figures 20.A-20.L.....	73
21.A. Axial velocity, SST, Re 5000, station -0.088m	74
21.B. Axial velocity, SST, Re 5000, station -0.064m	74

21.C. Axial velocity, SST, Re 5000, station -0.048m	74
21.D. Axial velocity, SST, Re 5000, station -0.02m.....	74
21.E. Axial velocity, SST, Re 5000, station -0.008m	74
21.F. Axial velocity, SST, Re 5000, station 0.0m	74
21.G. Axial velocity, SST, Re 5000, station 0.008m	75
21.H. Axial velocity, SST, Re 5000, station 0.016m	75
21.I. Axial velocity, SST, Re 5000, station 0.024m	75
21.J. Axial velocity, SST, Re 5000, station 0.032m	75
21.K. Axial velocity, SST, Re 5000, station 0.06m	75
21.L. Axial velocity, SST, Re 5000, station 0.08m	75
21.M. Legend for figures 21.A-21.L.....	76
22.A. Axial shear stress, SST, Re 5000, station -0.088m.....	77
22.B. Axial shear stress, SST, Re 5000, station -0.064m.....	77
22.C. Axial shear stress, SST, Re 5000, station -0.048m.....	77
22.D. Axial shear stress, SST, Re 5000, station -0.02m	77
22.E. Axial shear stress, SST, Re 5000, station -0.008m	77
22.F. Axial shear stress, SST, Re 5000, station 0.0m	77
22.G. Axial shear stress, SST, Re 5000, station 0.008m.....	78
22.H. Axial shear stress, SST, Re 5000, station 0.016m.....	78
22.I. Axial shear stress, SST, Re 5000, station 0.024m.....	78

22.J. Axial shear stress, SST, Re 5000, station 0.032m.....	78
22.K. Axial shear stress, SST, Re 5000, station 0.06m.....	78
22.L. Axial shear stress, SST, Re 5000, station 0.08m	78
22.M. Legend for figures 22.A-22.L.....	79
23.A. Axial velocity, BSL, Re 6500, station -0.088m	80
23.B. Axial velocity, BSL, Re 6500, station -0.064m	80
23.C. Axial velocity, BSL, Re 6500, station -0.048m	80
23.D. Axial velocity, BSL, Re 6500, station -0.02m.....	80
23.E. Axial velocity, BSL, Re 6500, station -0.008m	80
23.F. Axial velocity, BSL, Re 6500, station 0.0m	80
23.G. Axial velocity, BSL, Re 6500, station 0.008m	81
23.H. Axial velocity, BSL, Re 6500, station 0.016m	81
23.I. Axial velocity, BSL, Re 6500, station 0.024m	81
23.J. Axial velocity, BSL, Re 6500, station 0.032m	81
23.K. Axial velocity, BSL, Re 6500, station 0.06m	81
23.L. Axial velocity, BSL, Re 6500, station 0.08m.....	81
23.M. Legend for figures 23.A-23.L.....	82
24.A. Axial shear stress, BSL, Re 6500, station -0.088m.....	83
24.B. Axial shear stress, BSL, Re 6500, station -0.064m.....	83
24.C. Axial shear stress, BSL, Re 6500, station -0.048m.....	83

24.D. Axial shear stress, BSL, Re 6500, station -0.02m	83
24.E. Axial shear stress, BSL, Re 6500, station -0.008m	83
24.F. Axial shear stress, BSL, Re 6500, station 0.0m	83
24.G. Axial shear stress, BSL, Re 6500, station 0.008m	84
24.H. Axial shear stress, BSL, Re 6500, station 0.016m	84
24.I. Axial shear stress, BSL, Re 6500, station 0.024m	84
24.J. Axial shear stress, BSL, Re 6500, station 0.032m	84
24.K. Axial shear stress, BSL, Re 6500, station 0.06m	84
24.L. Axial shear stress, BSL, Re 6500, station 0.08m	84
24.M. Legend for figures 24.A-24.L.....	85
25.A. Axial velocity, SST, Re 6500, station -0.088m	86
25.B. Axial velocity, SST, Re 6500, station -0.064m	86
25.C. Axial velocity, SST, Re 6500, station -0.048m	86
25.D. Axial velocity, SST, Re 6500, station -0.02m.....	86
25.E. Axial velocity, SST, Re 6500, station -0.008m	86
25.F. Axial velocity, SST, Re 6500, station 0.0m	86
25.G. Axial velocity, SST, Re 6500, station 0.008m	87
25.H. Axial velocity, SST, Re 6500, station 0.016m	87
25.I. Axial velocity, SST, Re 6500, station 0.024m	87
25.J. Axial velocity, SST, Re 6500, station 0.032m	87

25.K. Axial velocity, SST, Re 6500, station 0.06m	87
25.L. Axial velocity, SST, Re 6500, station 0.08m	87
25.M. Legend for figures 25.A-25.L.....	88
26.A. Axial shear stress, SST, Re 6500, station -0.088m.....	89
26.B. Axial shear stress, SST, Re 6500, station -0.064m.....	89
26.C. Axial shear stress, SST, Re 6500, station -0.048m.....	89
26.D. Axial shear stress, SST, Re 6500, station -0.02m	89
26.E. Axial shear stress, SST, Re 6500, station -0.008m	89
26.F. Axial shear stress, SST, Re 6500, station 0.0m	89
26.G. Axial shear stress, SST, Re 6500, station 0.008m.....	90
26.H. Axial shear stress, SST, Re 6500, station 0.016m.....	90
26.I. Axial shear stress, SST, Re 6500, station 0.024m.....	90
26.J. Axial shear stress, SST, Re 6500, station 0.032m.....	90
26.K. Axial shear stress, SST, Re 6500, station 0.06m.....	90
26.L. Axial shear stress, SST, Re 6500, station 0.08m	90
26.M. Legend for figures 26.A-26.L.....	91
27.A. Axial velocity along axis, laminar, Re 500	93
27.B. Axial velocity along axis, laminar, Re 2000	93
27.C. Axial velocity along axis, SST, Re 2000	93
27.D. Axial velocity along axis, BSL, Re 2000	94

27.E. Axial velocity along axis, SST, Re 3500	94
27.F. Axial velocity along axis, BSL, Re 3500	94
27.G. Axial velocity along axis, SST, Re 5000	95
27.H. Axial velocity along axis, BSL, Re 5000	95
27.I. Axial velocity along axis, SST, Re 6500	95
27.J. Axial velocity along axis, BSL, Re 6500	96
28.A. Wall pressure profile, laminar, Re 500	98
28.B. Wall pressure profile, laminar, Re 2000	98
28.C. Wall pressure profile, SST, Re 2000	98
28.D. Wall pressure profile, BSL, Re 2000	99
28.E. Wall pressure profile, SST, Re 3500	99
28.F. Wall pressure profile, BSL, Re 3500	99
28.G. Wall pressure profile, SST, Re 5000	100
28.H. Wall pressure profile, BSL, Re 5000	100
28.I. Wall pressure profile, SST, Re 6500	100
28.J. Wall pressure profile, BSL, Re 6500	101
29.A. Wall shear stress profile, laminar, Re 500	102
29.B. Wall shear stress profile, laminar, Re 2000	102
29.C. Wall shear stress profile, SST, Re 2000	103
29.D. Wall shear stress profile, BSL, Re 2000	103

29.E. Wall shear stress profile, SST, Re 3500.....	103
29.F. Wall shear stress profile, BSL, Re 3500.....	104
29.G. Wall shear stress profile, SST, Re 5000.....	104
29.H. Wall shear stress profile, BSL, Re 5000.....	104
29.I. Wall shear stress profile, SST, Re 6500.....	105
29.J. Wall shear stress profile, BSL, Re 6500.....	105
30.A. Hemolysis index, Laminar, Re 500.....	106
30.B. Hemolysis index, Laminar, Re 2000.....	106
30.C. Hemolysis index, SST, Re 2000.....	106
30.D. Hemolysis index, BSL, Re 2000.....	106
30.E. Hemolysis index, SST, Re 3500.....	106
30.F. Hemolysis index, BSL, Re 3500.....	106
30.G. Hemolysis index, SST, Re 5000.....	107
30.H. Hemolysis index, BSL, Re 5000.....	107
30.I. Hemolysis index, SST, Re 6500.....	107
30.J. Hemolysis index, BSL, Re 6500.....	107

LIST OF SYMBOLS

D	Diameter
r	Radius
L_d	Development Length
Re	Reynolds Number
T	Time
u	Velocity in axial direction
μ	Dynamic viscosity
ρ	Density
τ	Shear stress
τ_0	Shear stress along the wall

1. INTRODUCTION

The study of blood flow through live tissue and organs has been a dedicated focus for many researchers since the early 1900's. Arterial diseases have been one of the highest leading causes of death and disability in the western countries [2]. Though it has not been recent that the laws of fluids have been understood; it has been recently that computer aided fluid flow has unveiled many diseases characteristics. As cited in Abraham et al. modeling of fluid flow has been examined for many different parameters and geometries, some of which include unsteady three dimensional fluid dynamic analysis [3]; others that focus on simplified geometries using Newtonian fluids focusing on simplified flow models all for examination of blood flow within body vessels.

Simplification of blood flows through different sections of a typical person's body has also been a greatly researched topic. Since it is currently not possible to model fluids at the atomic level, making the correct assumptions for Reynolds averaged Navier Stokes modeling becomes critical. It has been seen that within large geometries, models can be simplified. Newtonian fluids modeled by the Navier-Stokes equations [4] can achieve quality, highly accurate predictions of rheological flows with similar wall shear stress values for large diametrical structures [5]. It has been found that when the diameter of the artery is less than 5mm, an additional step of re-scaling the Newtonian viscosity is sufficient to model the Non-Newtonian behavior of the flow [6]. With smaller geometries, small arteries and capillaries, true non-Newtonian behavior must be modeled to obtain an accurate representation of the viscoelastic, shear-thinning, thixotropic behavior of blood [7]. Contrary to this simplification (assumption of a Newtonian fluid) Nakamura et al., [27] has shown that non-Newtonian models should be used for non-steady flows. In this study full non-Newtonian models are used when modeling highly diseased arteries. Using a sudden expansion configuration with a smooth walled tube, the investigation looks at two Reynolds flows, $Re = 200$ and 400 . Using the results referenced by Layek et al., [28] it finds that the

viscosity of high moduli vessels changes with the hematocrit level, which is also influenced by the arterial radius.

Focusing these simplifications on areas of the body, where applicable, leaves a vast opportunity for research. Since the main focus of arterial disease involves the heart and arteries around the heart, it falls exactly into the zone where artificial devices (and this Newtonian simplification) can apply. Looking closer into the development of artificial devices leaves a major concern open. Reviewed in depth by Carswell, et al. [8] the shear stress placed on to the hemoglobin has a direct result on the elastic deformation and damage that may be bestowed mechanically on the blood. It has been shown that a pressure range between 0.1 – 20 Pa maybe experienced within arteries and veins of health humans [9]. Research in the area determining when a particular flow can be hemolysis free has been shown to be in the range of 150 – 800 Pa [10-13].

Metrics of estimating the hemolysis have been developed throughout the years. As seen in Blackshear et al. [14], approximations measuring the blood cell wall interaction time (related to an average mass transfer coefficient) lead to a hemolysis level. Since these correlations were derived using couette flow, Blackshear et al., [14] estimated that for turbulent flow the hemolysis rate may be increased by a factor of 10. Later improvements were developed by Giersiepen et al. [16] and later refined by Song et al., [15] using experimental data found by Heuser et al., [17]. Giersiepen et al., [16] developed a power law blood hemolysis model that effectively predicted the damage bestowed on the red blood cells. Hb represents the hemoglobin content and dHb represents the released hemoglobin content. The ratio of dHb/Hb is generally called the hemoglobin index (HI).

$$dHb/Hb = C \cdot \tau^\alpha \cdot T^\beta \quad (1)$$

Giersiepen et al., [16] found the constants of equation 1 be: $C = 3.62e^{-7}$, $\alpha = 2.416$, $\beta = 0.785$. Later updates by Song et al., [15] found the values to be: $C = 1.8e^{-6}$, $\alpha = 1.991$, $\beta = 0.765$. Published after Song et al., [15] it was noted in Goubergrits et al., [29] that there are two different sets of constants for equation 1. These sets of numbers depended on what type of fluid damage the particular research was focused on. Goubergrits et al., [29] noted that the original constants were valued for the HI. Platelet lysis, which is also part of the total blood damage model, was able to be calculated by equation 1 but used a different set of constants. The values of $C = 3.66e^{-6}$, $\alpha = 3.075$, $\beta = 0.77$ were noted in Goubergrits et al., [29] for the platelet lysis index values. It should be noted that in this paper the HI index will be found using the HI index constants from Goubergrits et al., [29].

Development of other equations has found that it is not only the rupturing of the red blood cell that is of concern when passing blood through artificial devices, but also other thromboembolic complications that must be accounted for. Platelet activation leading to thrombus formation must also be estimated in the fluid flow. Discussed and reviewed in Bluestein et al., [18] Yin et al., [19] Alemu et al., [20] and Dumont et al., [21] the shear stress and exposure time of the fluid field estimated using a Lagrangian approach for platelet activation approximations.

Further developments to the blood damage models have yielded three conditions that should be check for the consistency of any derived model. Quoted from Grigioni et al., [22] these conditions are:

“Condition 0 – it must not clash with the principle of causality, thus preventing the paradoxical result of a reduction of damage due to mechanical loading in the presence of a decreasing shear stress, Grigioni et al., [23].

Condition 1 – it must be able to reproduce what Eq. (1) predicts when a uniform mechanical load is acting on blood cells; in fact, Eq. (1) is a mathematical correlation

extrapolated from experimental data under condition of uniform shear stress, this being the condition of its rigorous validity.

Condition 2 – it must be able to account for the load history sustained by blood cells. If in a previous time interval, two particles sustained different mechanical loadings, and in a subsequent time interval both corpuscles sustain the same stress, the effect of the latest loading is expected to be different for the two particles, under the damage accumulation hypothesis."

Equation 2, shown below, was developed by Grigioni et al., [22]. and was able to match empirical data with high accuracy while meeting conditions 0-2. The constants a, b , and C are commonly used as proposed by Giersiepen et al., [16]; $a = 0.785, b = 2.416$, and $C = 3.72 \cdot 10^{-5}$. "The term into the square brackets in equation (2) is representative of the whole mechanical dose acting on the erythrocyte moving along a path line from the starting observation time until the i th instant (conventionally assumed as time instant $t_0 = 0$ and i th observation interval, respectively), while $(\tau(t_i)^{b/a} \Delta t_i)$ is the elementary mechanical dose sustained by the red cell in the i th interval, (from instant t_{i-1} until instant t_i). Equation (2) states that the i th experienced dose (the term inside the square brackets) is a weighted summation on the observation time intervals Δt_j coming before time i ($j = 1, \dots, i$), the j th weight being the value of shear stress $\tau(t_j)$ (elevated to b/a value) sustained during the j th time interval" [22].

$$BDI = \sum_{i=1}^N C a \left[\sum_{j=1}^i \tau(t_j)^{b/a} \Delta t_j + D(t_0) \right]^{a-1} \tau(t_i)^{b/a} \Delta t_i \quad (2)$$

It can be noted here that the blood damage index is the amount of damage sustained to the red blood cell which contains the hemoglobin that is often released upon rupture.

Concluding the new formulation for a better estimation of the blood damage index, Nobili et al., [25] adapted equation 2 to include thrombogenic aspects of artificial devices. Equation 3 shows the modification Nobili et al., [25] made to account for platelet activation states (PAS)

$$PAS_k = \int_{t_0}^t Ca \left[\int_{t_0}^{\phi} \tau(\xi)^{b/a} d\xi + \frac{PAS_k(t_0)^{1/a}}{C} \right]^{a-1} \tau(\phi)^{b/a} d\phi \quad (3)$$

Describing equation 3, $PAS_k(t_0)$ relates the the value of activation at time t_0 for the platelet k while the shear stress τ as the function of time $\tau(t)$. The constants of the model were calculated by Norbili et al., [25] in the original formulation; these were shown as: $a = 1.3198$, $b = 0.6256$, and $C = 10^{-5}$. "Using this formulation the shear stress history sensed by blood particulates is resolved: the effects of the shear stress previously sustained on the subsequent activation/damage (senescence) is captured" [24].

While equation 2 and 3 lead to the development of equations that represent the platelet activation as well as the blood hemolysis index; a re-evaluation of the original model was performed by Goubergrits et al., [29]. In this study it was not that the original models were wrong as it is the application of the equation and the time dependency it has to the shear stress, Goubergrits et al., [29].

While the blood damage and platelet activation models have been developing, many of the simulations to predict the nature of the flow (to sometimes include the blood damage) have remained relatively geometrically simple. Seen in Borisyuk [26], the examination of a simple sudden expansion followed by ridged and elastic pipes were examined for pressure fluctuations as well as monitoring of the reattachment point. Further research has used a simple sudden expansion to model the flow conditions of full blood models as well as simplified blood models. These has shown very promising results

furthering the understanding of biomechanical fluid mechanics; some examples of these can be seen in Nakamura et al., [27] and Layek et al., [28].

Further simplifications of flows and geometry's of flows have been examined by Yamaguchi et al. [32], and Hyun et al. [33]. Yamaguchi et al. [32] was able to show the recirculation region of a stepped flow bifurcating into two different outlet channels. In this case the numerical approximation was able to align with the bifurcated stepped flow. In this bifurcated stepped flow, Yamaguchi et al [32] was also able to show an almost symmetric flow pattern upon the axial region of the cylindrical flow geometry. Hyun et al. [33] concluded the onset thrombosis and restenosis effects of a sharp sudden expansion as well as a slightly smoothed sudden expansion in aorta like configurations. Within this study the conclusion of the sharp sudden expansion leading to high partial deposition was concluded. It was also shown by Hyun et al. [33] that sharp sudden expansion geometries lead to the largest recirculation regions and flow reattachment points that were the furthest downstream.

This paper focuses on the simulation of flow through a converging/diverging nozzle. The experimental data, for this study, was performed by the FDA in reference to how well simulation practices could first predict blood fluid flows in future design of artificial organs. The experimental data as well as other simulation data can be found in references S.F.C. Stewart et al., [1] and S.F.C. Stewart et al., [30]. Further discussions, in this paper other than in the results section, will be limited to only the simulation performed here.

Solvers used in these simulations performed for this paper included laminar, shear stress transport (SST) and base line modeling (BSL). The simulations were further broken down into laminar, transitional, and turbulent runs with each having one or multiple of the solver methods used. The laminar, transitional, and turbulent simulation cases were based off of runs with Reynolds number 500, 2000, 3500, 5000, and 6500.

Multiple pre solution simulations were performed to optimize the model size as well as an optimized mesh study. The final geometrical model and mesh were then used to solve all the flow cases.

Investigated in this paper were the characteristics of how well the experimental data could be simulated using multiple solving methods. Plots were constructed to investigate velocity and shear stress characteristics. These were further used to compare flow fields of the simulated and experimental data. The reattachment position was then used to evaluate how well the model predicted the flow nature. Finally, equation 1 was used to evaluate a blood damage index for later use in the FDA's studies.

2. METHODS

2.1. Model

Geometry of this analysis was constructed of a development length region, a convergence/divergence region, and finally a length of tube for the flow to reestablish mono-directional, fully developed flow. Figure 1, S.F.C. Stewart et al., [1], shows the convergence divergence area of the model used. Figure 1 also denoted the flow direction investigated in this paper. Figure 2, S.F.C. Stewart et al., [1], shows the dimensions of the converging/diverging area.

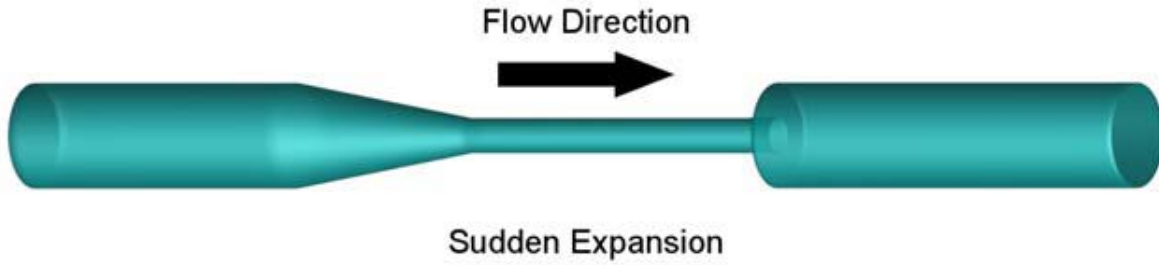


Figure 1. Flow direction and model of center model geometry

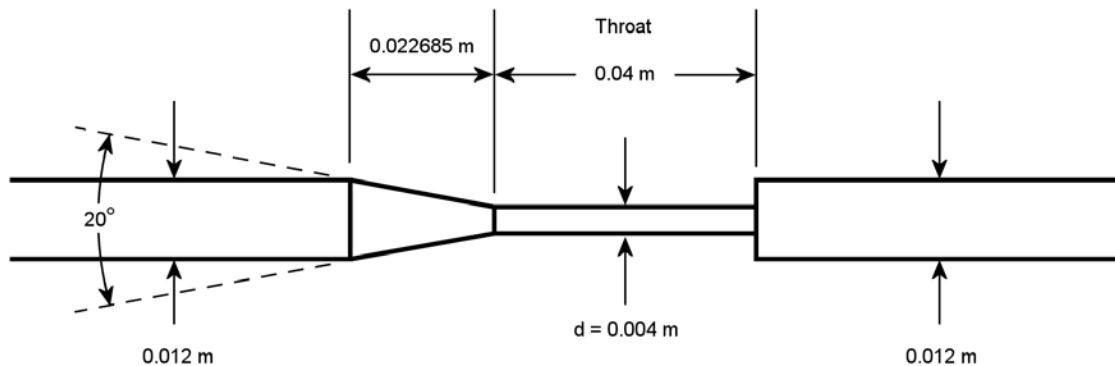


Figure 2. Geometry sizing of the convergence/divergence section

As previously noted, the geometry in figure 1 was used in a sudden expansion configuration. In addition to what is shown in figure 1, the entrance and the exit were extended to provide an entrance development region as well as a reattachment region. The entrance and exit regions were first sized to match the values used within the experimental data setup. For reference of this paper the point of origin will be the exact transition of the sudden expansion following the region where the geometry has been reduced to a 0.004m diameter.

Since the approach to the analysis was to establish a high accuracy boundary layer, an axisymmetric modeling approach was taken. This approach resulted in taking only a 5 degree slice of the geometry described above. This 5 degree axial slice was then meshed and modeled with the appropriate boundary conditions later discussed.

Optimizing for analysis the length of the entrance and a pre guess to the exit region were calculated using the standard expressions of entrance development length. Equation 4 donates the expression used for laminar flow profiles. Equation 5 donates the expression used for turbulent flow profiles.

$$L_d = 0.06DR_e \quad (4)$$

$$L_d = 4.4DR_e^{1/6} \quad (5)$$

Using the laminar expression (equation 1) for Reynolds number up to 2000, it was noted that the development length of this flow profile was 1.44m. In contrast the longest development region for turbulent profiles of Reynolds numbers up to 6500 was 0.2281m.

Using these numbers at the start of the meshing study the entrance and exit length were then adjusted to values that allowed a fully developed profile to be developed before

the flow entered the sudden expansion geometry as well as allowed a fully developed profile before the end of the full geometry. This allowed the simulation to be optimized to use one mesh for all the runs performed.

Concluding pre-analysis rounds for evaluation of the mesh study and evaluation of the entrance/exit length, the study drove the entrance geometry to a final value of 1.248m additional entrance length along with an exit length of 1.5m.

2.2. Boundary Conditions

Boundary conditions for the simulation were set to all facets of the 5 degree slice model; shown in figure 3. The two pie face cuts generated from the 5 degree slice were given an axis-symmetric boundary condition along the entire face.

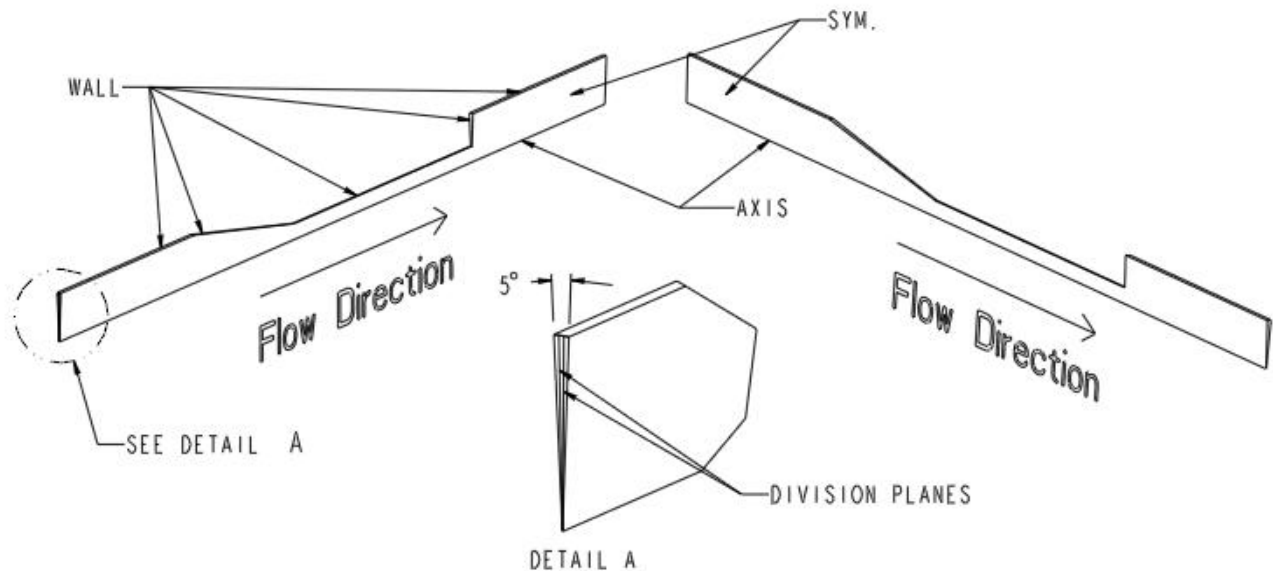


Figure 3. Geometry boundary conditions and divisions

The inlet boundary condition, for all runs, was set to resemble the original FDA experiment data. In the paper for the FDA experimental data setup, it was noted that a flow straightening device was used at the beginning of the added flow development geometry. To best simulate this, experimental simulation runs were then performed with the criteria of

matching the -0.088m position velocity profile. Reference of this position can be seen in figure 4, S.F.C. Stewart et al., [1].

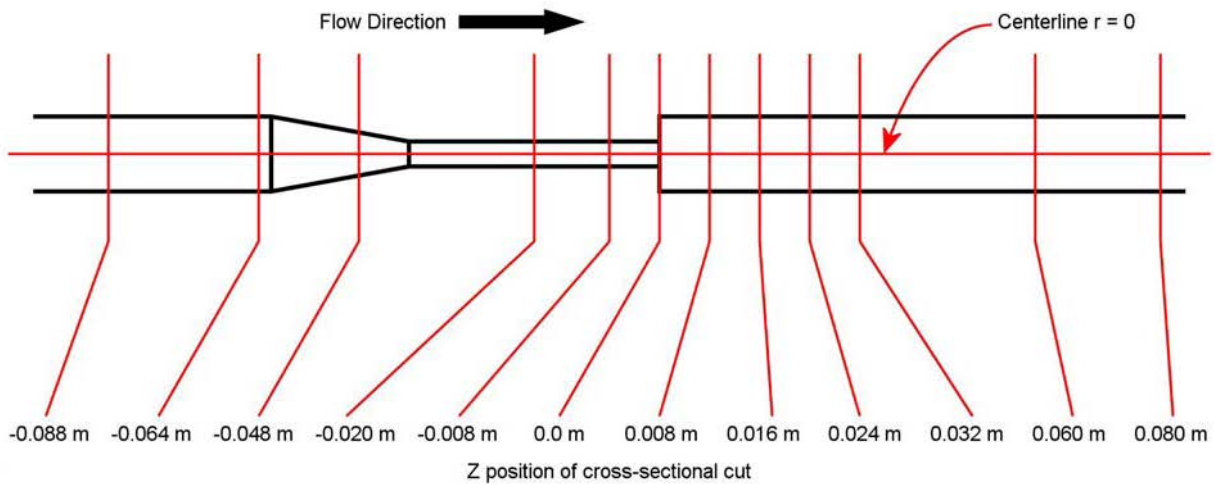


Figure 4. Cross sectional markers for geometry

With the goal of mating the starting position velocity profile, differing inlet profiles and turbulent conditions were simulated. The profiles examined for the simulations were:

- Laminar:
 - Zero-gradient
 - 50% partial developed flow (performed by calculating a velocity profile half way between fully developed and zero-gradient).
 - Fully developed flow.
- Turbulent/Transitional:
 - Zero-gradient, 0% initial turbulents
 - 3% initial turbulents
 - 5% initial turbulents
 - 7% initial turbulents

Final inlet boundary conditions used and giving the highest alignment to the FDA experimental data were: Zero-gradient for all laminar runs and 5% initial turbulent for all

turbulent/transitions runs. The last inlet boundary condition setting used was the flow rate for the differing Reynolds cases. Shown in table 1 are calculations of all the flow rates used of the differing Reynolds cases. All cases were calculated from the Reynolds number throat velocity (0.004m section), converted to a mass flow rate. From the mass flow rate the inlet velocity was calculated from the inlet diameter of the geometry (0.012m section). The corresponding velocity of the Reynolds number was applied to the inlet boundary condition.

Table 1. Reynolds numbers cases and entrance velocities

Tube Diameter (m)	Reynolds Number	Dyn. Viscosity (kg/m-s)	Density (kg/m ³)	Velocity (m/s)
0.004	500	0.0035	1056	0.4143
0.004	2000	0.0035	1056	1.6572
0.004	3500	0.0035	1056	2.9001
0.004	5000	0.0035	1056	4.1430
0.004	6500	0.0035	1056	5.3859
0.012	167	0.0035	1056	0.0460
0.012	667	0.0035	1056	0.1841
0.012	1167	0.0035	1056	0.3222
0.012	1667	0.0035	1056	0.4603
0.012	2167	0.0035	1056	0.5984

Running the pre-simulation boundary condition runs it was also found that the initial guess to the outlet boundary condition needed to be re-evaluated. The initial outlet boundary condition was set to a zero outlet pressure with zero differential pressure gradient. Using this boundary condition, it was found that the solver would create a second recirculation region across the outlet boundary. Elimination of this recirculation region was

solved by allowing the simulation to apply a 0.05Pa pressure gradient along opening. Final exit boundary conditions, resulting in the highest alignment with the experimental data, were found with a zero pressure outlet condition with a 0.05Pa pressure differential gradient along the outlet opening

Moving from the outlet of the geometry to the boundary condition for the exterior circular portion of the model; the exterior circular wall, through the length of the model, was given a no-slip wall boundary condition. This included the exterior walls of the convergence/divergence region of the model as well as the entrance and re-development region. The wall boundary condition was the only boundary condition, aside from the inlet velocity, that held variations from laminar and transitional/turbulent simulation runs. Table 2 donates the boundary condition set for each simulation case.

Table 2. Wall Boundary conditions for simulation

Simulation	Reynolds Number	Solution Method	Wall Boundary Condition	Wall Roughness	Specified Roughness
500 Lam	500	Laminar	No-Slip	Na	Na
2000 Lam	2000	Laminar	No-Slip	Na	Na
2000 SST	2000	SST	No-Slip	5.00E-07	2.50E-07
2000 BSL	2000	BSL	No-Slip	5.00E-07	2.50E-07
3500 SST	3500	SST	No-Slip	5.00E-07	2.50E-07
3500 BSL	3500	BSL	No-Slip	5.00E-07	2.50E-07
5000 SST	5000	SST	No-Slip	5.00E-07	2.50E-07
5000 BSL	5000	BSL	No-Slip	5.00E-07	2.50E-07
6500 SST	6500	SST	No-Slip	5.00E-07	2.50E-07
6500 BSL	6500	BSL	No-Slip	5.00E-07	2.50E-07

2.3. Computational Method

Average Reynolds Navier Stokes methods used for the analysis consisting of three different solution methods; solution methods of laminar, SST and BSL were used for the simulations. All simulations were performed using Ansys CFX 14.0. Table 2 includes the methods used for each of the Reynolds cases.

2.4. Mesh Study

A grid refinement studies was performed using Ansys ICEM and Ansys CFD to find the final mesh used in the simulation. To keep the mesh study limited to one defined mesh for all Reynolds cases, the 6500 SST characteristics was used for the mesh study evaluated.

At the start of the grid refinement study a more standard equation was used to estimate the total laminar boundary layer; equation 6 shows this equation. These values can be seen in table 3.

$$y = 10.0rR_e^{-1/2} \quad (6)$$

Table 3. Boundary layer thickness, traditional methods

Radius (m)	Reynolds Number	Thickness (m)
0.002	500	0.0004
0.002	2000	0.0002
0.002	3500	0.0002
0.002	5000	0.0001
0.002	6500	0.0001

Following calculation for the laminar boundary layer the 5 deg axie-symmetric mesh was modeled by divided, axially, into three different nodal regions. These regions were established by running two planes running through the axis and fanned out towards the outer tube wall. From this point the planes were given an angular control off the side wall symmetry with a spacing of 5/3 degrees each. This created three equally sized pie shaped cross sections normal to the flow direction and parallel to the major axis. Division of the model into three pie shape sections can be seen in figure 5.

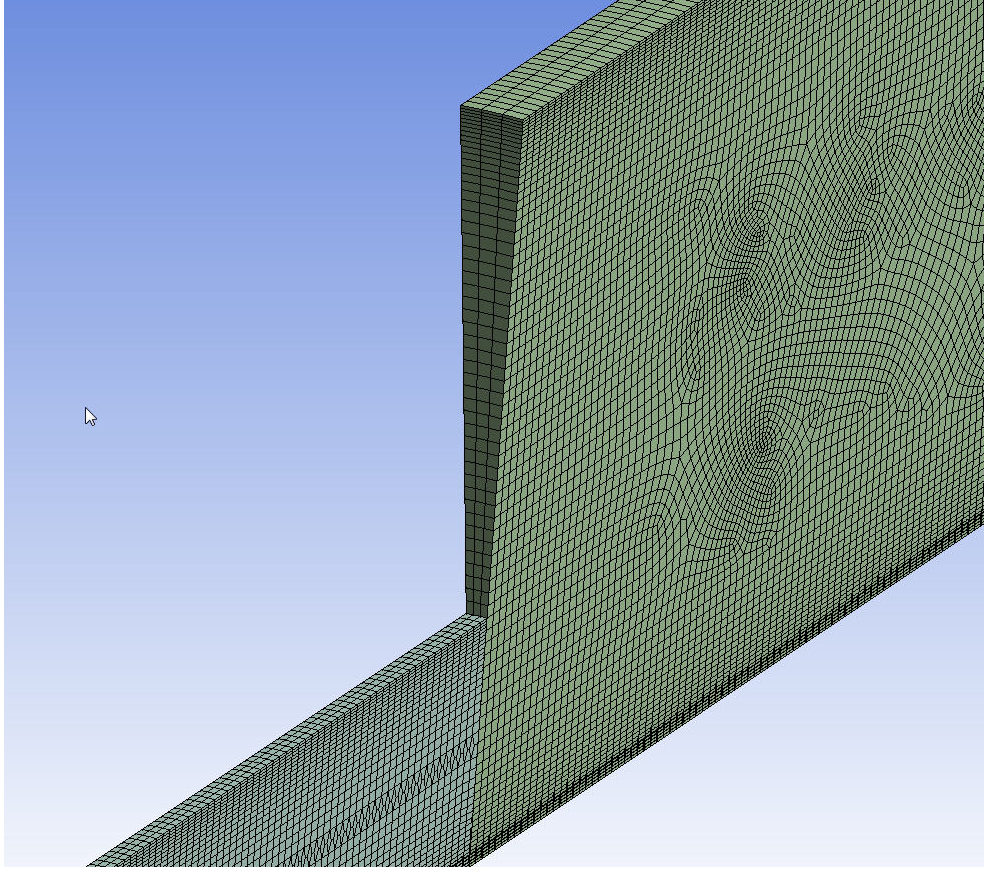


Figure 5. Entrance development length to converging/diverging mesh interface

From this point the mesh model was divided into three different sections along the length of the model. These sections; the entrance development length (all the geometry in front of the -0.088m mark), the converging/diverging section, and the reattachment region (all the geometry in back of the 0.08m mark) were used to control different body and inflation layer meshing regions.

The entrance development region as well as the reattachment region were both meshed with the same parameters. The implementation of a much smaller more controlled mesh was used for the converging/diverging section. The refined control of this section lead to a sizing that was about 1/5 the mesh size of either two prior sections. The resulting mesh of the geometry lead to a total body mesh that yielded most of the results wanted in the study but was also still solvable on a single high performance workstation.

Upon generation of the initial mesh, it was noted that many singularities and data discrepancies seem to be exhibited. Later mesh refinement runs found that increasing the number of nodes within the boundary layer and also reducing the boundary layer resulted in better accuracy.

Since meshing of the model was performed in Ansys ICEM, sizing of the first layer distance was controlled manually by the deduction of the wall shear stress. This was performed by comparing the difference in wall shear stress from one run to another run while reducing the spacing of the first layer by half the distance of the previous run. When the shear stress value reached considerable low differential value ($1e-6$ difference) between the current and prior run, the first layer approximation was considered to be valid. Since the total boundary layer was calculated from using equations 6 the first layer grid spacing was reduced by increasing the total number of nodes within the boundary layer while also using an exponential growth of the nodes to the free stream velocity.

Following the pre-analysis runs to evaluate the first layer sizing as well as general body mesh sizing, it became apparent that the total inflation layer was no longer limited to just the high shear stress portion of the wall flow field. Reviewing the size of the boundary layer size; it was quickly noticed that the initial approximations for the boundary layer were off by $\sim 2X$. Researching different types of boundary layer approximations lead to the finding of an expression that Prandtl found for turbulent flows. The seventh root law was able to predict a boundary layer thickness that closely matched the refined mesh of what analysis was driving too.

The Seventh Root Law (SRL) is “an expression for turbulent velocity distribution using only the resistance law for turbulent flow through smooth tubes” [31]. The expression was found to be applicable when “(1) the velocity distribution in the immediate neighborhood of the wall does not depend on the radius of the tube but is determined

completely by μ and ρ , as well as by the shear stress τ_0 at the wall; (2) the velocity distribution curves remain similar with increasing velocity" [31].

Equation 7 shows the SRL equation. The result of this equation set can be seen in table 4.

$$y = \frac{64.8r}{Re^{7/8}} \quad (7)$$

Table 4. Boundary layer thickness, seventh root law

Radius (m)	Reynolds Number	SRL thickness (m)
0.002	500	0.00059
0.002	2000	0.00018
0.002	3500	0.00011
0.002	5000	0.00008
0.002	6500	0.00006

Comparing the results of tables 3 and 6, it can be seen that the boundary layer thickness value for the simulation at 6500 Reynolds number is ~2X the value. This trend explained the previously reduction in the mesh and boundary layer that the mesh study exhibited.

Final updates to the body and boundary layer mesh control parameters can be seen in tables 5 and 6. The final refinements to the mesh, driven from the SRL as well as other found attributes, lead to pre-simulation mesh studies that were highly aligned to the velocity profiles for most all the Reynolds cases.

Table 5. Mesh control parameters, entrance/exit

Mesh Definition	Method	Body	Axis	Wall
General				
Method	Swept	--	--	--
Free Face Mesh Type	All Quads	--	--	--
Sweep Number Divisions	3	--	--	--
Sweep Bias Type	No Bias	--	--	--
Element Size	--	5.0e-4 (<i>m</i>)	--	--
Inflation layer				
Inflation Control Area	Total Thickness	--	--	--
Number of layers	--	--	5	5
Growth Rate	--	--	1.2	1.2
Maximum Thickness	--	--	1.0e-3 (<i>m</i>)	1.0e-3 (<i>m</i>)

Table 6. Mesh control parameters, converging/diverging section

Mesh Definition	Method	Body	Axis	Wall
General				
Method	Swept	--	--	--
Free Face Mesh Type	All Quads	--	--	--
Sweep Number Divisions	3	--	--	--
Sweep Bias Type	No Bias	--	--	--
Element Size	--	1.0e-4 (<i>m</i>)	--	--
Inflation layer				
Inflation Control Area	Total Thickness	--	--	--
Number of layers	--	--	20	20
Growth Rate	--	--	1.08	1.08
Maximum Thickness	--	--	1.0e-3 (<i>m</i>)	1.0e-3 (<i>m</i>)

Final body and boundary layer mesh metrics can be seen in table 7. Figure 6 shows the images of the final body and boundary layer mesh.

Table 7. Mesh metrics, all simulation runs

Total Mesh Nodes	3024326
Total Mesh Elements	586015
Calculated first layer, throat ($y^+ = 1$)	$8.1e-5$ (m)
Mesh first layer, throat	$2.1e-5$ (m)

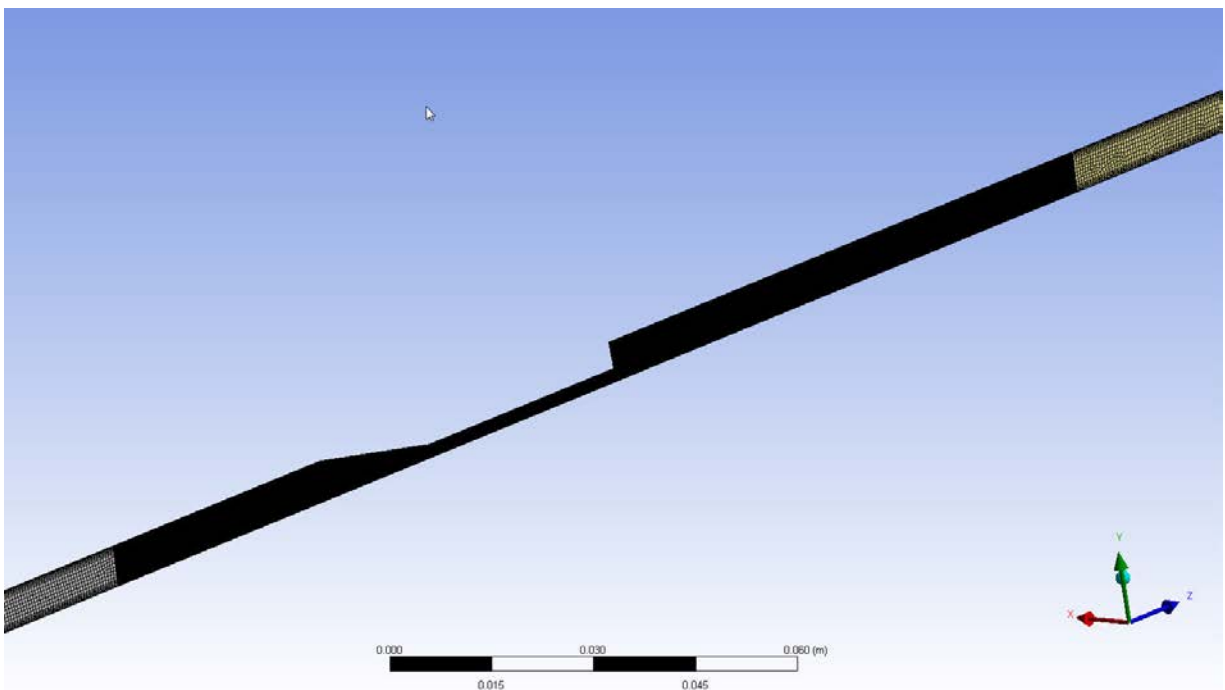


Figure 6.A. Mesh of converging/diverging section

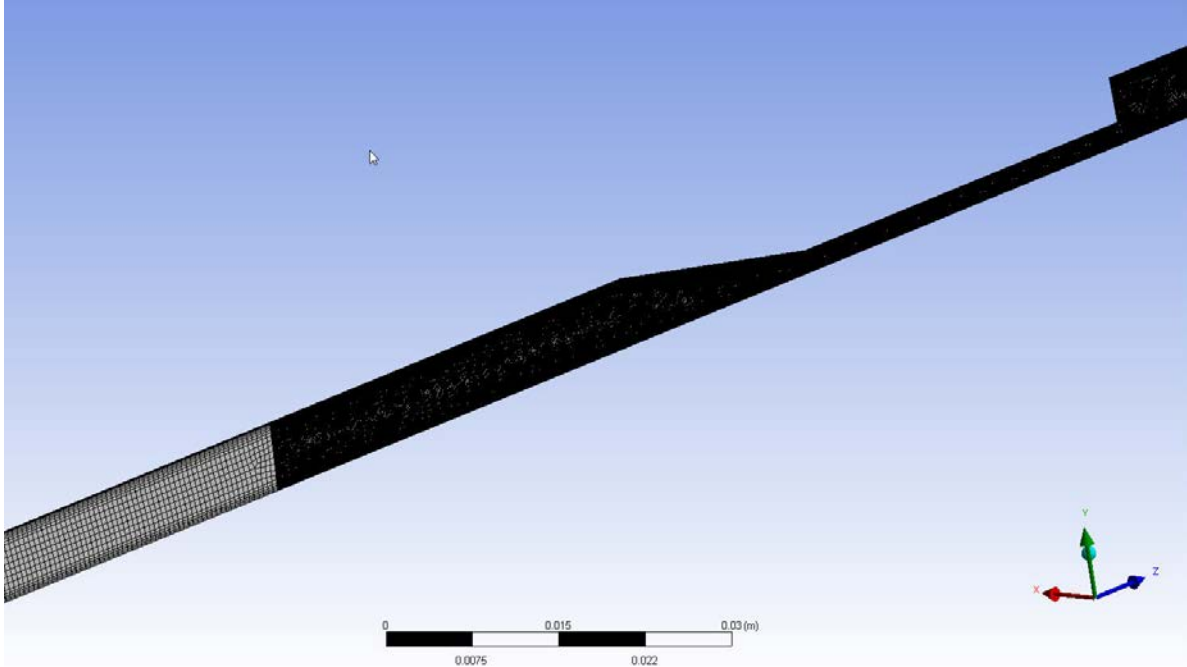


Figure 6.B. Mesh of converging/development section, zoom out

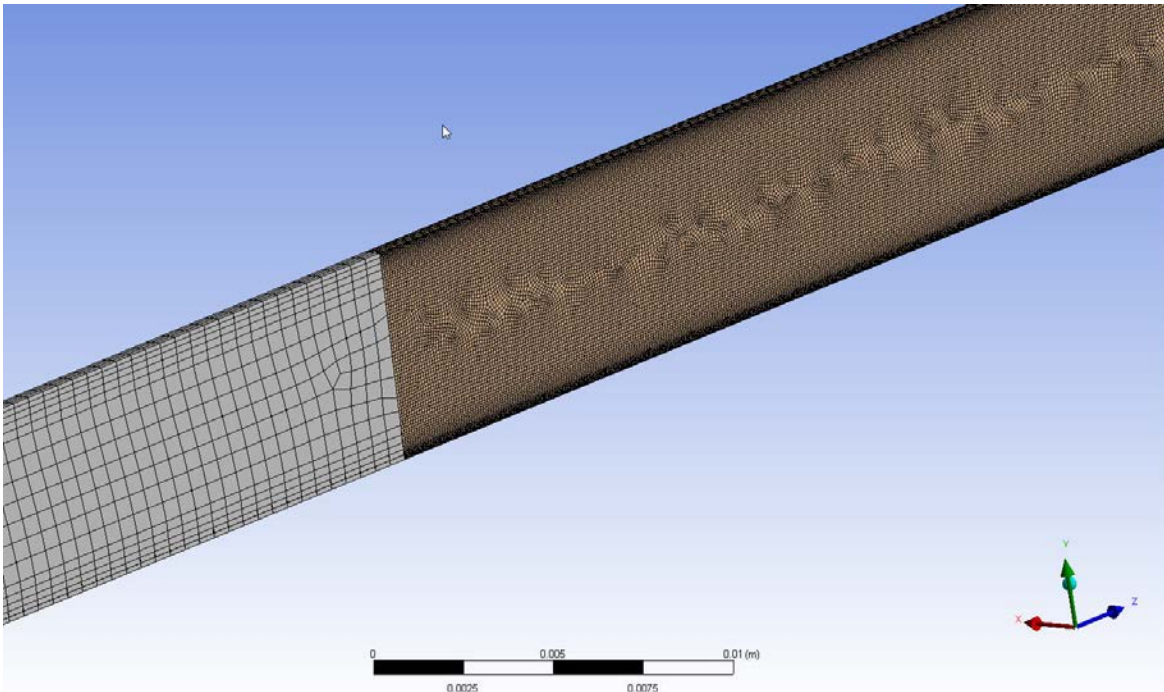


Figure 6.C. Mesh of converging/development section, zoom in

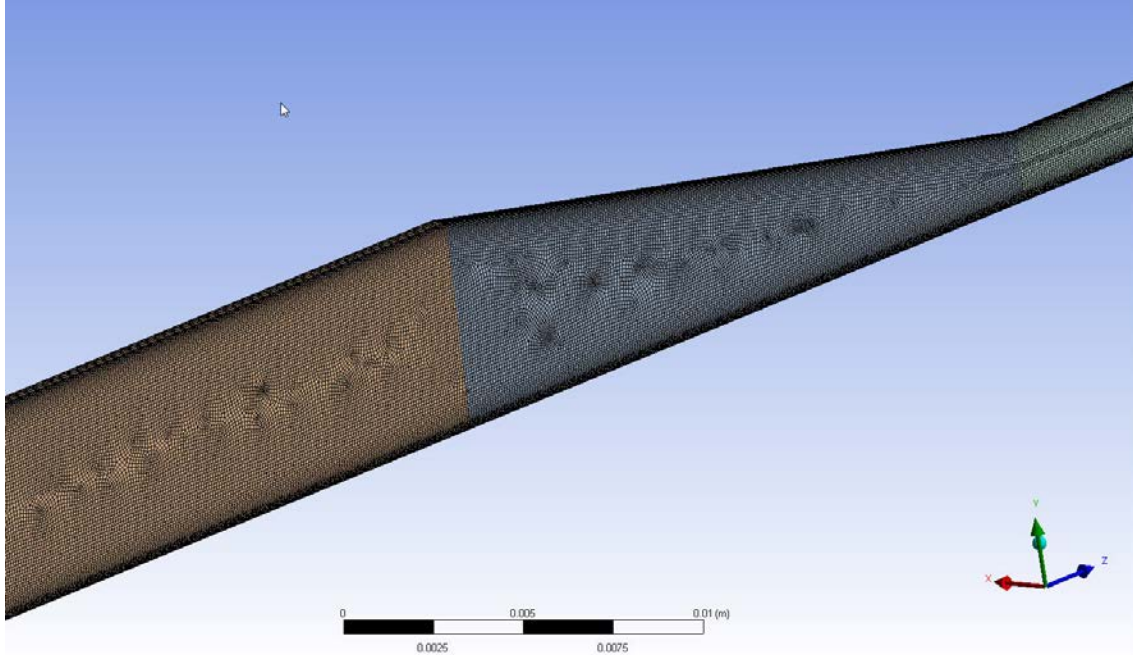


Figure 6.D. Mesh of convergence section

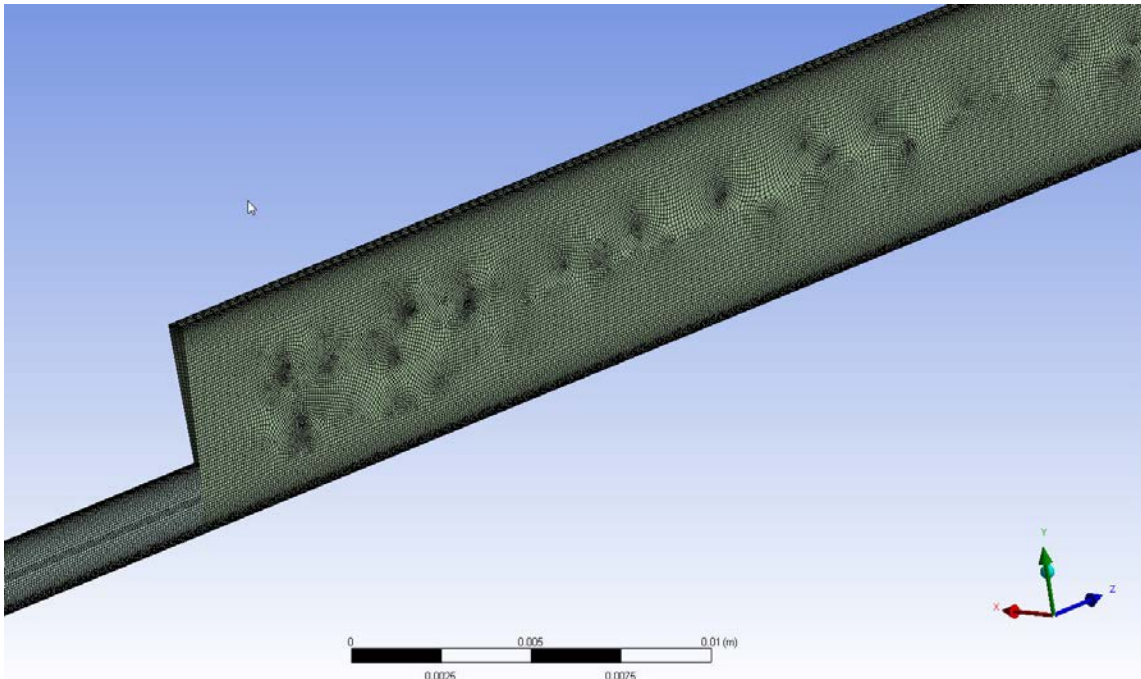


Figure 6.E. Mesh of expansion section

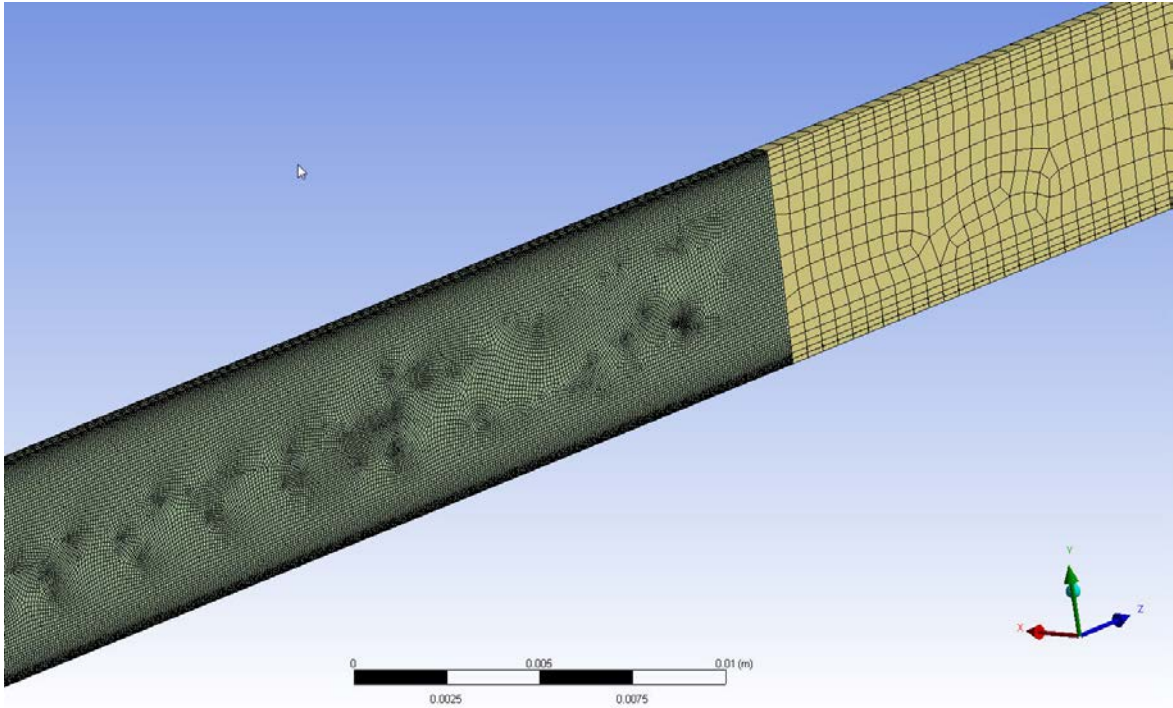


Figure 6.F. Mesh of expansion/reattachment section

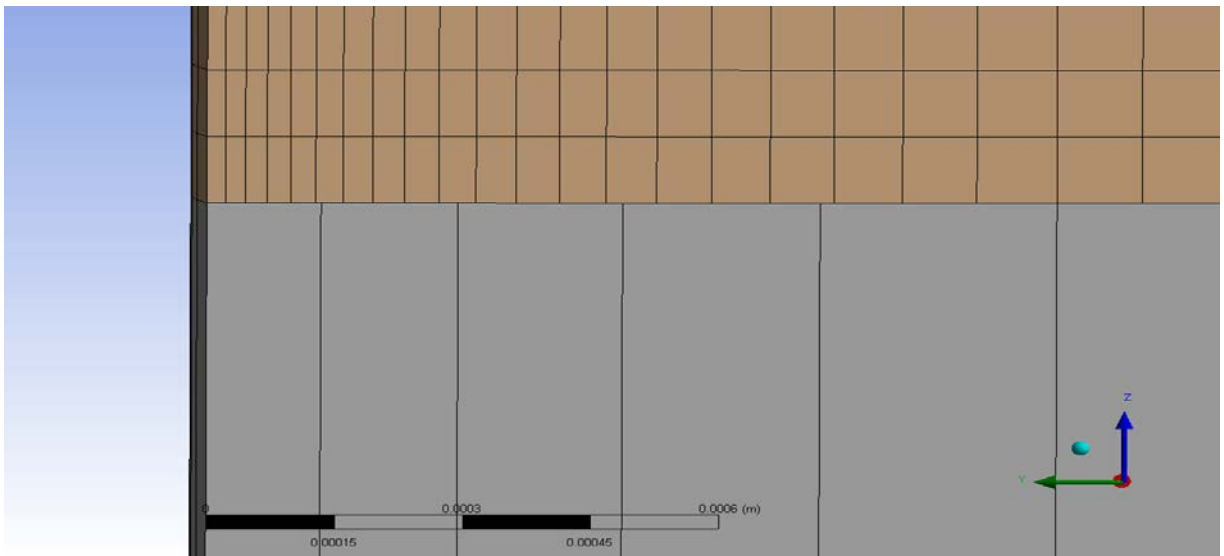


Figure 6.G. Mesh of development to convergence, first layer

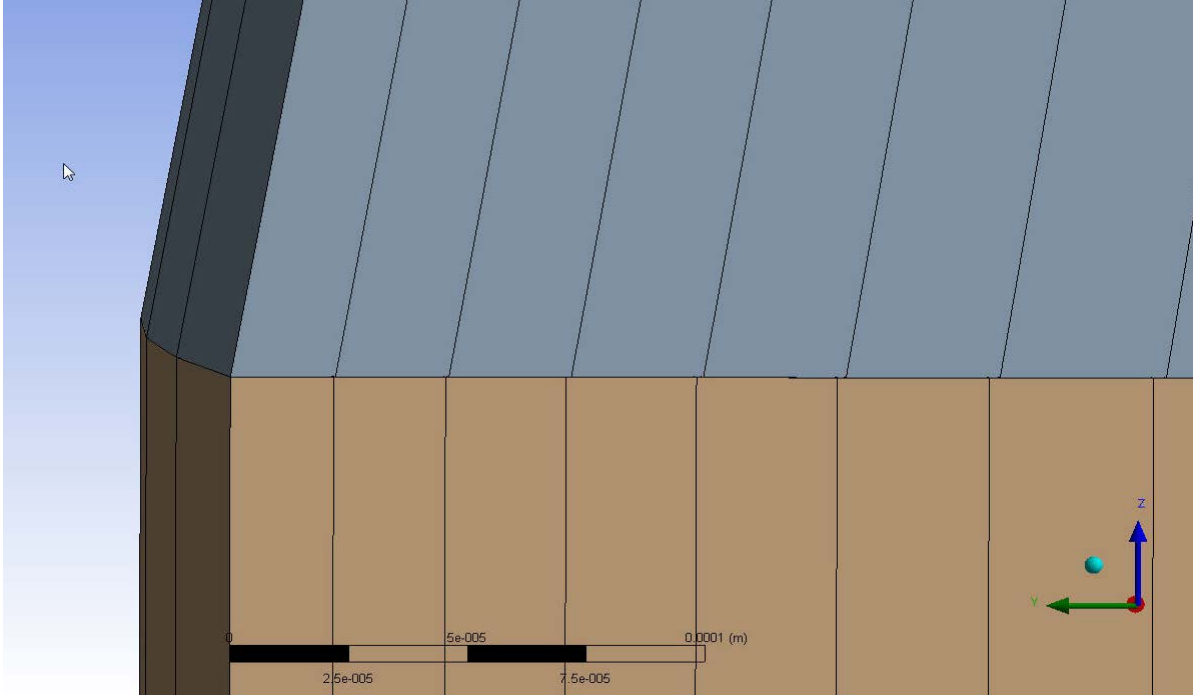


Figure 6.H. Mesh of converging section, first layer

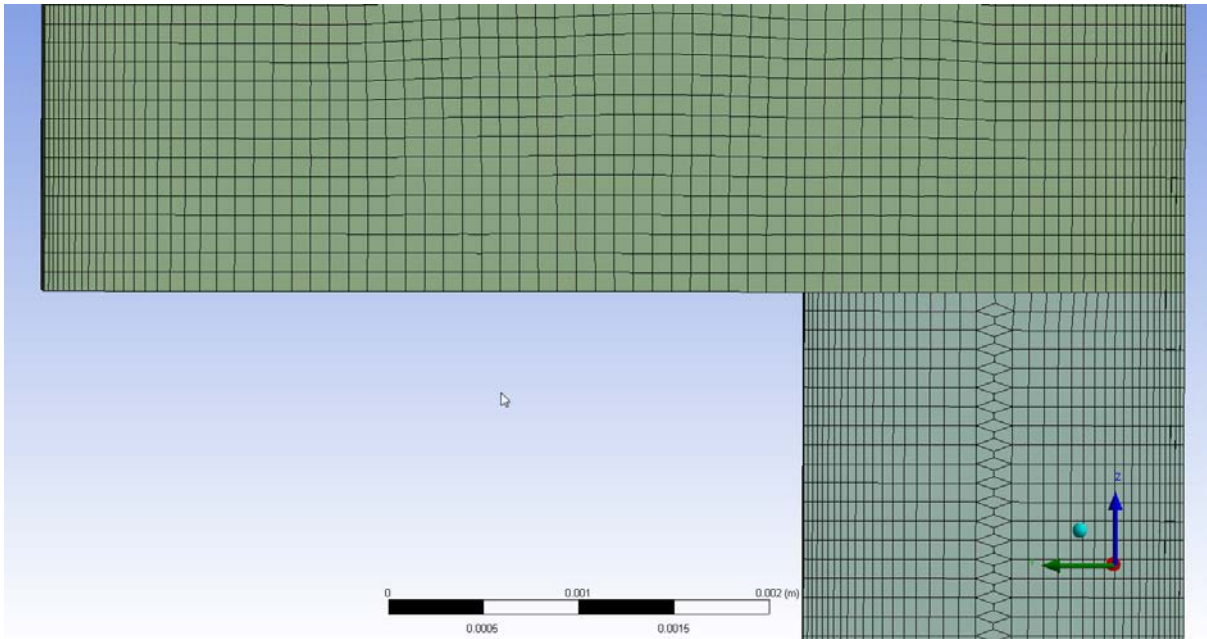


Figure 6.I. Mesh of sudden expansion, zoom in

2.5. Fluid Properties

The fluid used in the analysis was modeled to simulate the calculated Newtonian fluid properties of the FDA study. A density of 1058 kg/m^3 was used along with a viscosity of $0.0035 \text{ N} \cdot \text{s/m}^2$. From the descriptions found in the papers by the FDA, the experimental data was found by using two different fluids. The first fluid, Sodium Iodide, was used for the partial velocity imaging studies. The Sodium Iodide fluid was used to gather velocity and stress data of the runs. The second fluid, Glycerin-Water, was used for pressure gradient measurements through the experimental setup. The averaged fluid properties values from the FDA data can be seen in table 9 averaged from the reference S.F.C. Stewart et al., [30]. Conversion of the flow results from the two Newtonian fluids in table 9 to the fluid proper used in the analysis were made using Reynolds numbers similarities. Equations 7, 8, and 9 show the equations used for the Reynolds number similarity conversions S.F.C. Stewart et al., [30].

Table 8. Fluid properties for the experimental data from the FDA

Fluid Property	Sodium Iodide Solution	Glycerin-Water
Dynamic Viscosity (cP)	~7.32	~3.65
Specific Gravity	~1.72	~1.06

$$\mathbf{u}_{blood} = \mathbf{u}_{NaI} \times \left(\frac{\mu_{blood} \rho_{NaI}}{\mu_{NaI} \rho_{blood}} \right) \quad (8)$$

$$\boldsymbol{\tau}_{blood} = \boldsymbol{\tau}_{NaI} \times \left(\frac{\mu_{blood}^2 \rho_{NaI}}{\mu_{NaI}^2 \rho_{blood}} \right) \quad (9)$$

$$\boldsymbol{\tau}'_{blood} = \boldsymbol{\tau}'_{NaI} \times \left(\frac{\mu_{blood}^2 \rho_{NaI}}{\mu_{NaI}^2 \rho_{blood}} \right) \quad (10)$$

The equations and properties of the sodium iodide as well as the glycerin-water are all listed for reference; equations 8-10. Data from the FDA was provided for this analysis with the conversation pre-performed. Please refer to references X and X for further detail on the experimental data as well as any setup parameter for this data.

2.6. Simulation Convergence and Solver Method

For all runs completed the simulation convergence was set to 1e-6 convergence for the conservation of mass as well as the conservation of momentum equations. The turbulence convergence of non-laminar runs was set to 1e-6 convergence but achieved 3e-6.

Highlighting the solver options; the activation schema as well as the turbulence numerical options were both set to high resolution for all simulation runs.

Included in the SST turbulence runs a Gamma Theta transitional turbulence option was selected. The Gamma Theta option was initially selected for only the transitional turbulence runs (Reynolds numbers of 2000 and 3500). This option was then adapted to all SST runs after metrics of the non-Gamma Theta SST runs yielded the same results for Reynolds numbers 5000 and 6500.

Final solution setup options included a wall surface roughness value implemented for all transitional and turbulent runs. The wall surface roughness value was taken from the FDA data of the experimental setup; this value was found to be 2.5e-4mm, S.F.C. Stewart et al., [30].

2.7. HI% Calculations

The HI% in this paper was calculated using equation 1 and the constants $C = 3.62e^{-7}$, $\alpha = 2.416$, $\beta = 0.785$. This was performed by dividing the geometry into 11 axial sections using the 12 different cross sectional markers noted in figure 4. After dividing the geometry into 11 axial sections, each section was divided into 30 equally spaced radial divisions. Using the velocity data of each section and each radial division, a time for a partial traveling through the section/division was then calculated. Once the values for each radial division for each section was calculated, an average of each section was found by the composition of the fractional area of each radial division in relation to the total area (meaning that the composing area for each radial division was calculated and then fractionalized by the total area of that section). The total HI% was then found by averaging the 11 sectional histogram values. The resultant of this HI% calculation for each data set is shown in the histogram like plots of figure 30.

3. DATA MANAGMENT

Data management for all the simulation results as well as the experimental data, from the FDA, was managed by scripting programs in Matlab. Construction of 5 total programs were written, each of which generating one or multiple of the figures found in the results and discussion section. Construction of each program included writing script for a search routine to scan through the data sets and find the data of interest. Upon finding the data the script would then scale and plot the experimental data to the simulation data for the figure of choice. In some cases additional confirmation metrics were incorporated into the script for added assurance of correctly plotted values.

All scripts written for plotting and managing data can be found in the appendix.

4. RESULTS & DISCUSSION

The results of the simulations trended to yield similarity to others groups in the FDA study. In some simulations, very good alignment of the entrance, exit, or converging/diverging section were found. In multiple cases high accuracy was found for multiple sections. Overall, comparison plots of the velocity profiles to the experimental data yielded the highest accuracy. Shear stress plots were within reason, but in some cases did not represent the experimental data profiles.

The result of this paper do not include the plotted results of others groups simulations but will make reference to it for comparison. Data from others groups simulations can be found in S.F.C. Stewart et al., [1].

The first set of plots review the laminar 500 Reynolds number case. Figure 7 (7.A-7.L) represents axial velocity for this case in twelve different axial locations. In these figures it can be seen that the simulation data and the experimental data align with marginal error. Figures 7.A through 7.L show the axial velocity upon radial cross sectional cuts of the converging/diverging section. The sectional location of the cuts can be compared to using figure 4 for reference.

Closer examination of figure 7 reviles that simulation convergence to the experimental data was almost completely within the marginal error of the experimental data. It is only seen in figure 7.B that the simulation over predicts the maximum center flow development profile outside the experimental data error margin by $\sim 0.003\text{m/s}$. This data also aligns, and is at the higher end, of results seen from other groups noted in S.F.C. Stewart et al., [1].

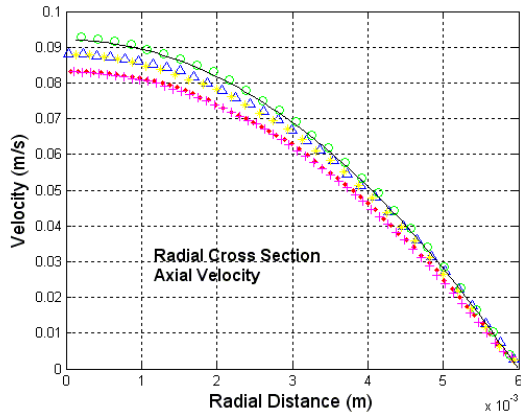


Figure 7.A. Axial velocity, laminar, Re 500, station -0.088m

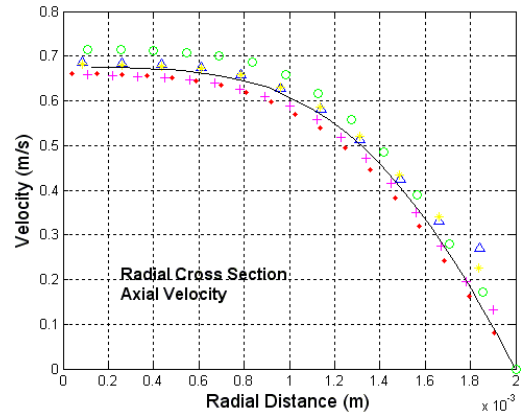


Figure 7.D. Axial velocity, laminar, Re 500, station -0.02m

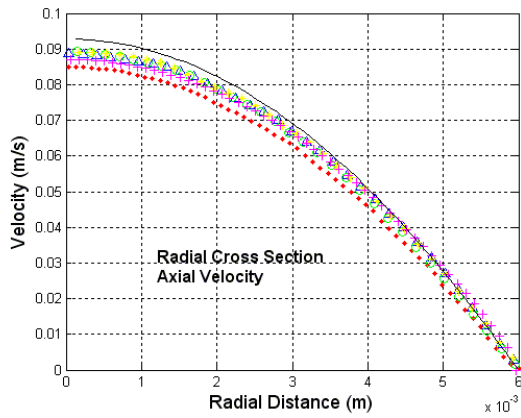


Figure 7.B. Axial velocity, laminar, Re 500, station -0.064m

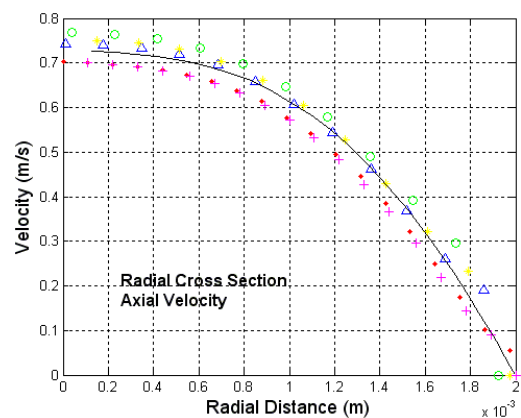


Figure 7.E. Axial velocity, laminar, Re 500, station -0.008m

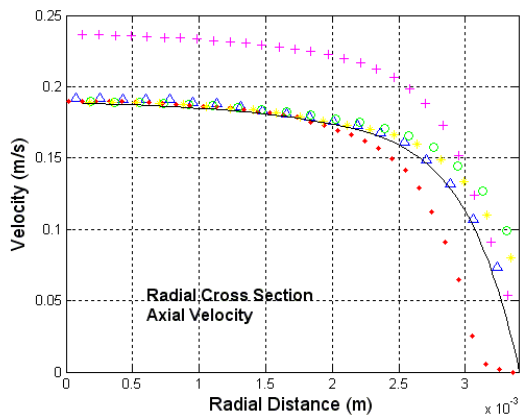


Figure 7.C. Axial velocity, laminar, Re 500, station -0.048m

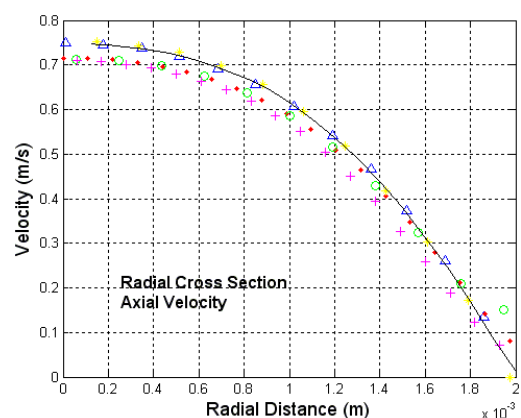


Figure 7.F. Axial velocity, laminar, Re 500, station 0.0m

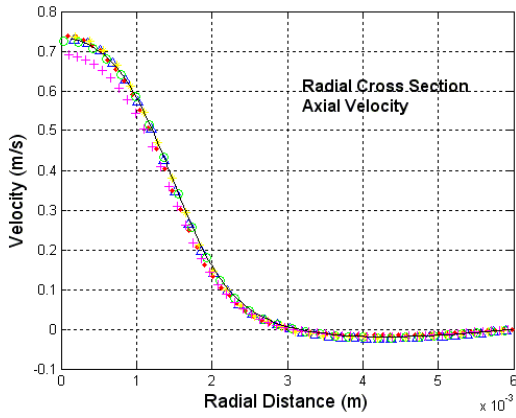


Figure 7.G. Axial velocity, laminar, Re 500, station 0.008m

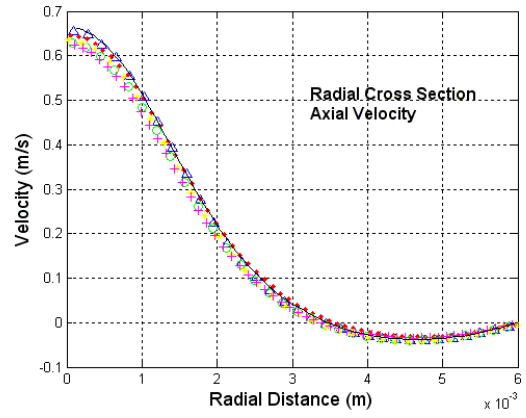


Figure 7.J. Axial velocity, laminar, Re 500, station 0.032m

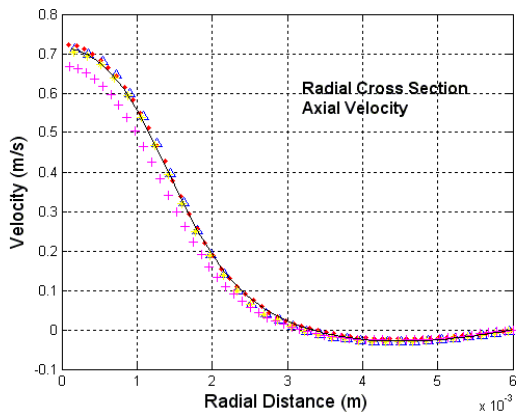


Figure 7.H. Axial velocity, laminar, Re 500, station 0.016m

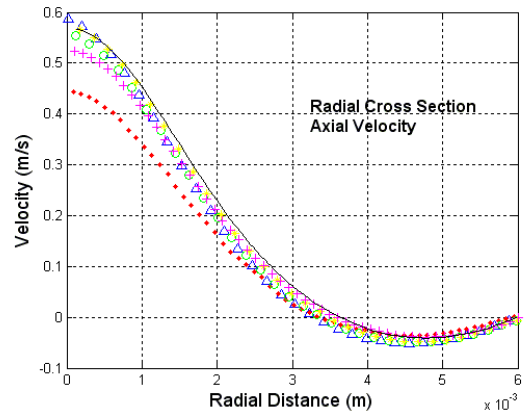


Figure 7.K. Axial velocity, laminar, Re 500, station 0.06m

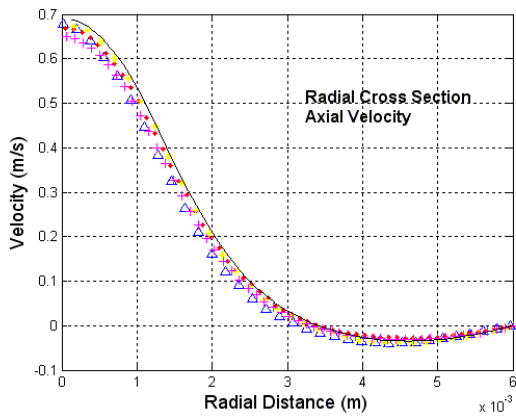


Figure 7.I. Axial velocity, laminar, Re 500, station 0.024m

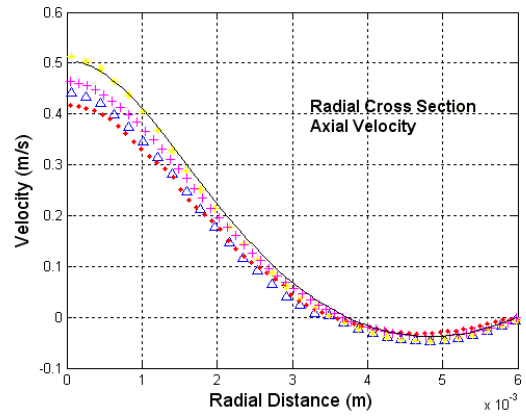


Figure 7.L. Axial velocity, laminar, Re 500, station 0.08m



Figure 7.M. Legend for figures 7.A-7.L

Figures 8 show the axial shear stress profile upon radial sectional cuts for the 500 Reynolds number laminar case. Figure 8 includes the 12 axial locations donated by figures 8.A-8.L

Though showing the same Reynolds case as the figures above, here it is noticeable that the simulation comes close to predicting the shear stress through the sections but is not quite as accurate as the velocity profiles above.

In these plots the first noticeable items is the divergence from the experimental data close to the outer wall in figures 8.A and 8.B. This is exhibited by the experimental data trending to decrease in shear stress while the simulation remains on the same predicted slope as the general flow shear stress. The second noticeable divergence in the simulation to the experimental data is the discrepancy with the velocity scaling to figure 8.C. In figure 8.C it is noticeable that the shear stress close to the wall aligns well but the shear stress at the center of the tub is over predicted by $\sim 0.1\text{Pa}$. The final noticeable item in figure 8 is again the small divergence in predicting the wall shear stress for figures 8.H-8.L.

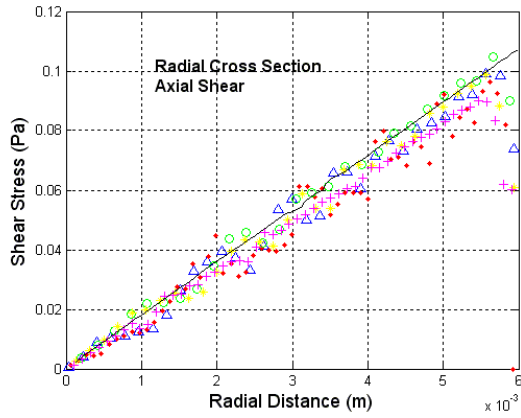


Figure 8.A. Axial shear stress, laminar, Re 500, station -0.088m

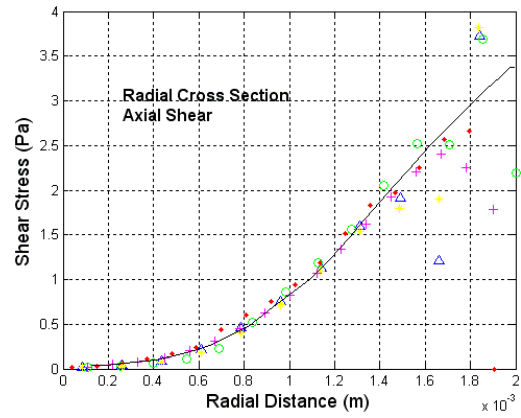


Figure 8.D. Axial shear stress, laminar, Re 500, station -0.02m

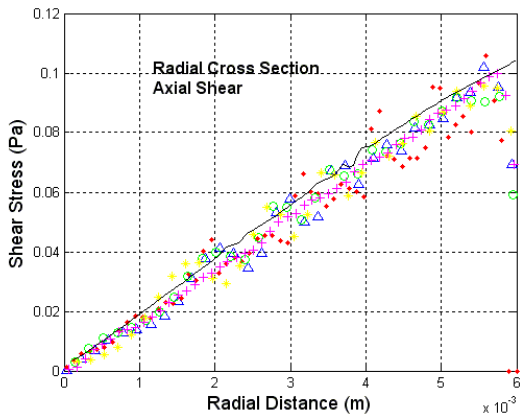


Figure 8.B. Axial shear stress, laminar, Re 500, station -0.064m

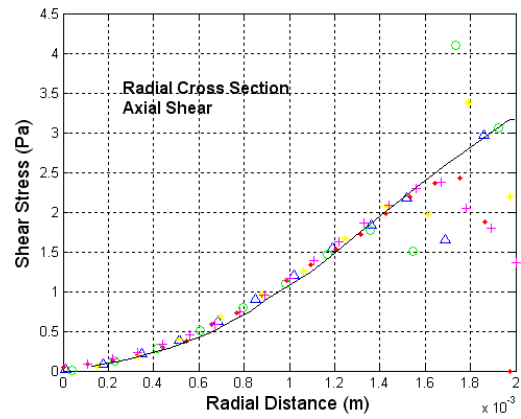


Figure 8.E. Axial shear stress, laminar, Re 500, station -0.008m

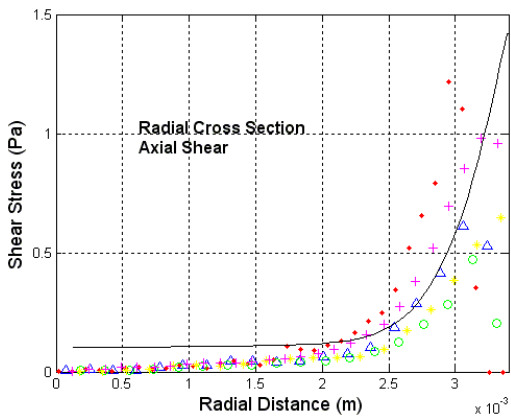


Figure 8.C. Axial shear stress, laminar, Re 500, station -0.048m

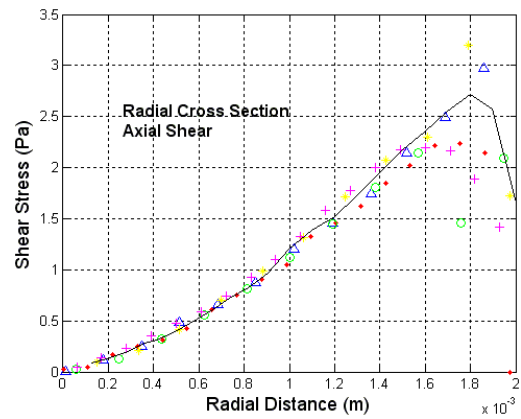


Figure 8.F. Axial shear stress, laminar, Re 500, station 0.0m

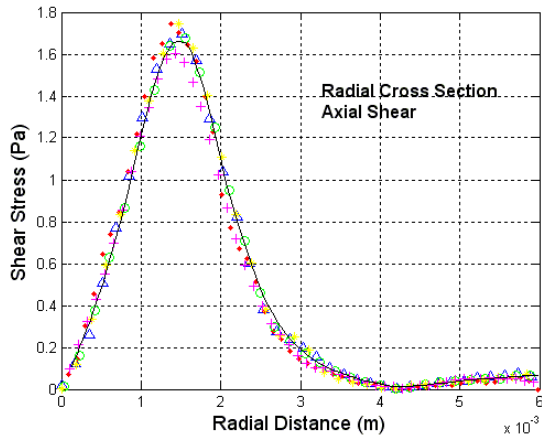


Figure 8.G. Axial shear stress, laminar, Re 500, station 0.008m

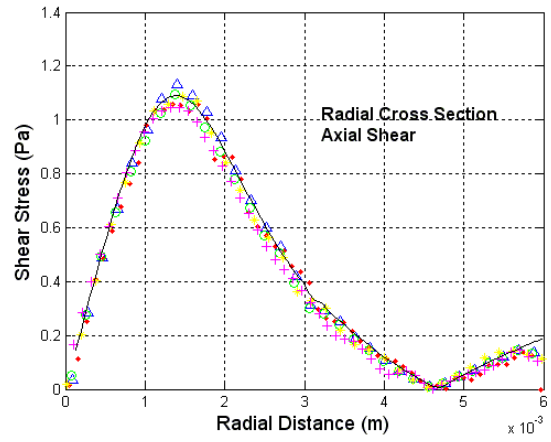


Figure 8.J. Axial shear stress, laminar, Re 500, station 0.032m

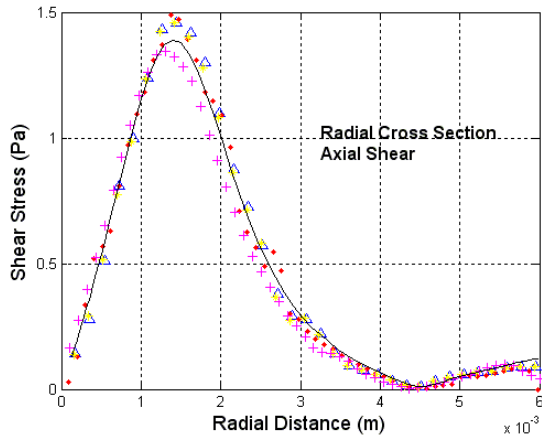


Figure 8.H. Axial shear stress, laminar, Re 500, station 0.016m

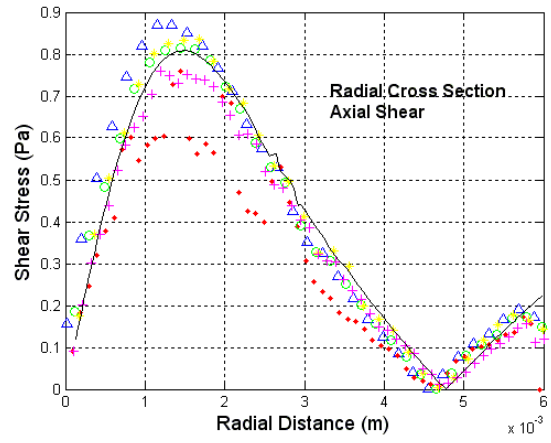


Figure 8.K. Axial shear stress, laminar, Re 500, station 0.06m

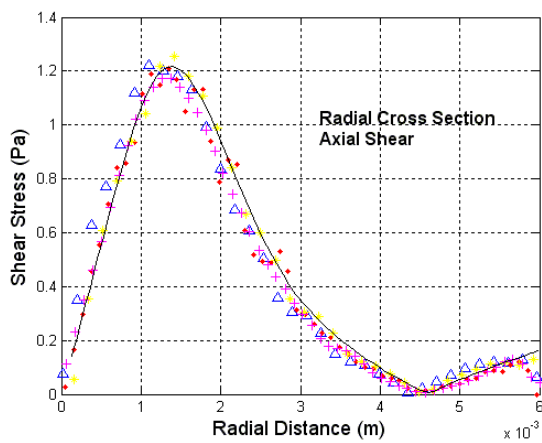


Figure 8.I. Axial shear stress, laminar, Re 500, station 0.024m

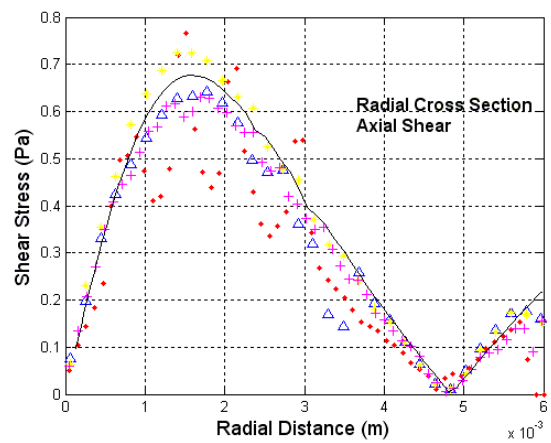


Figure 8.L. Axial shear stress, laminar, Re 500, station 0.08m



Figure 8.M. Legend for figures 8.A-8.L

Moving to the 2000 Reynolds laminar case, figure 9 shows case plots for the axial velocity of the radial section cuts. Figure 9 includes figures 9.A-9.L for the twelve different axial locations.

In figure 9 it is visible that the velocity profiles align with the experimental data very well until sections 0.06m and 0.08m (figures 8.K and 8.L). In these figures the laminar simulation characteristics predict the flow to carry a high velocity profile at the center of the tub while the experimental data velocity profile is starting to show higher dampening of the velocity profile. Also noticeable in figure 8.K there is a large spread in the experimental data sets; two data sets following one velocity profile while the other three following there, seemingly, own trend. The velocity profiles in figures 9 seem to align closely with the velocity profiles seen by others, S.F.C. Stewart et al., [1].

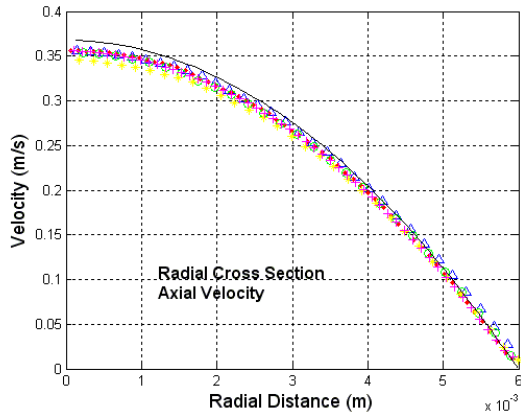


Figure 9.A. Axial velocity, laminar, Re 2000, station -0.088

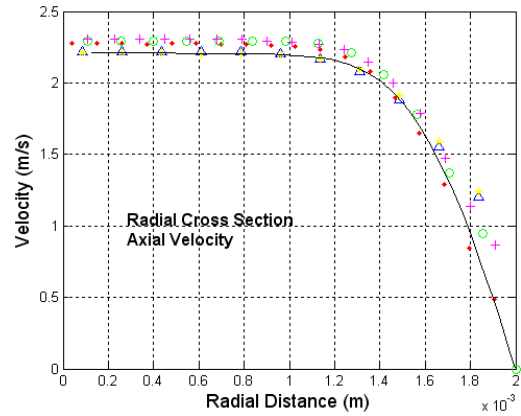


Figure 9.D. Axial velocity, laminar, Re 2000, station -0.02m

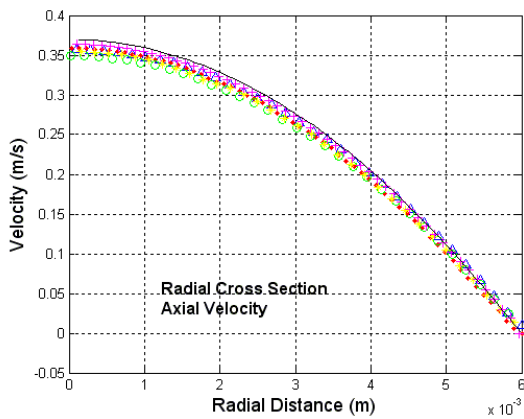


Figure 9.B. Axial velocity, laminar, Re 2000, station -0.064m

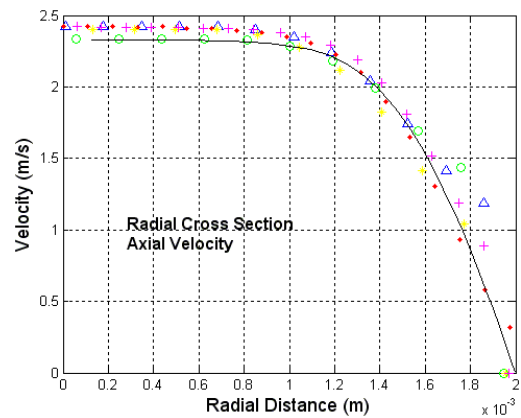


Figure 9.E. Axial velocity, laminar, Re 2000, station -0.008m

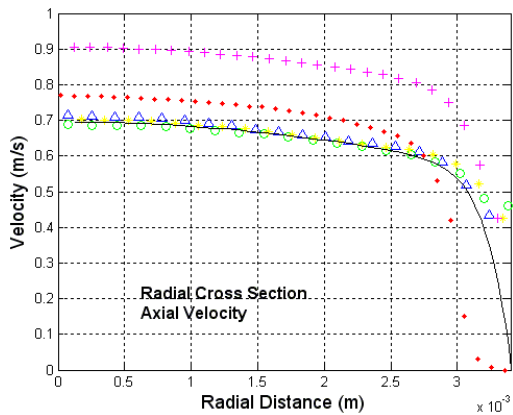


Figure 9.C. Axial velocity, laminar, Re 2000, station -0.048m

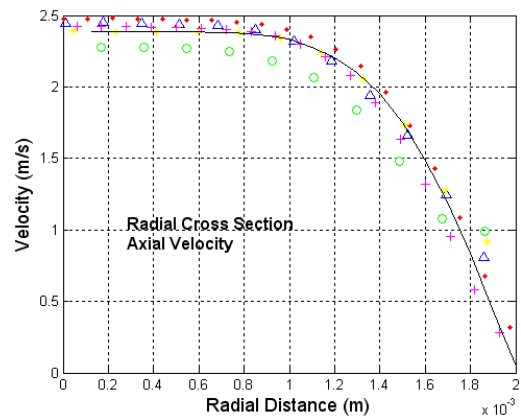


Figure 9.F. Axial velocity, laminar, Re 2000, station 0.0m

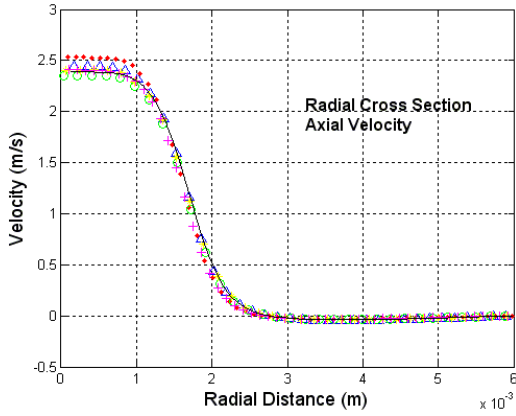


Figure 9.G. Axial velocity, laminar, Re 2000, station 0.008m

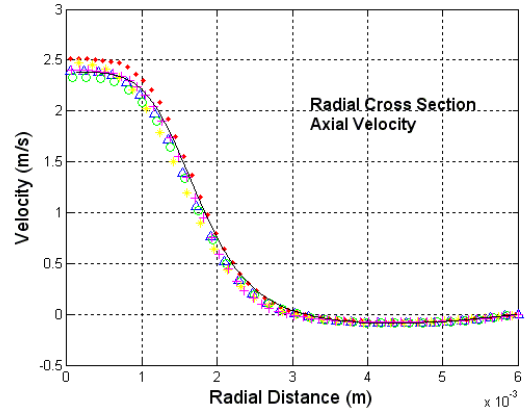


Figure 9.J. Axial velocity, laminar, Re 2000, station 0.032m

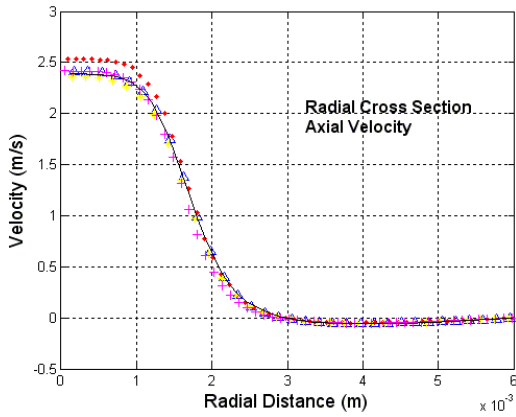


Figure 9.H. Axial velocity, laminar, Re 2000, station 0.016m

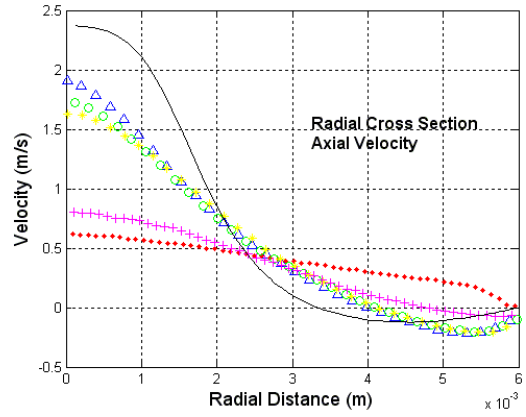


Figure 9.K. Axial velocity, laminar, Re 2000, station 0.06m

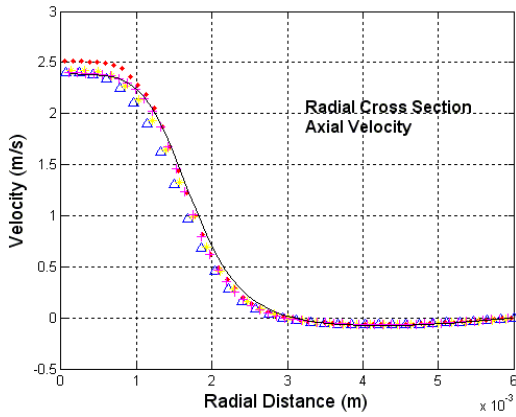


Figure 9.I. Axial velocity, laminar, Re 2000, station 0.024m

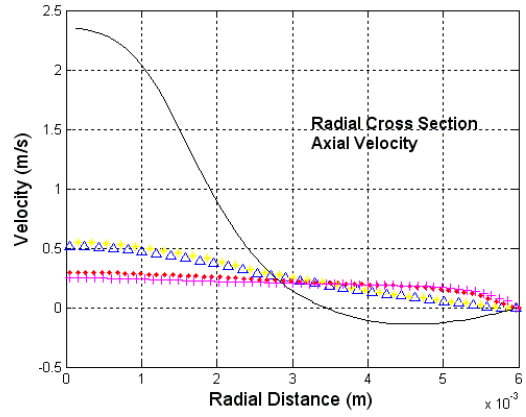


Figure 9.L. Axial velocity, laminar, Re 2000, station 0.08m



Figure 9.M. Legend for figures 9.A-9.L

Continuing with the axial shear stress for the radial sectional cuts of the 2000 Reynolds number laminar case, figure 10 depicts the alignment of the simulation shear stress to the experimental data. Figure 10 includes figures 10.A-10.L, donating the 12 different axial locations along the flow path.

In figure 10 most all of the sections (except for 10.K and 10.L) align with the experimental data falling within the error of the data sets. As seen in the velocity profiles of the 2000 Reynolds Laminar case, figures 10.K and 10.L trend to over predict the shear stress value from the estimated carried flow earlier in the tub section.

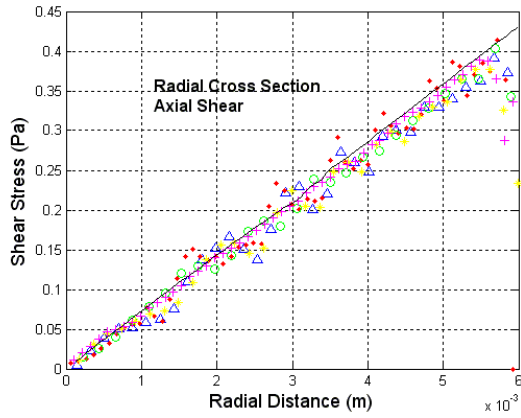


Figure 10.A. Axial shear stress, laminar, Re 2000, station -0.088m

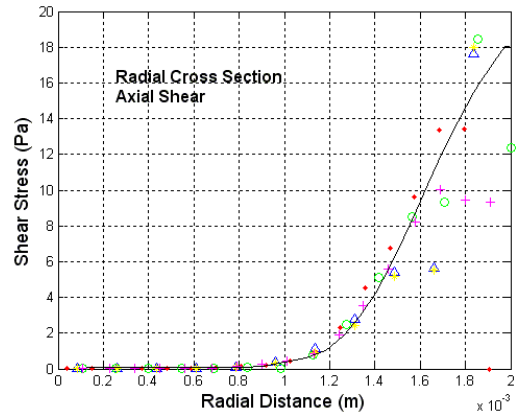


Figure 10.D. Axial shear stress, laminar, Re 2000, station -0.02

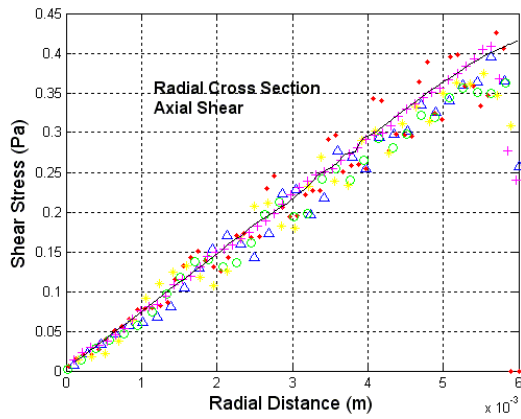


Figure 10.B. Axial shear stress, laminar, Re 2000, station -0.064m

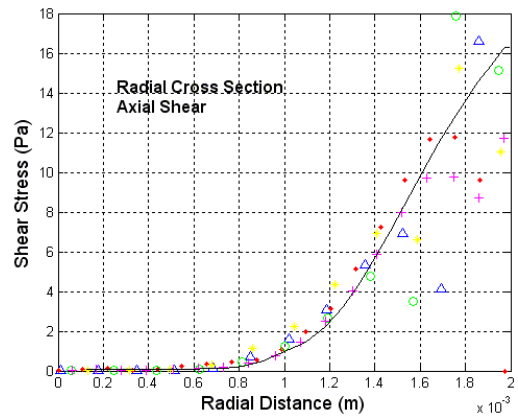


Figure 10.E. Axial shear stress, laminar, Re 2000, station -0.008m

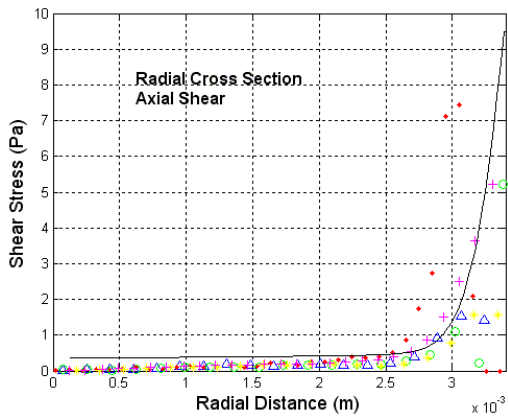


Figure 10.C. Axial shear stress, laminar, Re 2000, station -0.048m

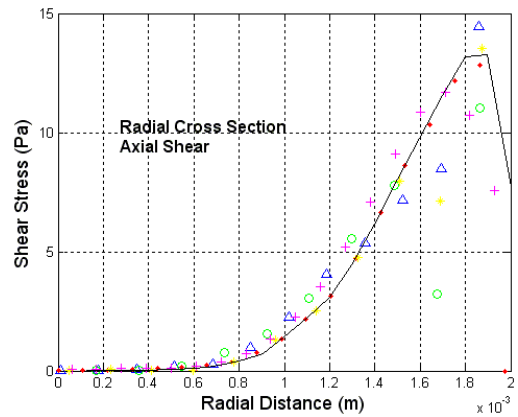


Figure 10.F. Axial shear stress, laminar, Re 2000, station 0.0m

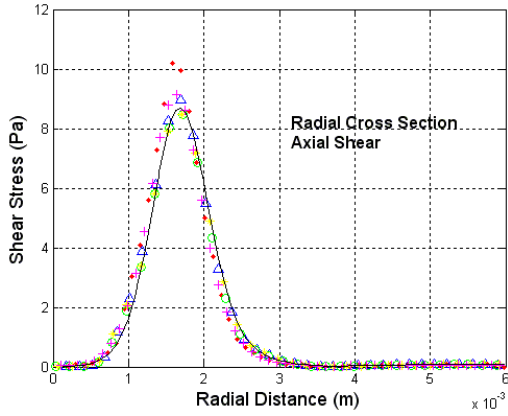


Figure 10.G. Axial shear stress, laminar, Re 2000, station 0.008m

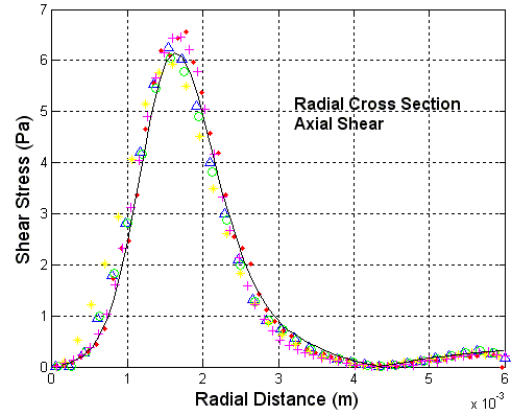


Figure 10.J. Axial shear stress, laminar, Re 2000, station 0.032m

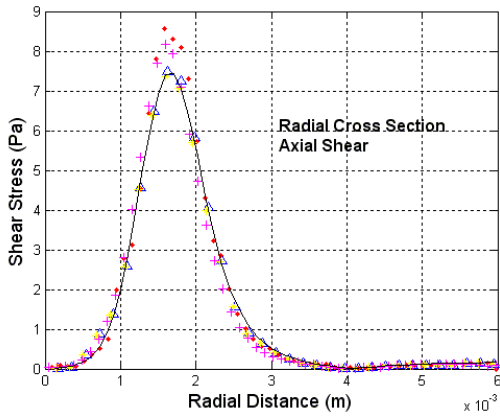


Figure 10.H. Axial shear stress, laminar, Re 2000, station 0.016m

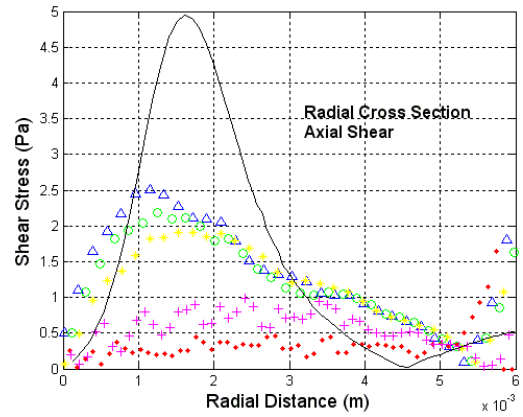


Figure 10.K. Axial shear stress, laminar, Re 2000, station 0.06m

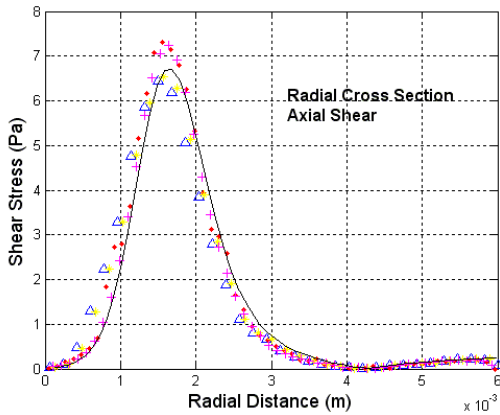


Figure 10.I. Axial shear stress, laminar, Re 2000, station 0.024m

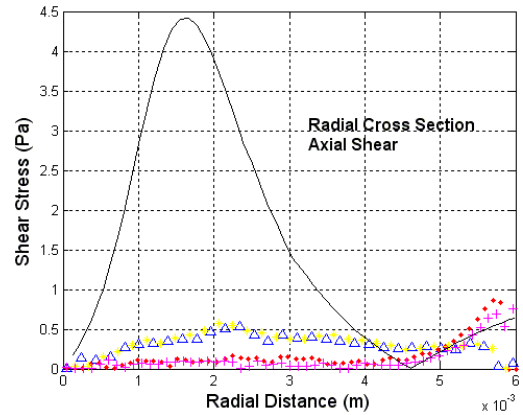


Figure 10.L. Axial shear stress, laminar, Re 2000, station 0.08m



Figure 10.M. Legend for figures 10.A-10.L

Moving to a different solution method, figure 11 shows the axial velocity profiles for the radial section cuts of 2000 Reynolds case using the BSL solver. Figure 11 includes figures 11.A-11.L, representing the twelve different axial locations.

In figure 11 a switch in trend from the earlier laminar profiles is shown. Starting at the back end of the tub section, figure 11.K shows an under predicted velocity profile in reference to the experimental data. Later in figure 11.L the solver appears to be better estimating the diminishing velocity profile as it almost aligns with two of the five data sets.

Other noticeable characteristics of the BSL solver in the 2000 Reynolds case is the under prediction of the velocity profile soon after the sudden expansion. Figures 11.H-11.K show the velocity profile separating from the experimental data, failing to hold the high gradients of the velocity profile as the experimental data does.

As the separation point for re-circulating flow is controlled in this experiment/simulation, another item noticed in the 2000 Reynolds BSL simulation is re-circulation area and how the simulation data aligns with the experiment. At section 0.008m (figure 11.G) the recirculation area is under predicted by the simulation. This remains the case up until the 0.06m section (figure 11.K).

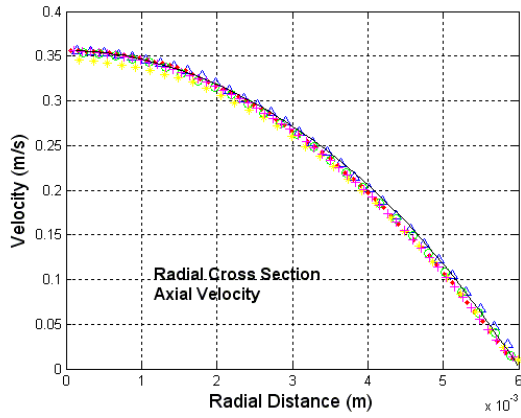


Figure 11.A. Axial velocity, BSL, Re 2000, station -0.088m

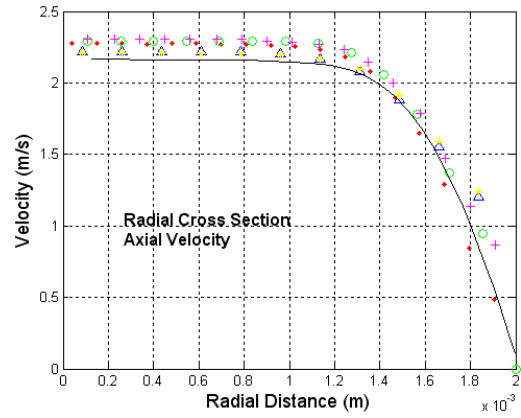


Figure 11.D. Axial velocity, BSL, Re 2000, station -0.02m

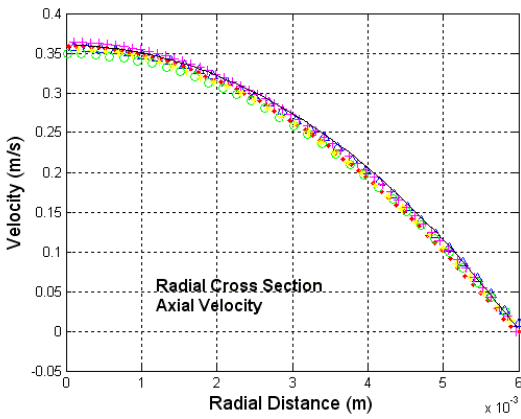


Figure 11.B. Axial velocity, BSL, Re 2000, station -0.064m

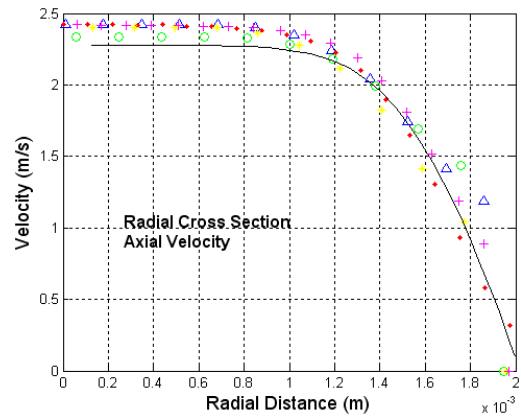


Figure 11.E. Axial velocity, BSL, Re 2000, station -0.008m

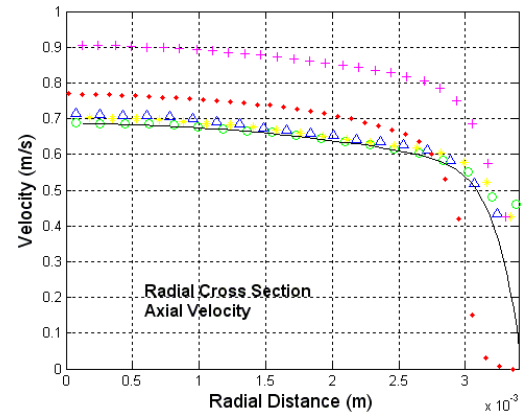


Figure 11.C. Axial velocity, BSL, Re 2000, station -0.048m

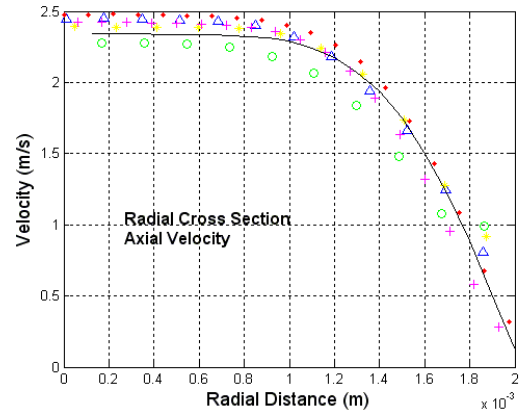


Figure 11.F. Axial velocity, BSL, Re 2000, station 0.0m

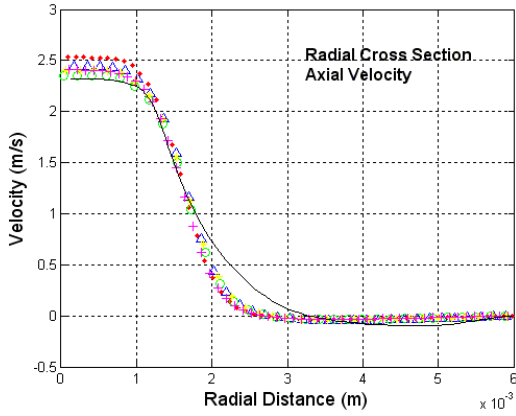


Figure 11.G. Axial velocity, BSL, Re 2000, station 0.008m

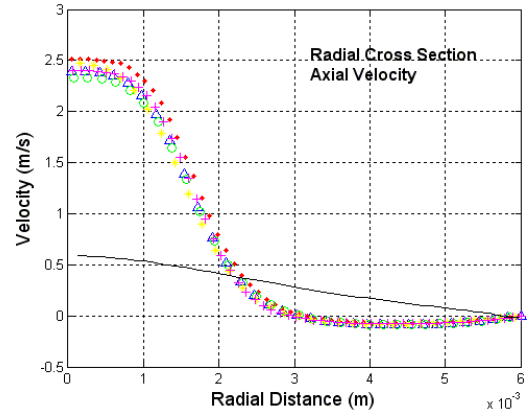


Figure 11.J. Axial velocity, BSL, Re 2000, station 0.032m

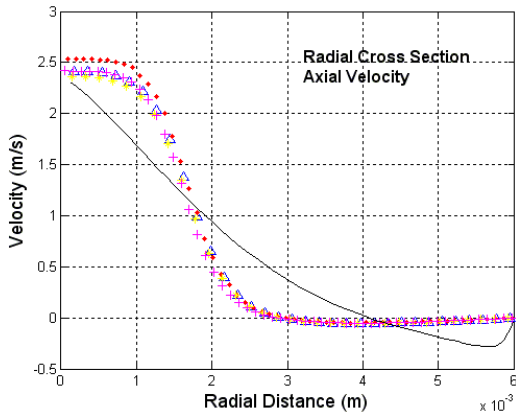


Figure 11.H. Axial velocity, BSL, Re 2000, station 0.016m

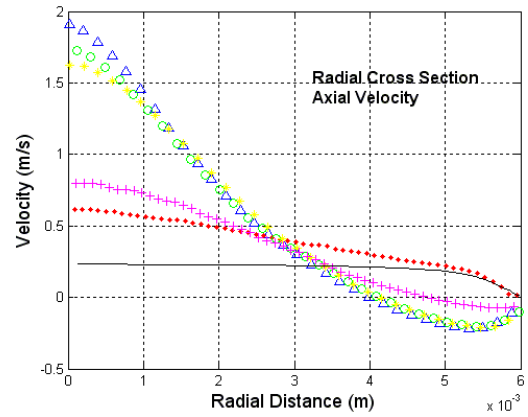


Figure 11.K. Axial velocity, BSL, Re 2000, station 0.06m

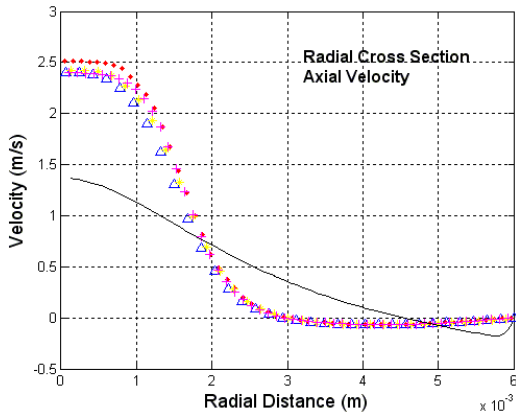


Figure 11.I. Axial velocity, BSL, Re 2000, station 0.024m

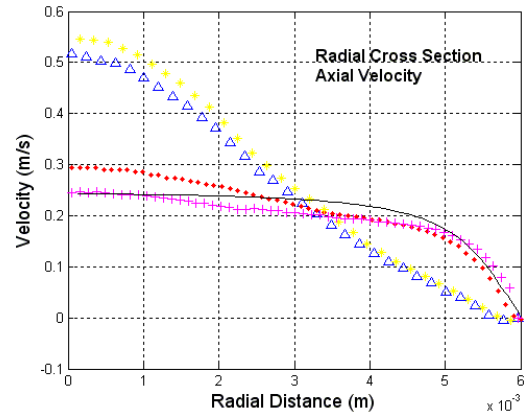


Figure 11.L. Axial velocity, BSL, Re 2000, station 0.08m



Figure 11.M. Legend for figures 11.A-11.L

Figures 12.A through 12.L show the shear stress profiles of the experimental data as well as the simulation for the 2000 Reynolds number BSL run. Similar to the velocity profiles the simulation manages to align with the experimental data up until the sudden expansion point (figure 12.G). After the point of the sudden expansion the simulation data tends to deviate from the experiment; once again under estimating the maximums that the data shows. It is not until the end of the tube at 0.08m (figure 12.L) that the simulation shear stress profile aligns with two of the experimental data sets.

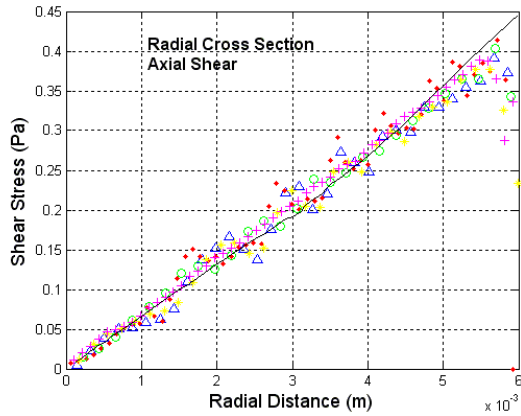


Figure 12.A. Axial shear stress, BSL, Re 2000, station -0.088m

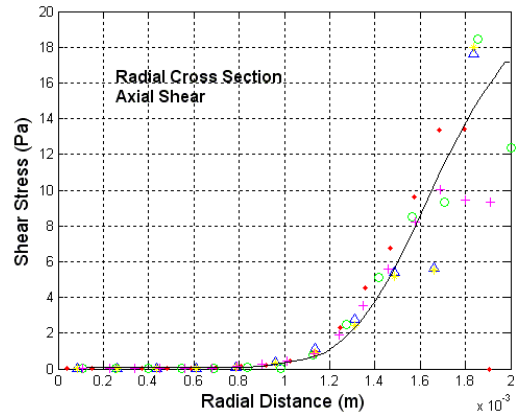


Figure 12.D. Axial shear stress, BSL, Re 2000, station -0.02m

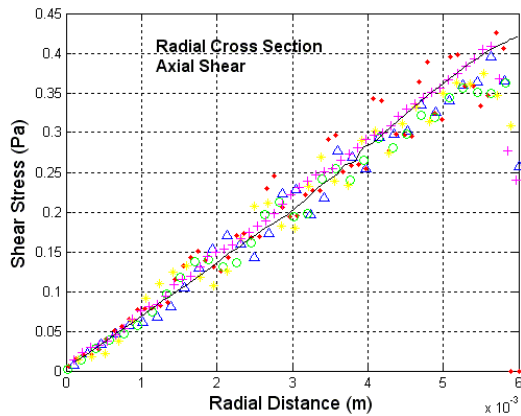


Figure 12.B. Axial shear stress, BSL, Re 2000, station -0.064m

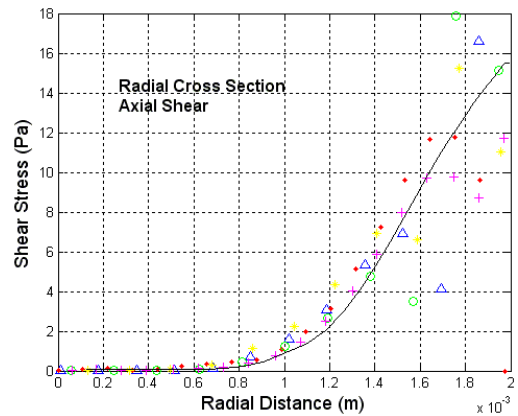


Figure 12.E. Axial shear stress, BSL, Re 2000, station -0.008m

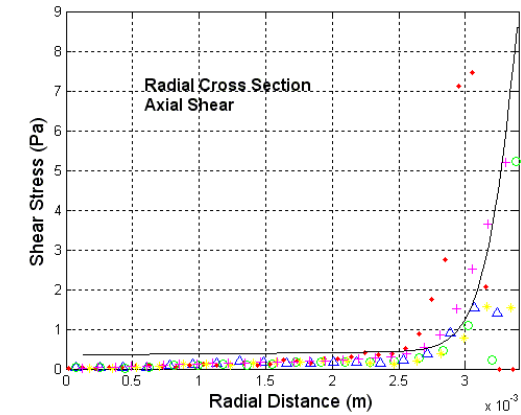


Figure 12.C. Axial shear stress, BSL, Re 2000, station -0.048m

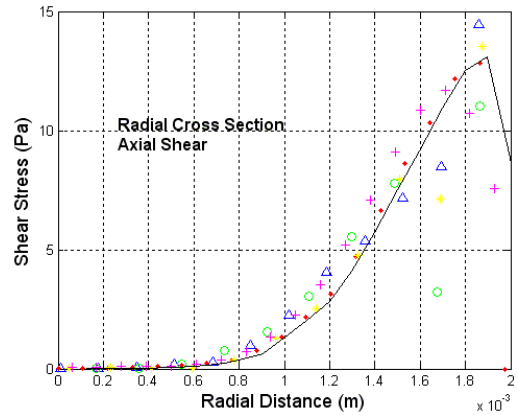


Figure 12.F. Axial shear stress, BSL, Re 2000, station 0.0m

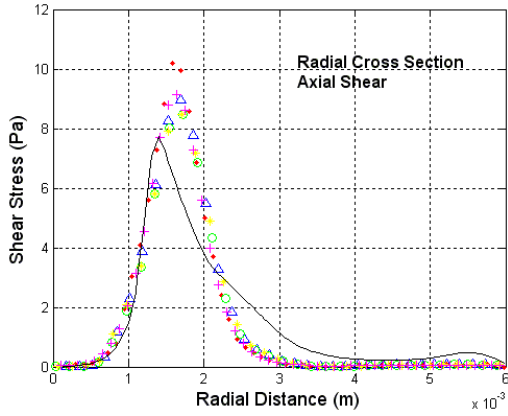


Figure 12.G. Axial shear stress, BSL, Re 2000, station 0.008m

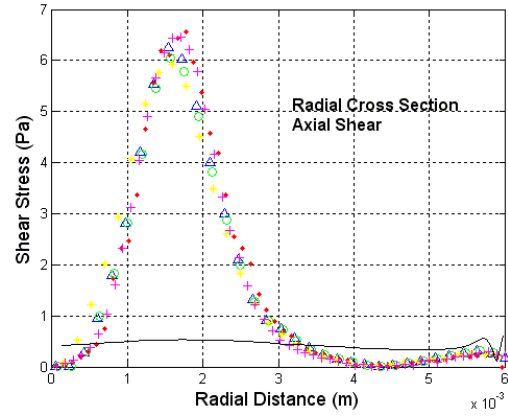


Figure 12.J. Axial shear stress, BSL, Re 2000, station 0.032m

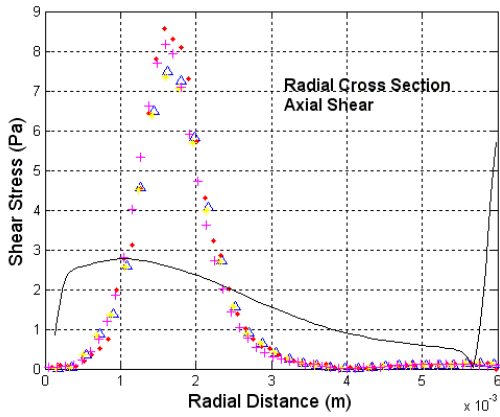


Figure 12.H. Axial shear stress, BSL, Re 2000, station 0.016m

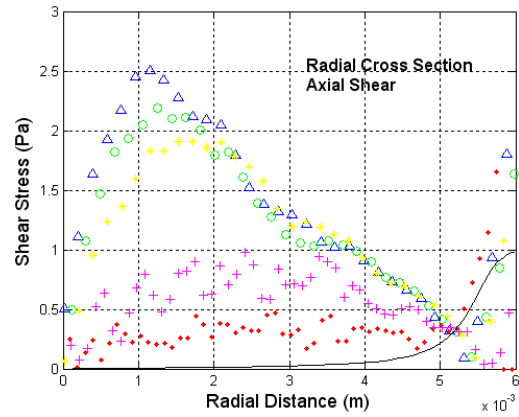


Figure 12.K. Axial shear stress, BSL, Re 2000, station 0.06m

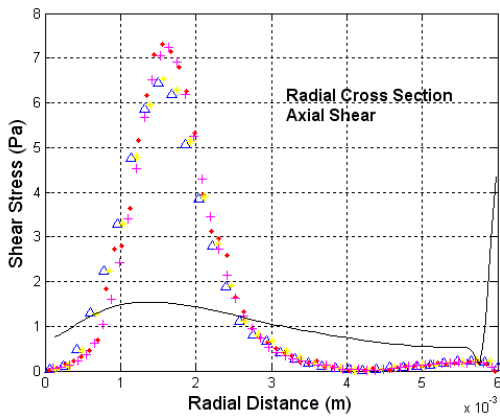


Figure 12.I. Axial shear stress, BSL, Re 2000, station 0.024m

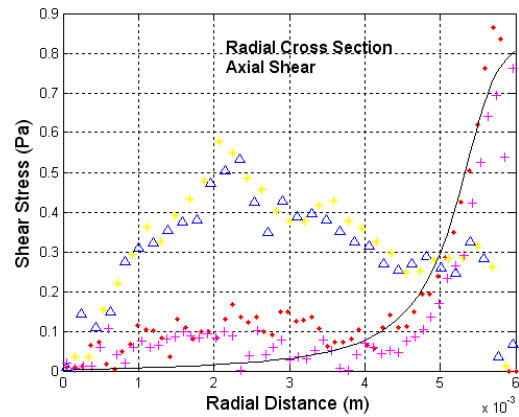


Figure 12.L. Axial shear stress, BSL, Re 2000, station 0.08m



Figure 12.M. Legend for figures 12.A-12.L

The velocity profiles for the 2000 Reynolds case SST can be seen in figures 13.A through 13.L. Up until the 0.16m mark (figure 13.H), the experimental data velocity profiles seem to be tracked well by the simulation results. At the 0.016m (figure 13.H) mark and further downstream, the velocity profile of the simulation seems to diverge from the experimental data as well as does not achieve the full velocity profile. It is not until the very last section (figure 13.L) that the velocity profile of the experimental data appears to line up with the experimental data.

The 2000 Reynolds SST simulation data also seem to exhibit the same trend in the recirculation zone as the 2000 Reynolds BSL simulation. As noted in figure 11, the recirculation zone of the simulation data seems to be under predicted until the 0.06m (figure 13.K) region.

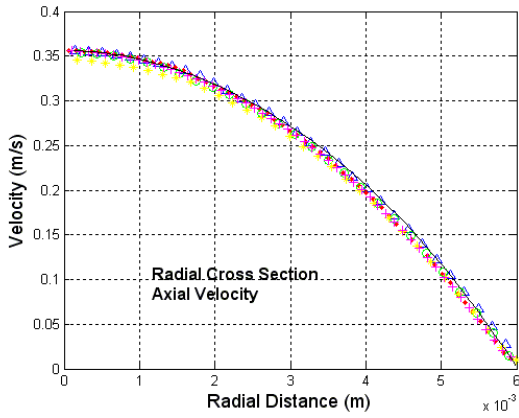


Figure 13.A. Axial velocity, SST, Re 2000, station -0.088m

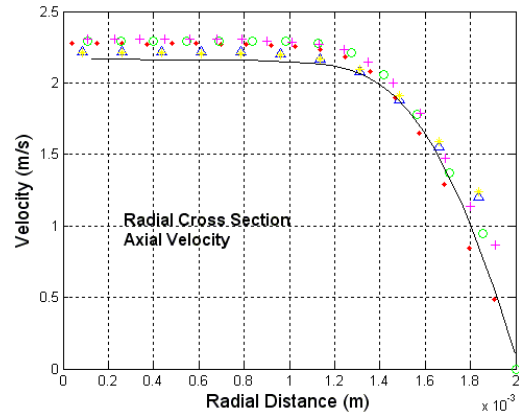


Figure 13.D. Axial velocity, SST, Re 2000, station -0.02m

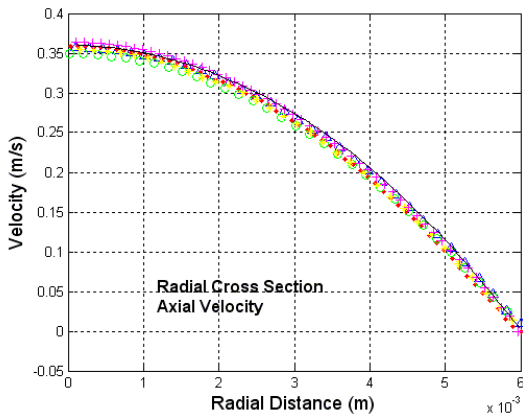


Figure 13.B. Axial velocity, SST, Re 2000, station -0.064m

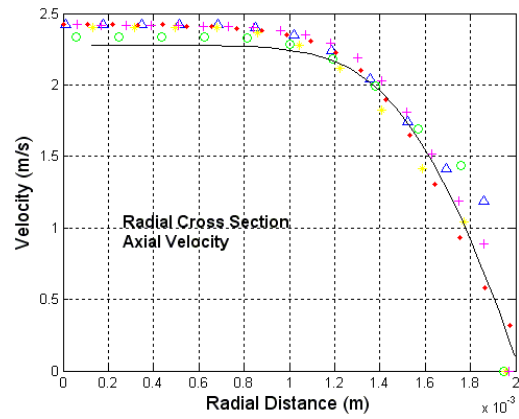


Figure 13.E. Axial velocity, SST, Re 2000, station -0.008m

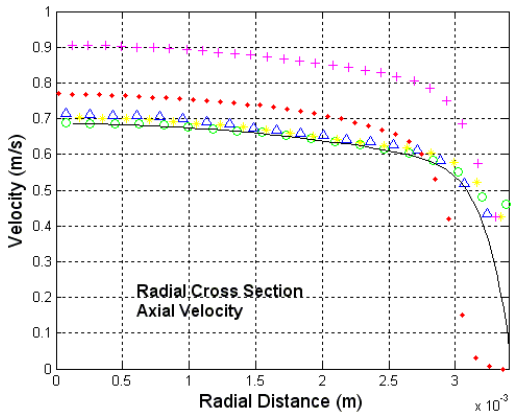


Figure 13.C. Axial velocity, SST, Re 2000, station -0.048m

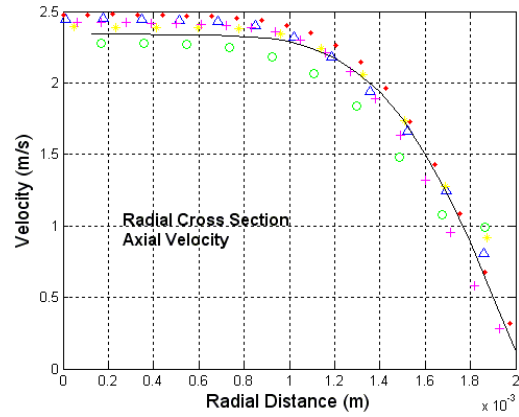


Figure 13.F. Axial velocity, SST, Re 2000, station 0.0m

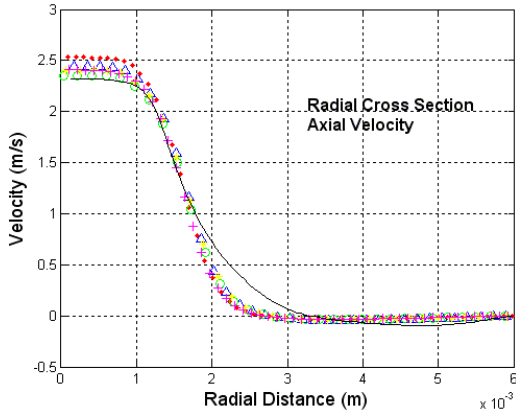


Figure 13.G. Axial velocity, SST, Re 2000, station 0.008m

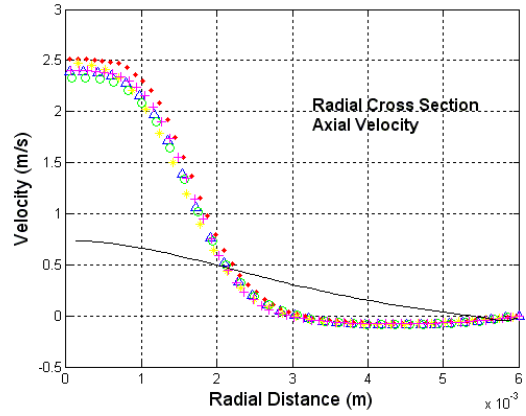


Figure 13.J. Axial velocity, SST, Re 2000, station 0.032m

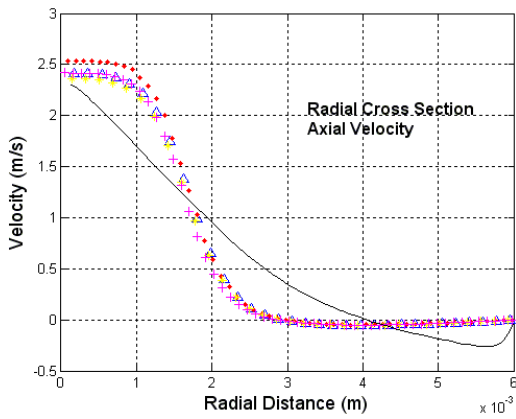


Figure 13.H. Axial velocity, SST, Re 2000, station 0.016m

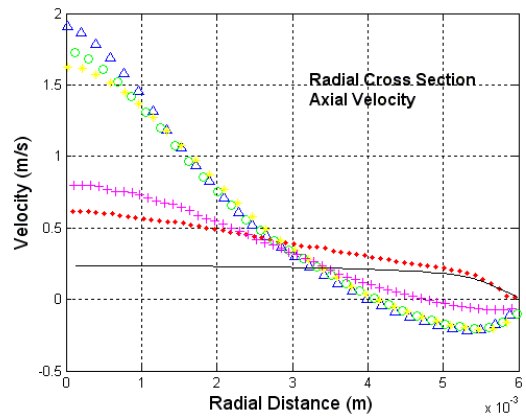


Figure 13.K. Axial velocity, SST, Re 2000, station 0.06m

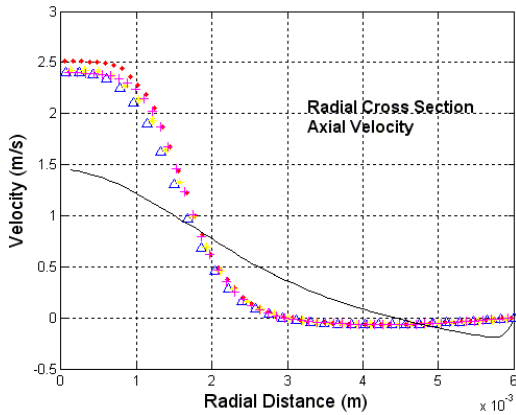


Figure 13.I. Axial velocity, SST, Re 2000, station 0.024m

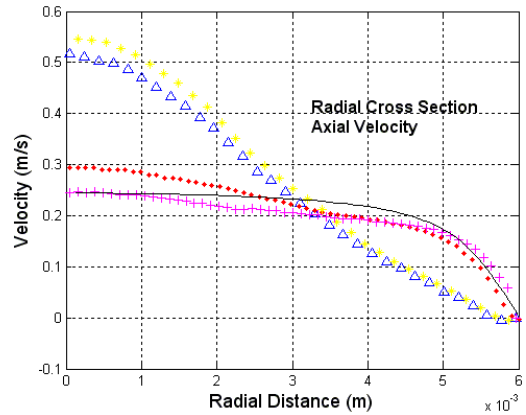


Figure 13.L. Axial velocity, SST, Re 2000, station 0.08m



Figure 13.M. Legend for figures 13.A-13.L

Figure 14 (14.A-14.L) shows the shear stress sectional plots for the 2000 Reynolds SST simulation at twelve different axial locations. Once again the plots seem to track the experimental within the experimental data error until the sudden expansion (section 0.0m or figure 14.F). After this point the shear stress values are very similar to the BSL solver and in the 2000 Reynolds case. In section 0.016m (figure 14.H) that the peak shear stress value at about the 0.0015m mark is not held as was in section 0.016m of figure 12.H. This was found to be one of the main differences in using the SST solver to the BSL solver as the SST solver allows for additional dampening parameters that are not accounted for in the BSL solver.

At the very at the end of the section, sections 0.06 and 0.08 or figures 14.K-14.L, the experimental data seems to exhibit two different types of profiles. It was seen in both types of solvers (the BSL as well as the SST) that the simulated solutions seem to follow the experimental data with higher wall shear stress values.

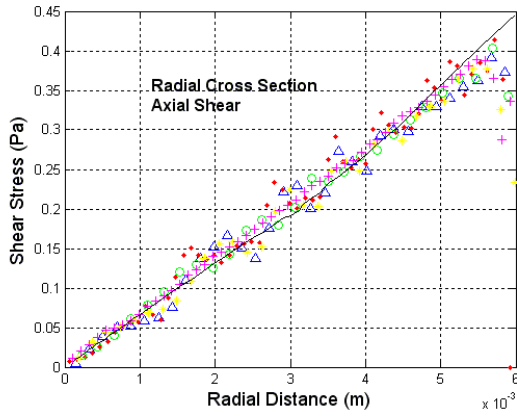


Figure 14.A. Axial shear stress, SST, Re 2000, station -0.088m

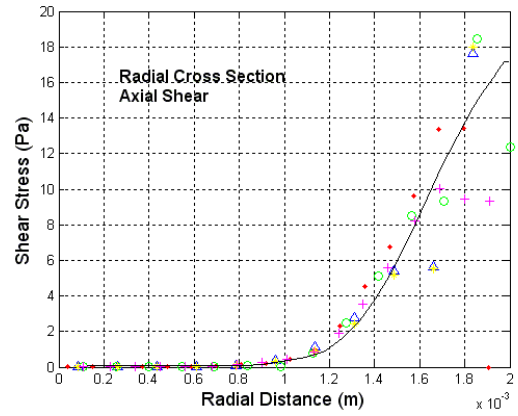


Figure 14.D. Axial shear stress, SST, Re 2000, station -0.02m

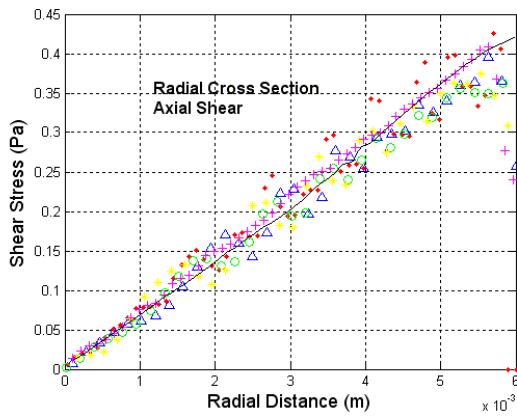


Figure 14.B. Axial shear stress, SST, Re 2000, station -0.064m

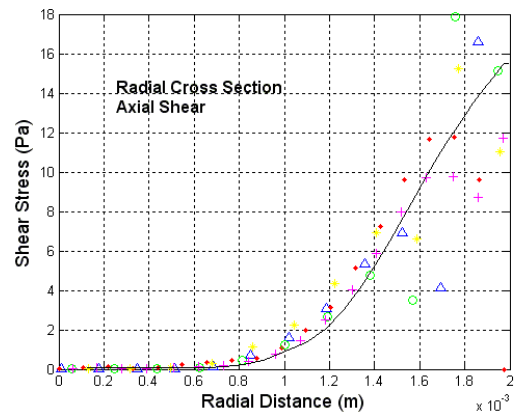


Figure 14.E. Axial shear stress, SST, Re 2000, station -0.008m

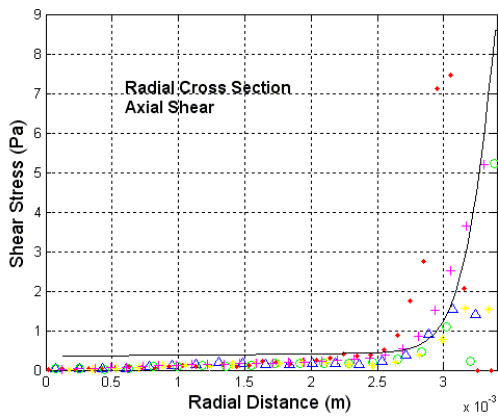


Figure 14.C. Axial shear stress, SST, Re 2000, station -0.048m

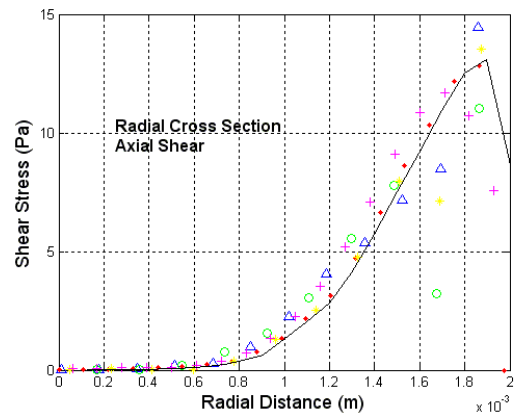


Figure 14.F. Axial shear stress, SST, Re 2000, station 0.0m

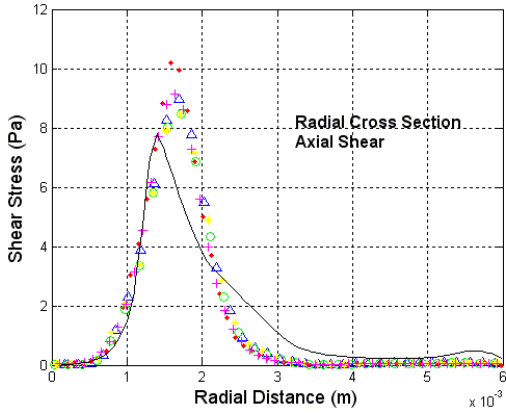


Figure 14.G. Axial shear stress, SST, Re 2000, station 0.008m

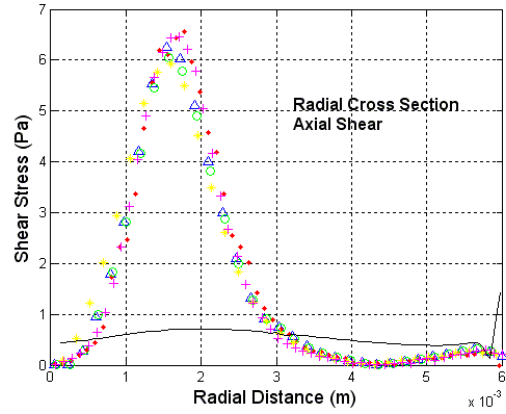


Figure 14.J. Axial shear stress, SST, Re 2000, station 0.032m

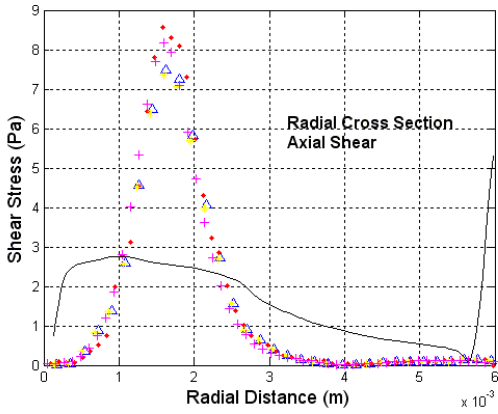


Figure 14.H. Axial shear stress, SST, Re 2000, station 0.016m

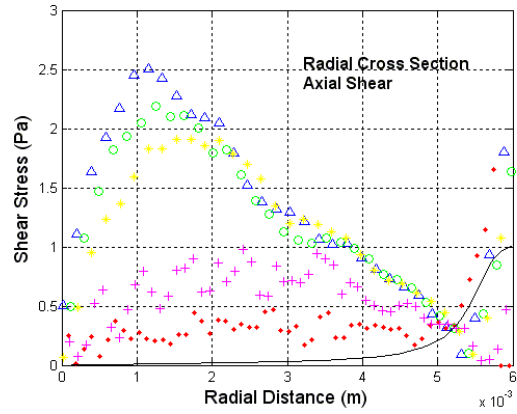


Figure 14.K. Axial shear stress, SST, Re 2000, station 0.06m

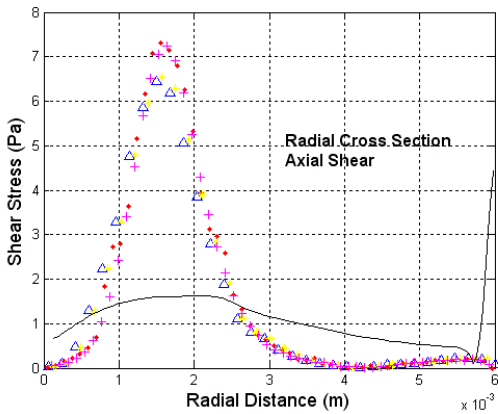


Figure 14.I. Axial shear stress, SST, Re 2000, station 0.024m

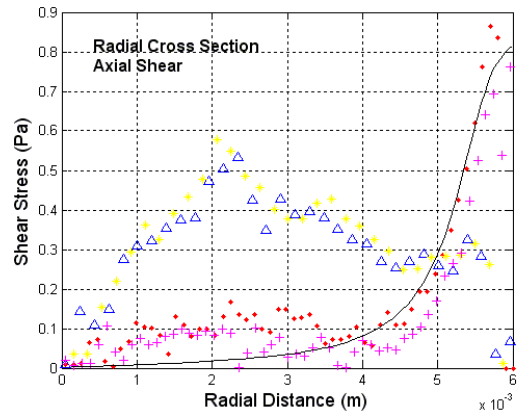


Figure 14.L. Axial shear stress, SST, Re 2000, station 0.08m



Figure 14.M. Legend for figures 14.A-14.L

The 3500 Reynolds BSL velocity profiles for 12 different axial locations are shown in figure 15 (15.A-15.L). Seen in the 2000 Reynolds cases as well as the laminar cases the trend of the simulation to the experimental data seem to follow each other closely up until the sudden expansion (section 0.0m or figure 15.F.). After this point the BSL solver tended to under estimate the max velocity and gradient of the velocity profile.

The recirculation zone at section 0.008m through 0.024m (figures 15.G.-15.I.) is also under predicted in size as was in the previous cases.

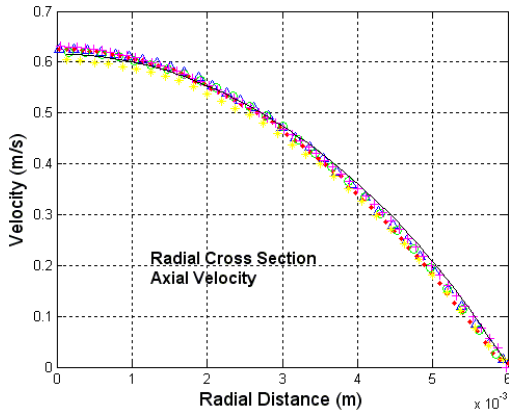


Figure 15.A. Axial velocity, BSL, Re 3500, station -0.088m

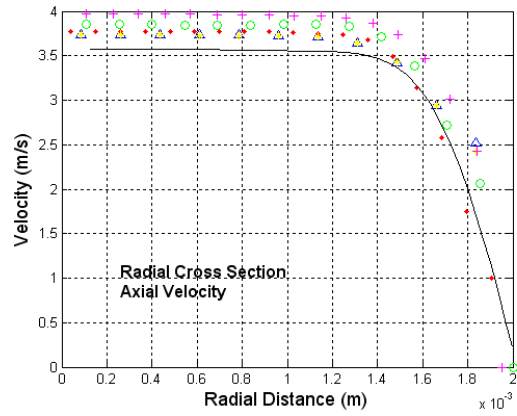


Figure 15.D. Axial velocity, BSL, Re 3500, station -0.02m

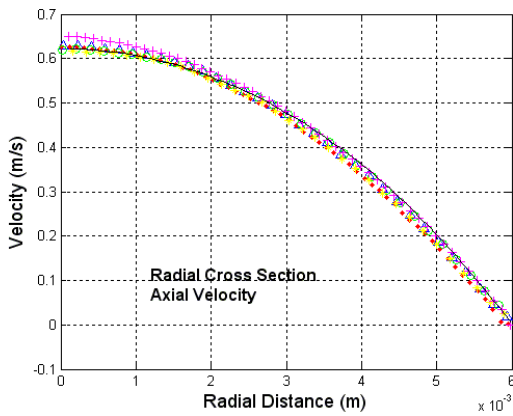


Figure 15.B. Axial velocity, BSL, Re 3500, station -0.064m

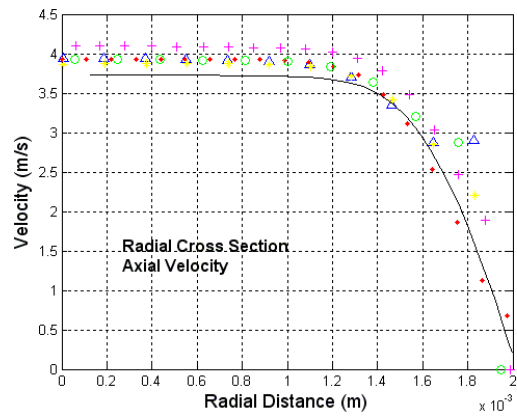


Figure 15.E. Axial velocity, BSL, Re 3500, station -0.008m

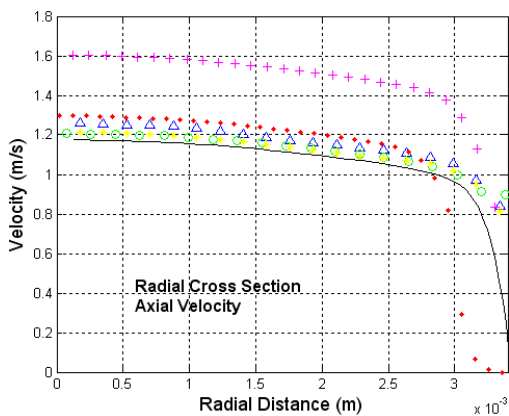


Figure 15.C. Axial velocity, BSL, Re 3500, station -0.048m

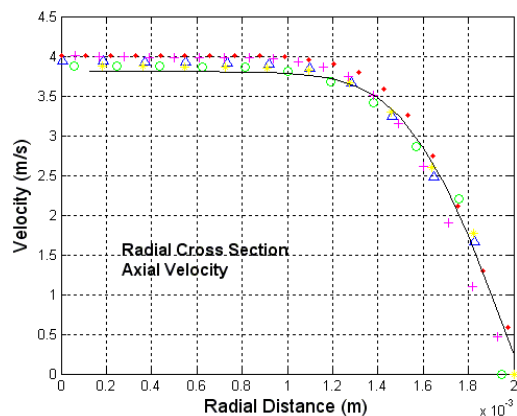


Figure 15.F. Axial velocity, BSL, Re 3500, station 0.0m

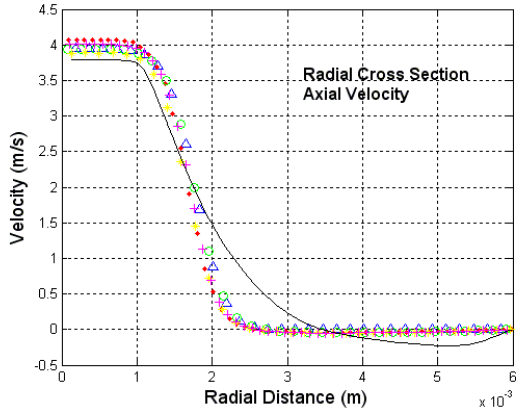


Figure 15.G. Axial velocity, BSL, Re 3500, station 0.008m

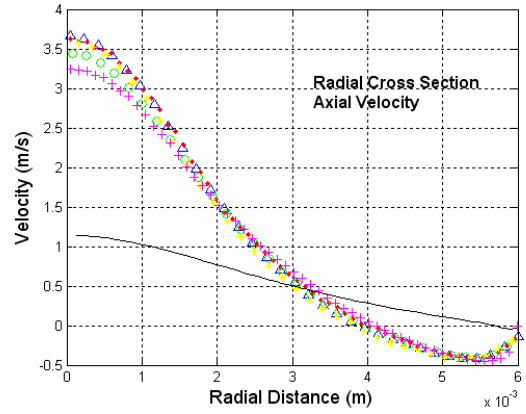


Figure 15.J. Axial velocity, BSL, Re 3500, station 0.032m

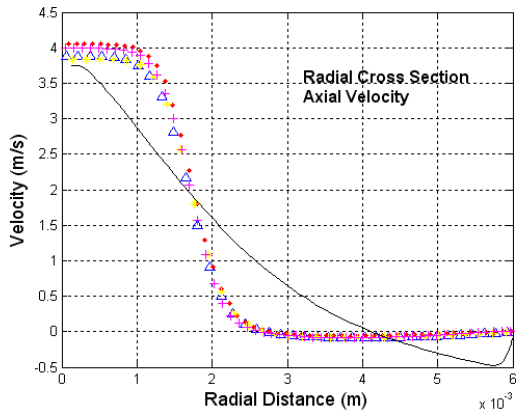


Figure 15.H. Axial velocity, BSL, Re 3500, station 0.016m

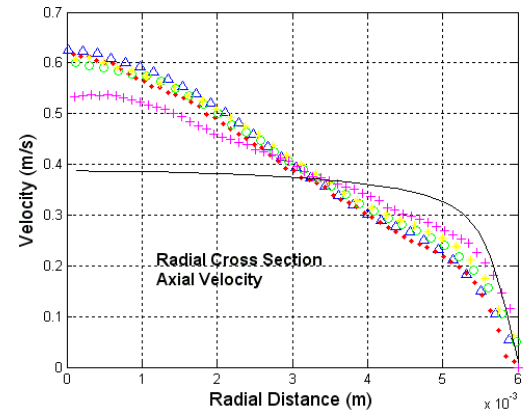


Figure 15.K. Axial velocity, BSL, Re 3500, station 0.06m

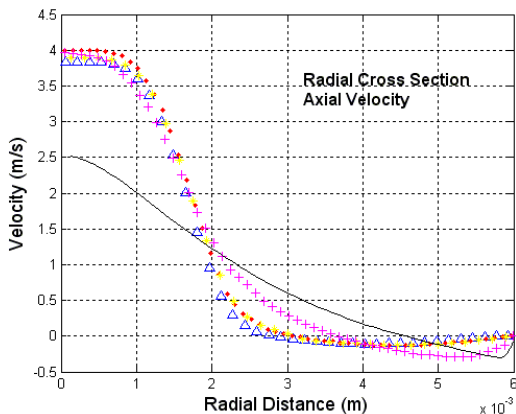


Figure 15.I. Axial velocity, BSL, Re 3500, station 0.024m

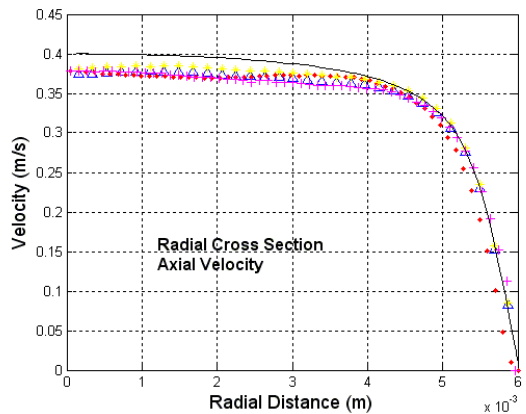


Figure 15.L. Axial velocity, BSL, Re 3500, station 0.08m



Figure 15.M. Legend for figures 15.A-15.L

The shear stress cross sections for the 3500 Reynolds BSL run can be seen in figure 16 (16.A-16.L). These figures represent the 12 axial locations of the flow path. Up until the sudden expansion the simulation data, of the 3500 Reynolds BLS runs, matches the experimental data. At section 0.0m it becomes noticeable that some singularities were not able to be massaged out of the simulation runs. As this error has been seen in previous cases as well as with different solvers, it is noted that the mesh in this area could be refined a little better than used for the results shown here. Though the singularity does not allow the simulation to highly align with the experimental data, the value and trend around the singularity is within the experimental data error and should have little effect to downstream velocity and shear stress values.

Final observations of the 3500 Reynolds BLS runs is the final shear stress profile at the last section of the measured flow (section 0.08m or figure 16.L). Here it is noted that the shear stress profile manages to re-align with the experimental data and follow the trend within the error of the experimental data.

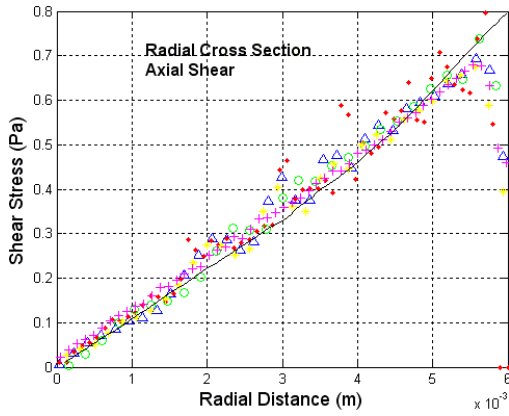


Figure 16.A. Axial shear stress, BSL, Re 3500, station -0.088m

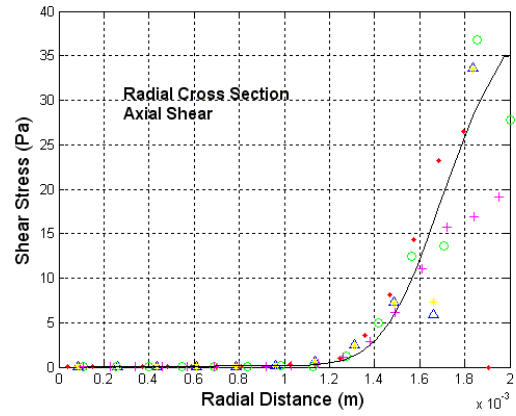


Figure 16.D. Axial shear stress, BSL, Re 3500, station -0.02m

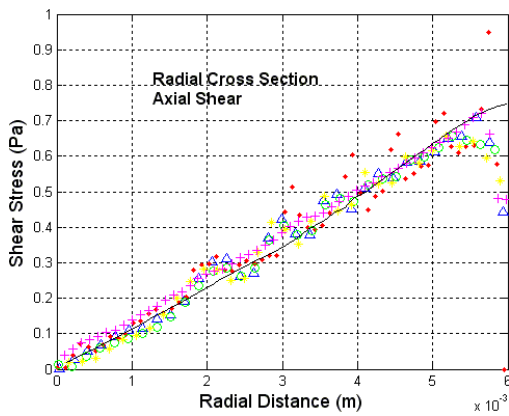


Figure 16.B. Axial shear stress, BSL, Re 3500, station -0.064m

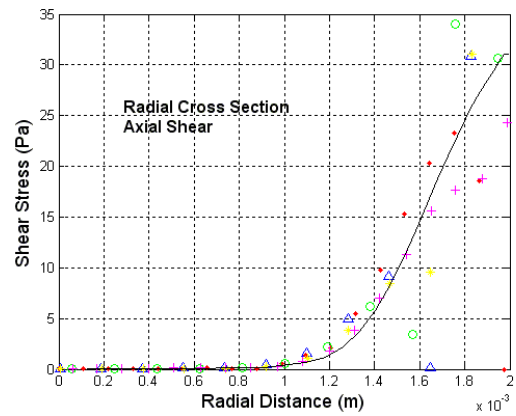


Figure 16.E. Axial shear stress, BSL, Re 3500, station -0.008m

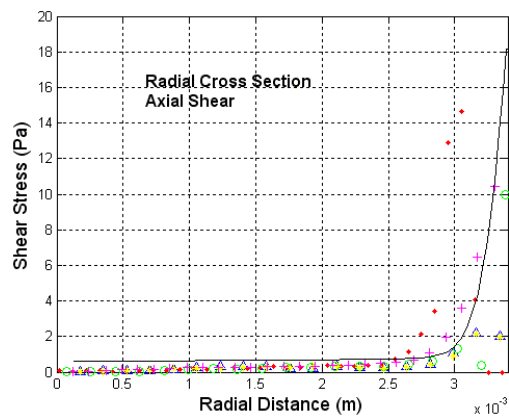


Figure 16.C. Axial shear stress, BSL, Re 3500, station -0.048m

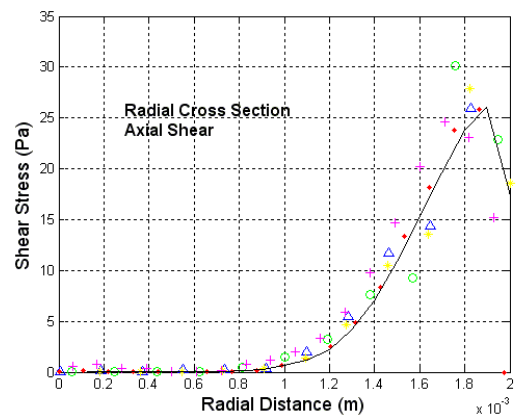


Figure 16.F. Axial shear stress, BSL, Re 3500, station 0.0m

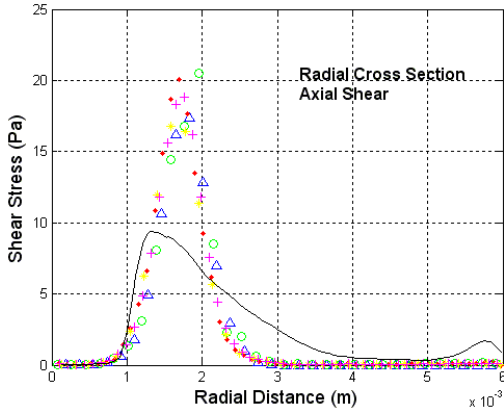


Figure 16.G. Axial shear stress, BSL, Re 3500, station 0.008m

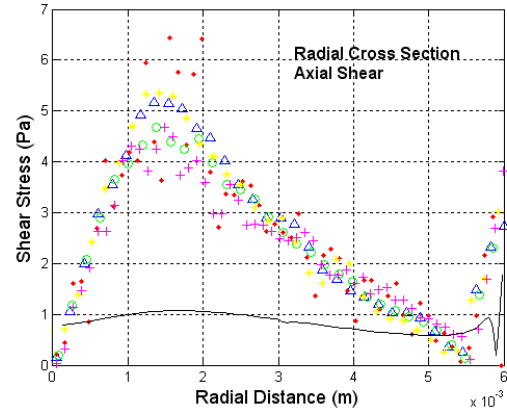


Figure 16.J. Axial shear stress, BSL, Re 3500, station 0.032m

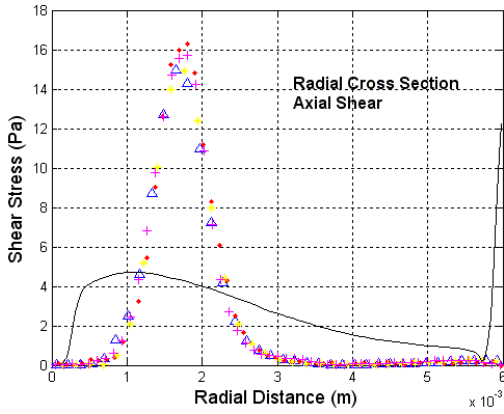


Figure 16.H. Axial shear stress, BSL, Re 3500, station 0.016m

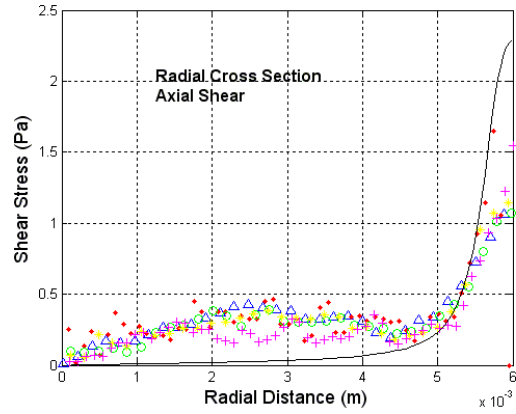


Figure 16.K. Axial shear stress, BSL, Re 3500, station 0.06m

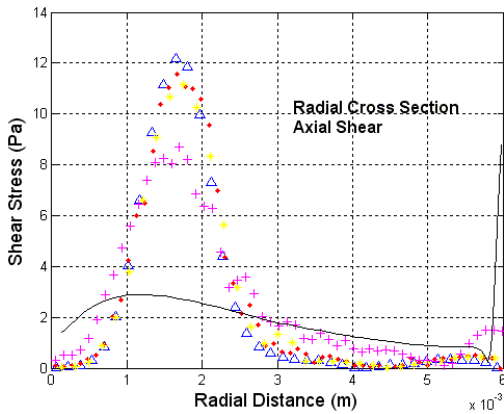


Figure 16.I. Axial shear stress, BSL, Re 3500, station 0.024m

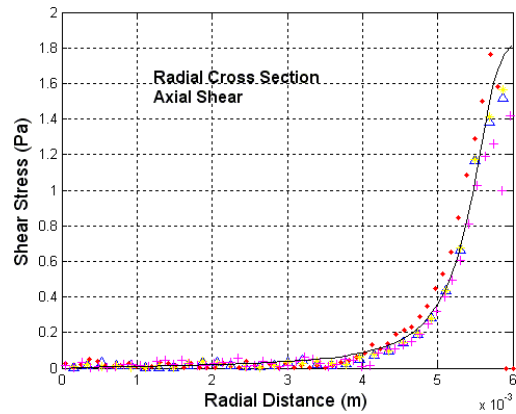


Figure 16.L. Axial shear stress, BSL, Re 3500, station 0.08m



Figure 16.M. Legend for figures 16.A-16.L

Figure 17 (17.A-17.L) shows the velocity profiles for the 3500 Reynolds SST case in 12 different axial locations. In these plots the velocity profile tracks the experimental data well up until sections after the sudden expansion.

Immediately after the sudden expansion (section 0.008m or figure 17.G), the simulation fails to follow the experimental data with the error of the experiment but the simulation starts track the data better than in the previous simulations. As seen at section 0.08m (figure 17.G) the simulation data tracks just under the experimental data until the $1.5e-3m$ radial distance; at this point the simulation starts to slightly over predict the flow profile until the $3.5e-3m$ radial distance at which it returns to slightly under predicting the velocity values. At this point the simulation trends the same as in the previous cases (under predicting the velocity maximum and gradients in figures 17.H-17.K) until the very end of the measured section.

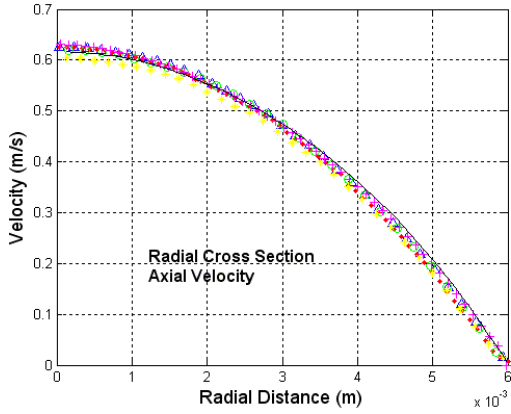


Figure 17.A. Axial velocity, SST Re 3500, station -0.088m

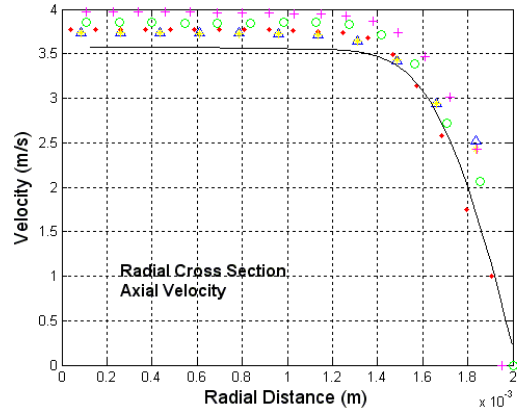


Figure 17.D. Axial velocity, SST Re 3500, station -0.02m

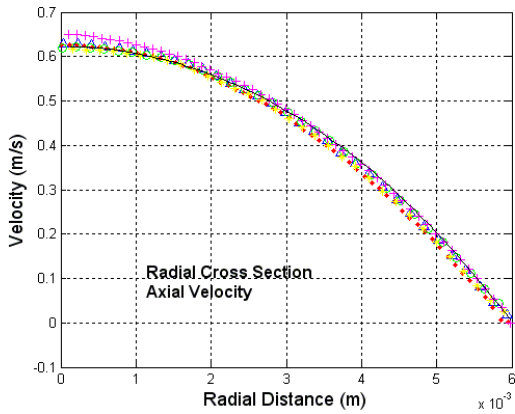


Figure 17.B. Axial velocity, SST Re 3500, station -0.064m

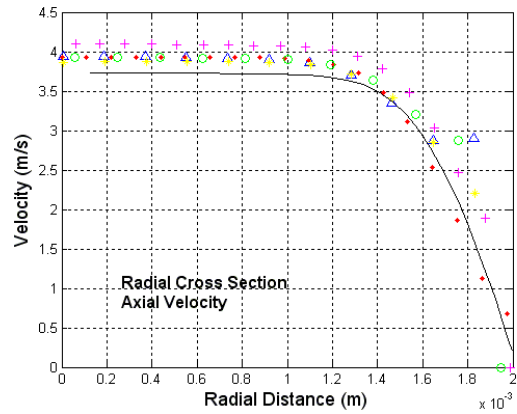


Figure 17.E. Axial velocity, SST Re 3500, station -0.008m

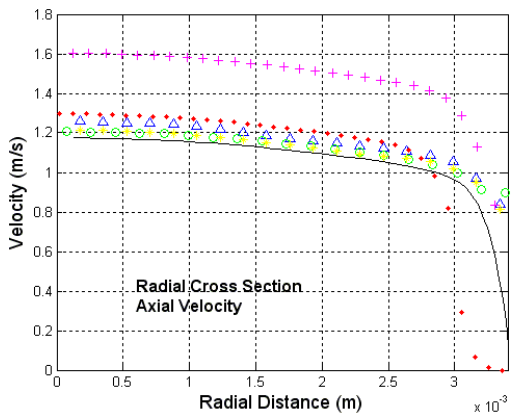


Figure 17.C. Axial velocity, SST Re 3500, station -0.048m

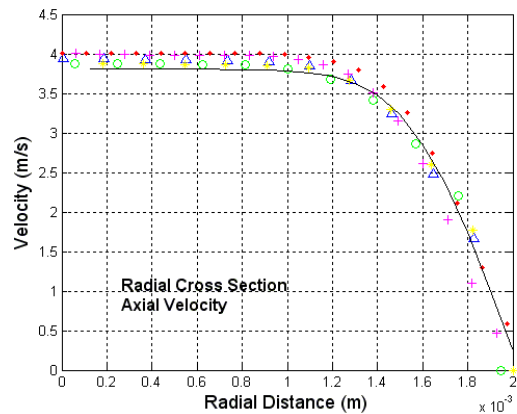


Figure 17.F. Axial velocity, SST Re 3500, station 0.0m

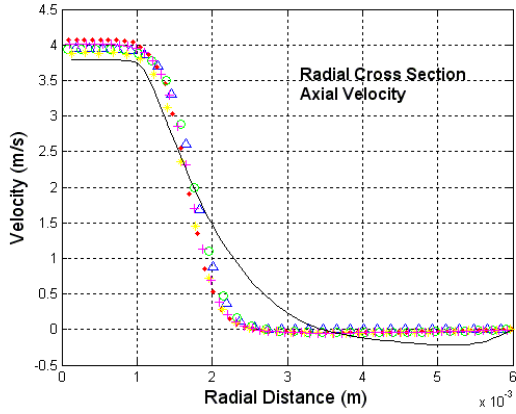


Figure 17.G. Axial velocity, SST Re 3500, station 0.008m

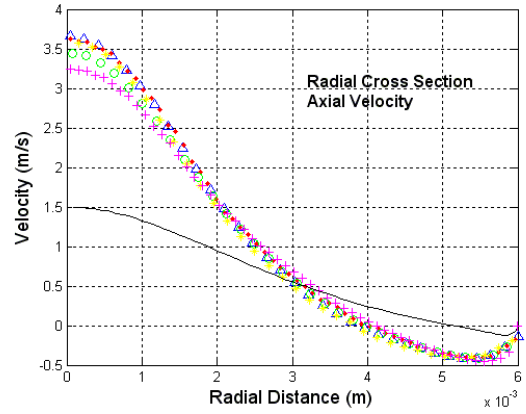


Figure 17.J. Axial velocity, SST Re 3500, station 0.032m

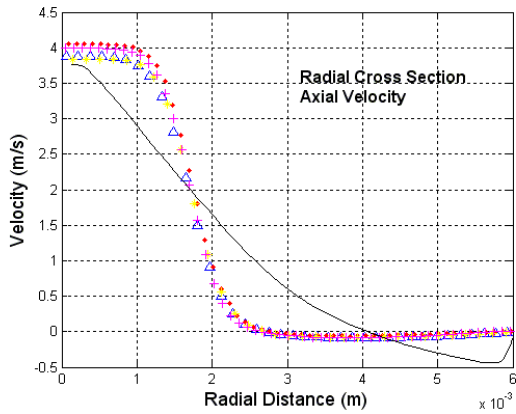


Figure 17.H. Axial velocity, SST Re 3500, station 0.016m

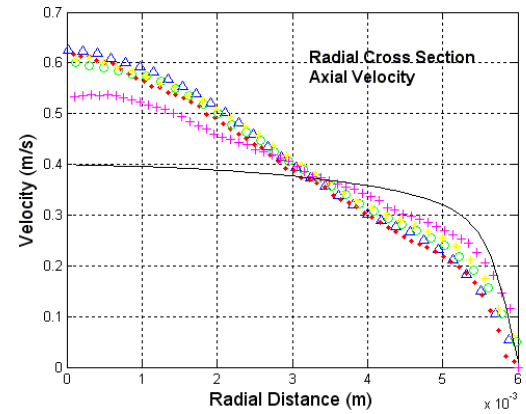


Figure 17.K. Axial velocity, SST Re 3500, station 0.06m

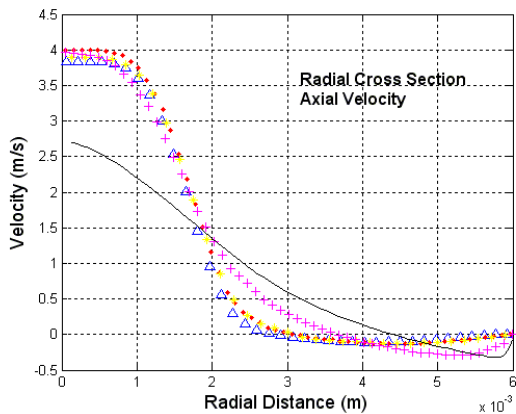


Figure 17.I. Axial velocity, SST Re 3500, station 0.024m

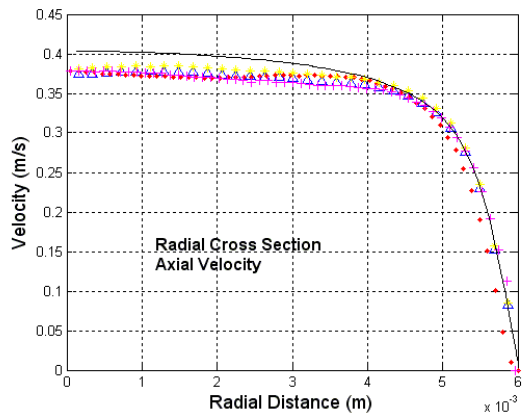


Figure 17.L. Axial velocity, SST Re 3500, station 0.08m



Figure 17.M. Legend for figures 17.A-17.L

Moving to the shear stress trends of the 3500 Reynolds SST simulation, figure 18 (18.A-18.L) displays the shear stress cross section along the converging/diverging section for 12 different axial locations.

The shear stress plots for the 3500 Reynolds SST simulation once again trends similar to results found in the 2000 Reynolds runs. At section 0.008m (figure 18.G) the simulated data under predicts the shear stress values along the cross section. Alignment of the experimental data and simulation data happens at the last cross section (section 0.08m or figure 18.L).

As noted in the 3500 Reynolds BSL solver run. The shear stress curve scalars start to align better to the simulation data than the previous transitional run does.

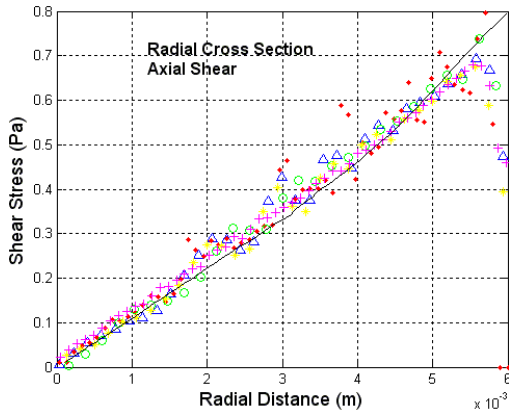


Figure 18.A. Axial shear stress, SST Re 3500, station -0.088m

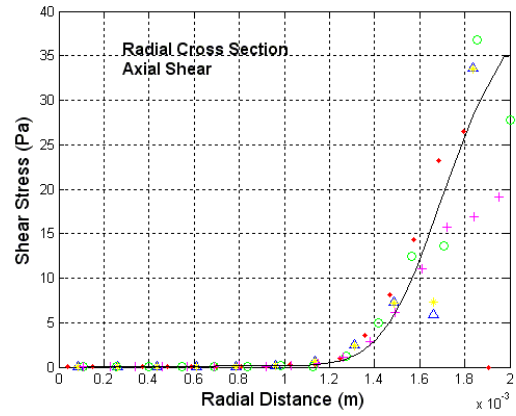


Figure 18.D. Axial shear stress, SST Re 3500, station -0.02m

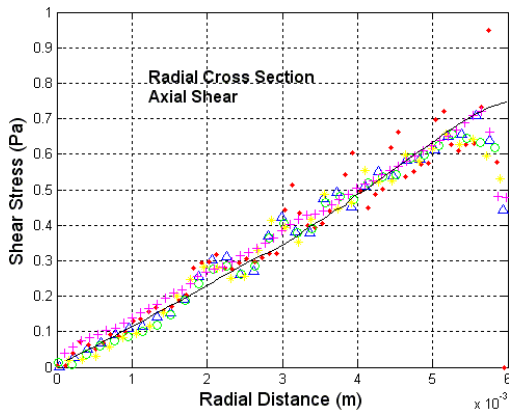


Figure 18.B. Axial shear stress, SST Re 3500, station -0.064m

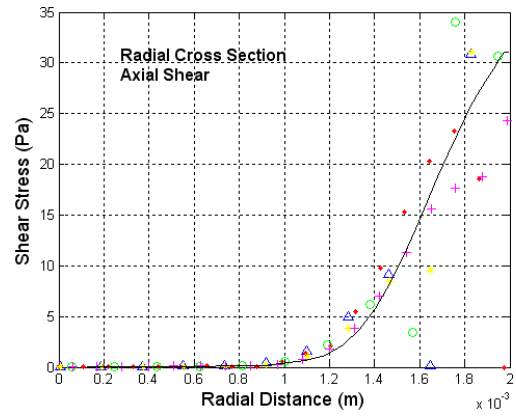


Figure 18.E. Axial shear stress, SST Re 3500, station -0.008m

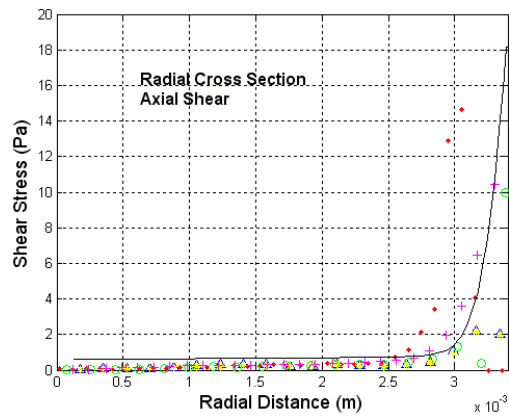


Figure 18.C. Axial shear stress, SST Re 3500, station -0.048m

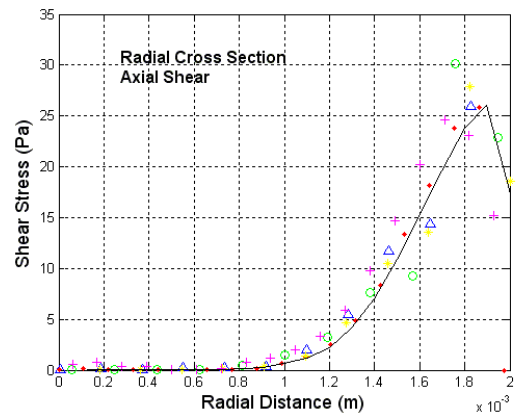


Figure 18.F. Axial shear stress, SST Re 3500, station 0.0m

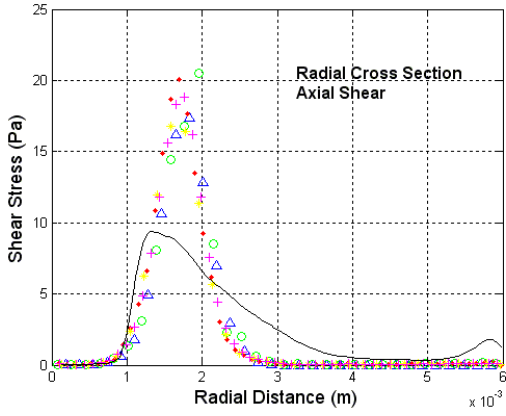


Figure 18.G. Axial shear stress, SST
Re 3500, station 0.008m

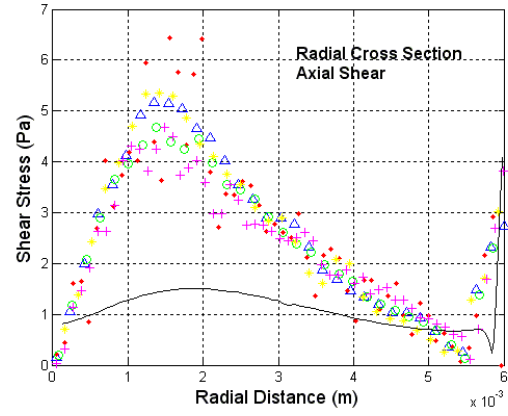


Figure 18.J. Axial shear stress, SST
Re 3500, station 0.032m

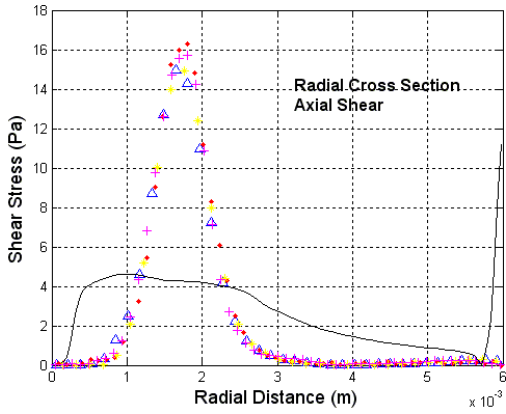


Figure 18.H. Axial shear stress, SST
Re 3500, station 0.016m

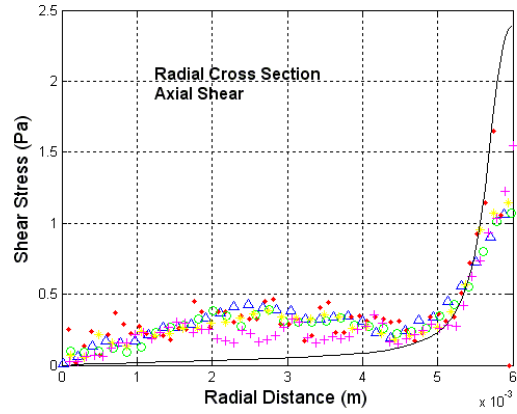


Figure 18.K. Axial shear stress, SST
Re 3500, station 0.06m

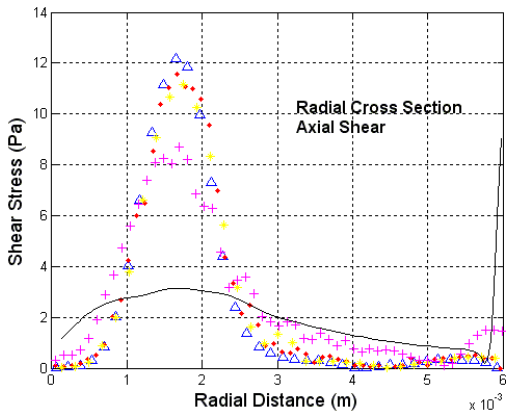


Figure 18.I. Axial shear stress, SST
Re 3500, station 0.024m

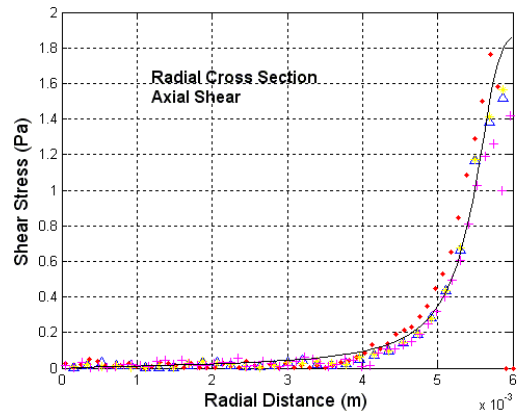


Figure 18.L. Axial shear stress, SST
Re 3500, station 0.08m



Figure 18.M. Legend for figures 18.A-18.L

Figure 19 (19.A-19.L) shows the velocity profiles for the 5000 Reynolds BSL simulation at 12 different axial locations. As can be seen in section -0.088m through 0.0m (figures 19.A-19.F), good alignment to the experimental data was attained. In two of these cross sections the analysis data was within the experimental data. For the rest of the cross section (figures 19.C-19.F) the simulation results, though under predicted, only had an averaged offset of $\sim 0.2\text{m/s}$. After the sudden expansion the velocity profiles also seem to align with the experimental data better than seen in any of the 2000 or 3500 Reynolds cases discussed before; section 0.008m through 0.08m (figures 19.G-19.L) show that the simulation results only under predict the experimental data but by much smaller margins than in prior cases. These plots also exhibit velocity gradients that start to align with the experimental data. The highest discrepancy shows up in section 0.032m. In this section the maximum value of the velocity profile is underestimated by $\sim 1.8\text{m/s}$ in reference to an averaged maximum flow of 3.5m/s .

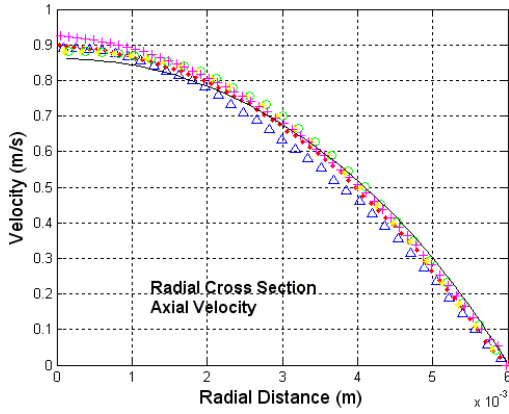


Figure 19.A. Axial velocity, BSL, Re 5000, station -0.088m

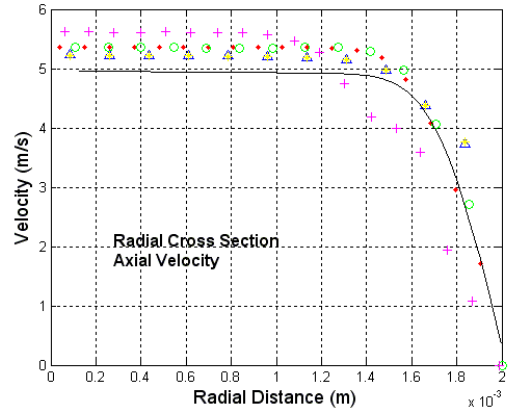


Figure 19.D. Axial velocity, BSL, Re 5000, station -0.02m

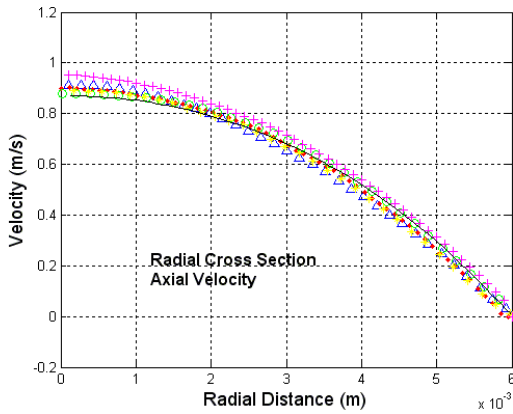


Figure 19.B. Axial velocity, BSL, Re 5000, station -0.064m

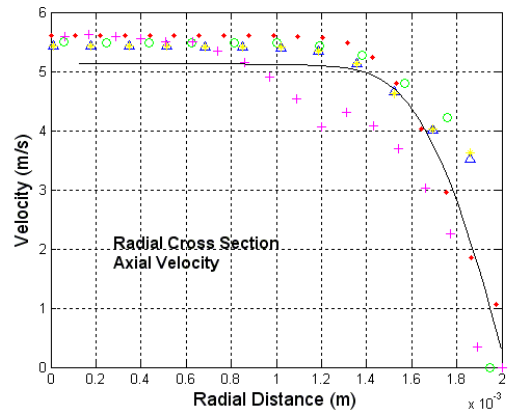


Figure 19.E. Axial velocity, BSL, Re 5000, station -0.008m

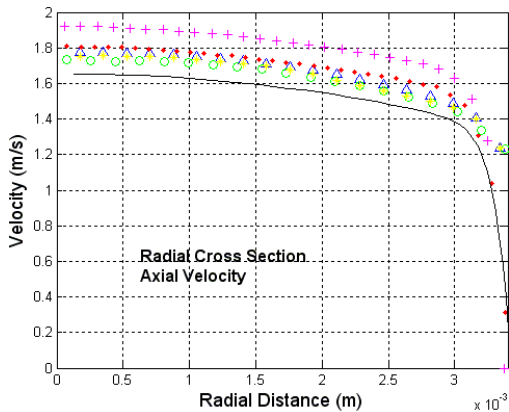


Figure 19.C. Axial velocity, BSL, Re 5000, station -0.048m

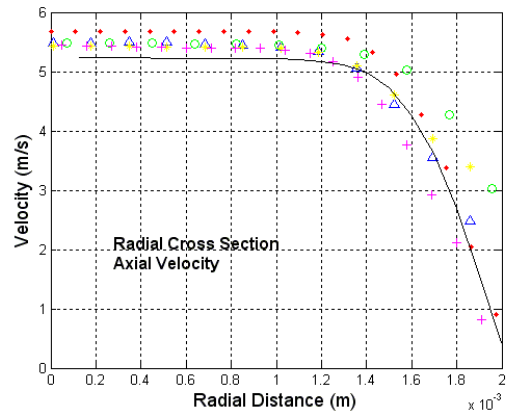


Figure 19.F. Axial velocity, BSL, Re 5000, station 0.0m

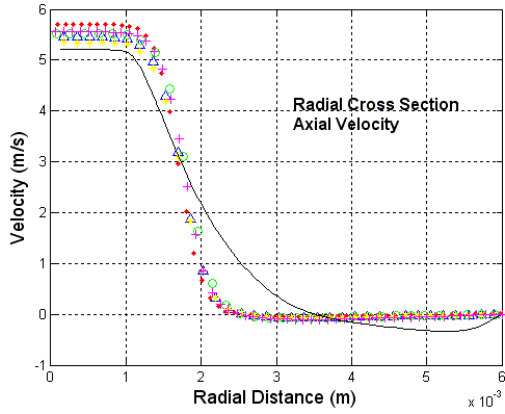


Figure 19.G. Axial velocity, BSL, Re 5000, station 0.008m

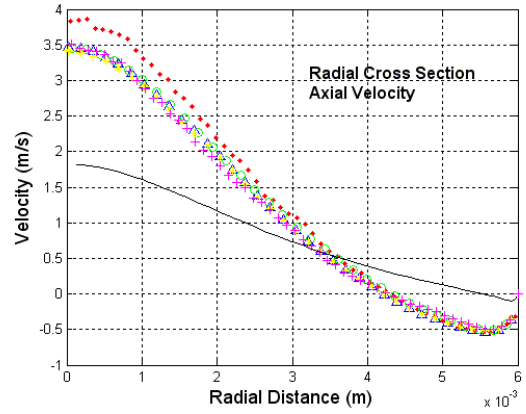


Figure 19.J. Axial velocity, BSL, Re 5000, station 0.032m

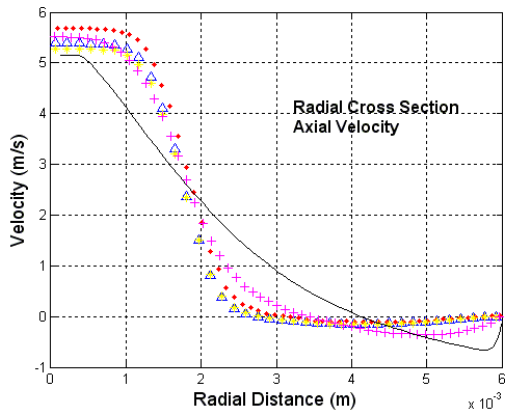


Figure 19.H. Axial velocity, BSL, Re 5000, station 0.016m

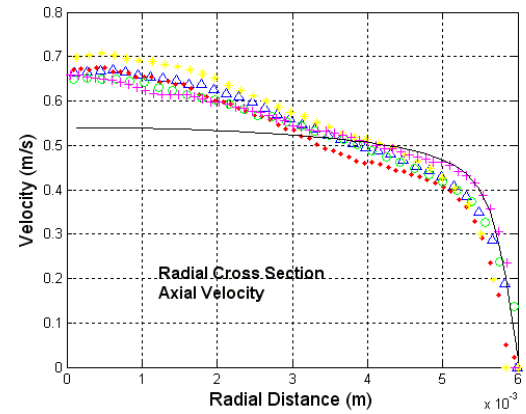


Figure 19.K. Axial velocity, BSL, Re 5000, station 0.06m

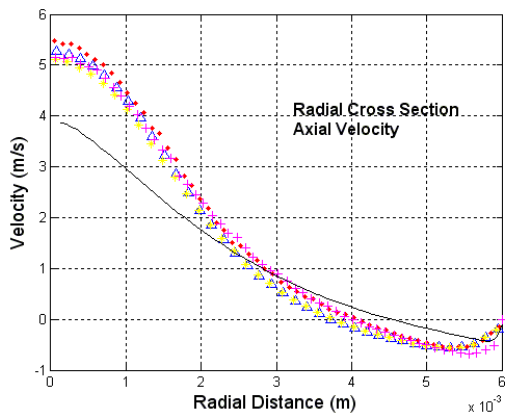


Figure 19.I. Axial velocity, BSL, Re 5000, station 0.024m

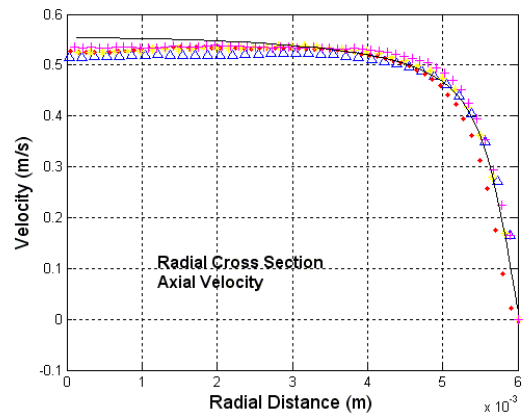


Figure 19.L. Axial velocity, BSL, Re 5000, station 0.08m



Figure 19.M. Legend for figures 19.A-19.L

Showing the shear stress cross section for the 5000 Reynolds BSL plots, figure 20 (20.A-20.L) shows the cross sections for this case at 12 different axial locations. As noted in the figure 19, the entrance profiles had good alignment comparing the experimental data to the simulation data. The same is noted for the shear stress cross section. One of the more noticeable characteristics at the start of these plots is the diverging shear stress towards the wall at the start of the converging/diverging area. Figure 20.A and 20.B show that the shear stress aligns well with the experimental data but once again there is a trend to not capture the decaying shear stress towards the wall of the tub. Since this trend is not present towards the middle and end sections of the converging/diverging section, it is believed that this discrepancy is due to the boundary wall node distribution in the entrance length section of the simulation. It is believed that since the entrance length section has a much coarser wall boundary inflation layer, it is not giving the analysis enough length to develop the correct shear stress distribution in time for the converging/diverging measurements section.

Past this entrance wall shear stress discrepancy we also see the singularity at the expansion of the tube show up (section 0.0m or figure 20.F) and the discrepancy of the data in the middle of the expanded section (sections 0.008m through 0.32m). The exception with the 5000 Reynolds case from the previous cases is section 0.06m (figure 20.J). In the 5000 Reynolds case simulation using the BSL solver, this section now aligns with the data within the experimental error of the experimental data. This trend in the data seeming to align better and better with higher Reynolds numbers would suggest that the BSL solver is better suited for flows of higher Reynolds numbers and has troubles with the transitional range of flow profiles.

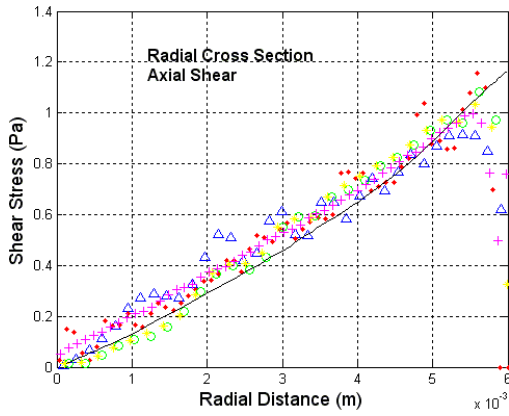


Figure 20.A. Axial shear stress, BSL, Re 5000, station -0.088m

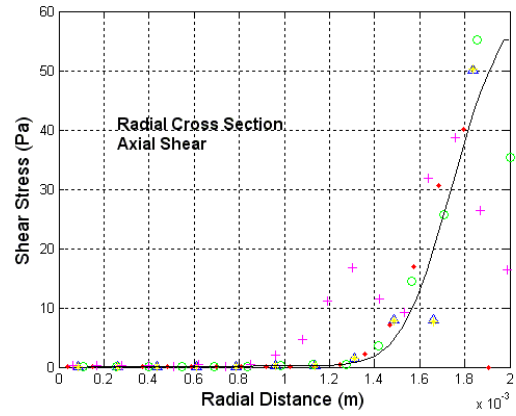


Figure 20.D. Axial shear stress, BSL, Re 5000, station -0.02m

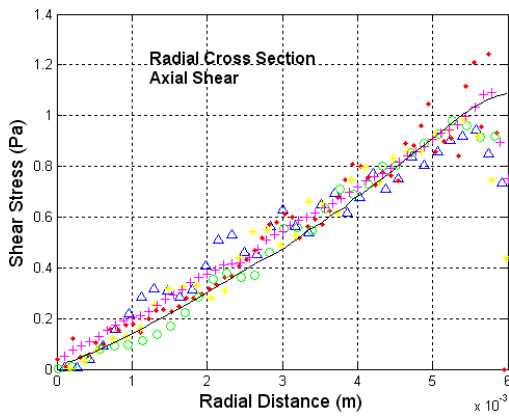


Figure 20.B. Axial shear stress, BSL, Re 5000, station -0.064m

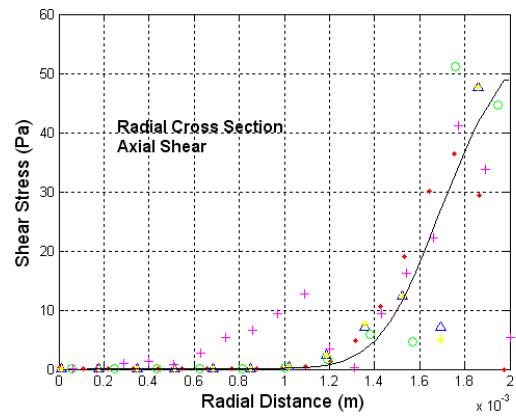


Figure 20.E. Axial shear stress, BSL, Re 5000, station -0.008m

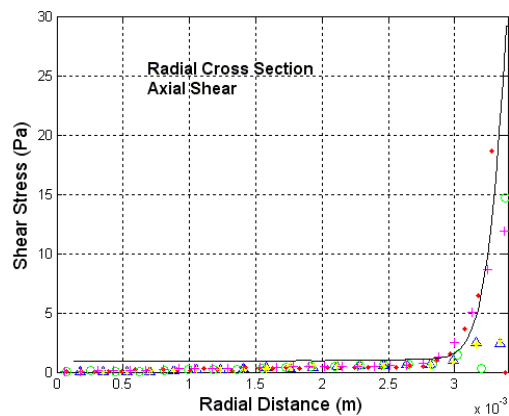


Figure 20.C. Axial shear stress, BSL, Re 5000, station -0.048m

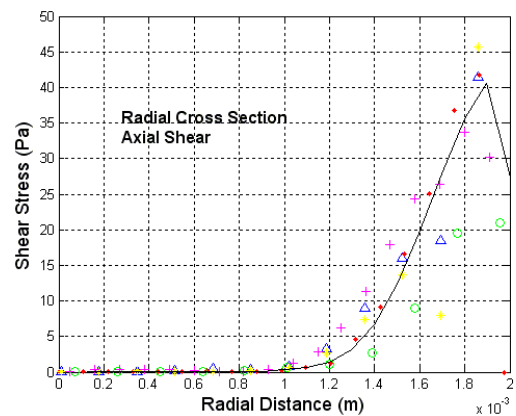


Figure 20.F. Axial shear stress, BSL, Re 5000, station 0.0m

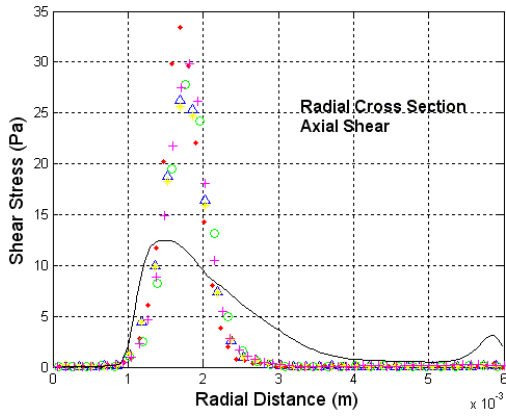


Figure 20.G. Axial shear stress, BSL, Re 5000, station 0.008m

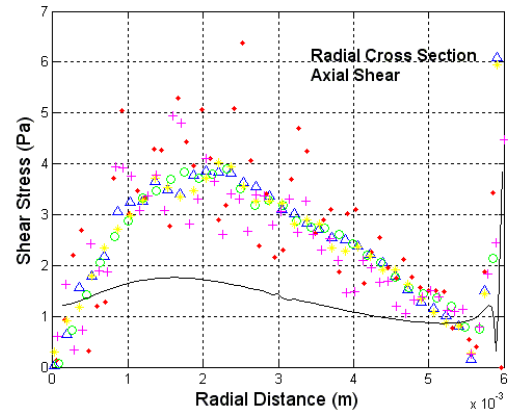


Figure 20.J. Axial shear stress, BSL, Re 5000, station 0.032m

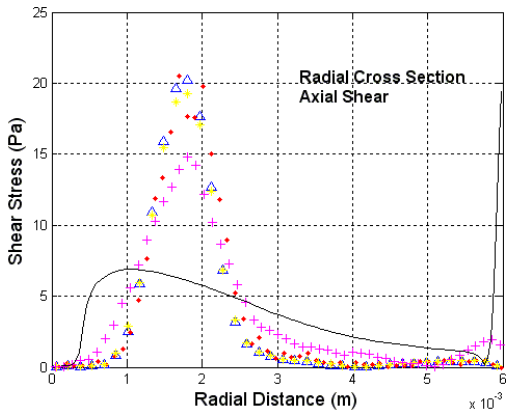


Figure 20.H. Axial shear stress, BSL, Re 5000, station 0.016m

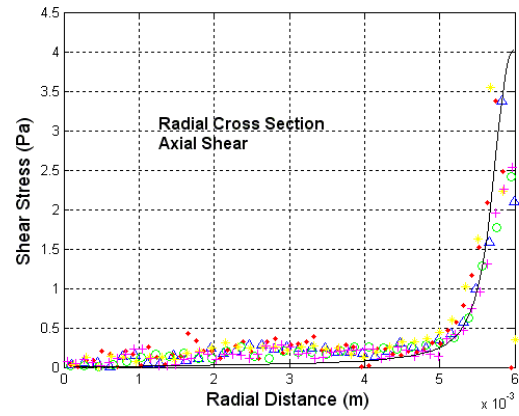


Figure 20.K. Axial shear stress, BSL, Re 5000, station 0.06m

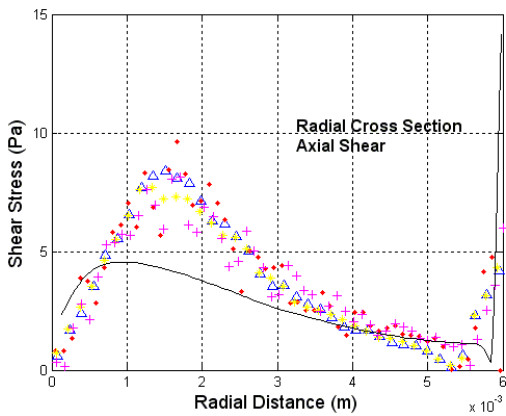


Figure 20.I. Axial shear stress, BSL, Re 5000, station 0.024m

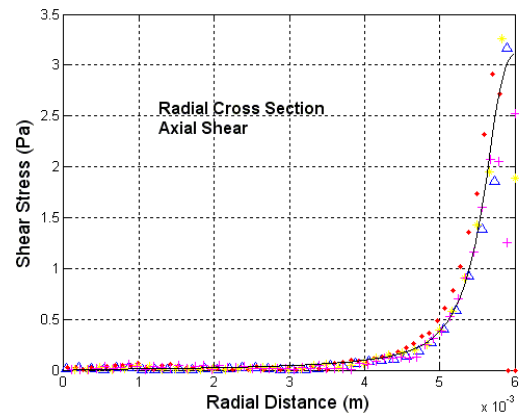


Figure 20.L. Axial shear stress, BSL, Re 5000, station 0.08m



Figure 20.M. Legend for figures 21.A-21.L

Moving to the 5000 Reynolds SST cases, figure 21 (21.A-21.L) shows the velocity profiles for the 12 different cross sections of the converging/diverging section of the modeled geometry. Once again we see very good alignment to the experimental data from sections -0.088m and -0.064m. From these section the simulation data maintains good alignment with the experimental data. This can be seen in section -0.048m through 0.0m (figures 21.C-21.F) as the velocity profiles underestimate the experimental data by $\sim 0.1\text{m/s}$ for the majority of the radial section.

Good alignment of the simulation data to the experimental data is even maintained in section 0.008m (figure 21.G). In figure 21.G it is noticeable that the velocity profile gradient is starting to align with the experimental data better than in the previous BSL and SST solution transitional and turbulent cases.

The alignment of the data is even maintained to a good fit through sections 0.016m through 0.06m (figures 21.H-21.K). In these sections the highest discrepancy is shown in section 0.032m (figure 21.J); here the maximum velocity is only underestimated by $\sim 1\text{m/s}$ in reference to a maximum velocity of 3.5 for the experimental data. Comparing this to the same section in the 5000 Reynolds number for the BSL solution, the SST case trends to align better to predicting lower Reynolds turbulent cases. In this particular case for this section of the geometry the SST solution yielded results $\sim 32\%$ better for maximum velocity perdition.

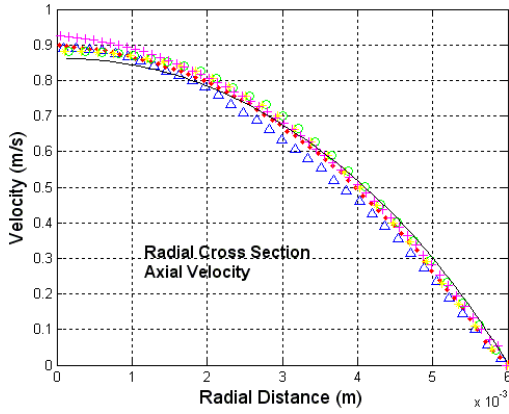


Figure 21.A. Axial velocity, SST, Re 5000, station -0.088m

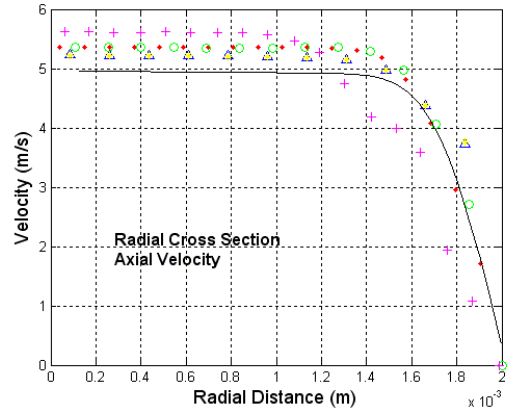


Figure 21.D. Axial velocity, SST, Re 5000, station -0.02m

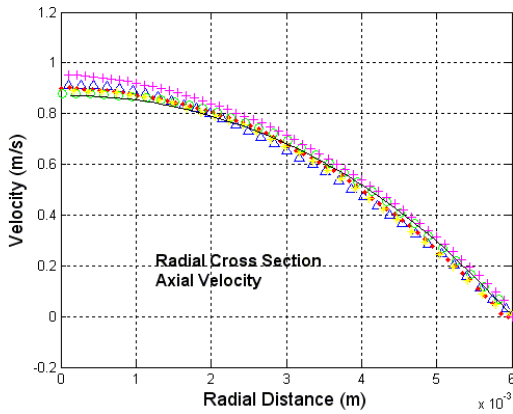


Figure 21.B. Axial velocity, SST, Re 5000, station -0.064m

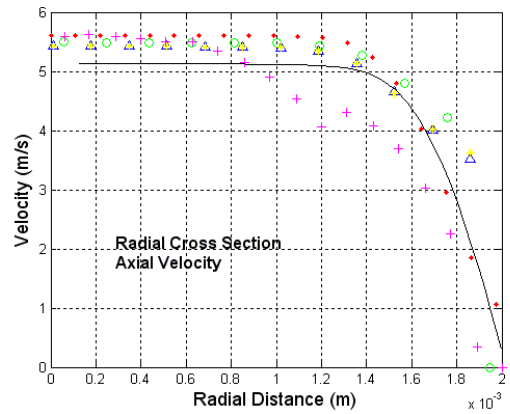


Figure 21.E. Axial velocity, SST, Re 5000, station -0.008m

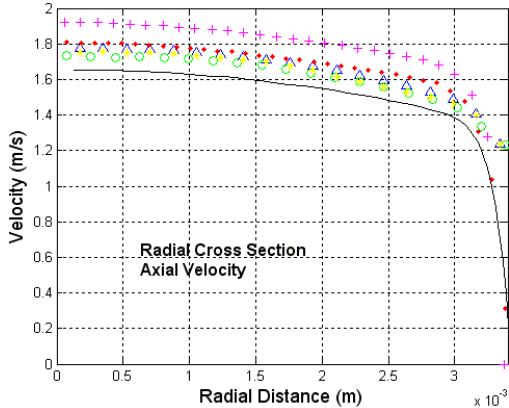


Figure 21.C. Axial velocity, SST, Re 5000, station -0.048m

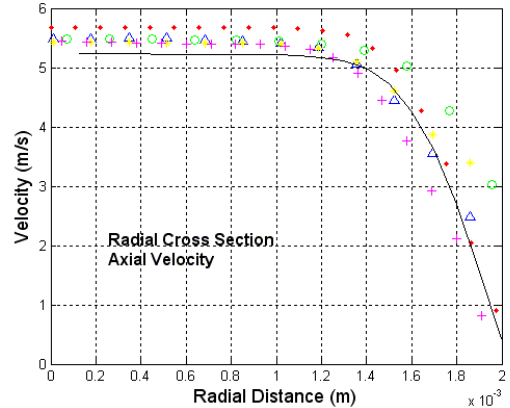


Figure 21.F. Axial velocity, SST, Re 5000, station 0.0m

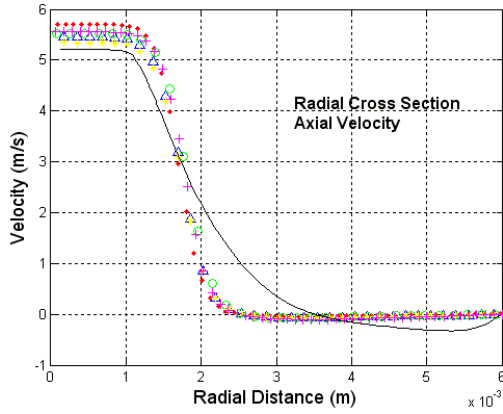


Figure 21.G. Axial velocity, SST, Re 5000, station 0.008m

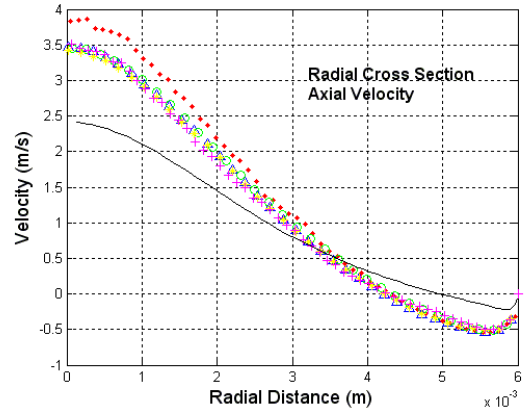


Figure 21.J. Axial velocity, SST, Re 5000, station 0.032m

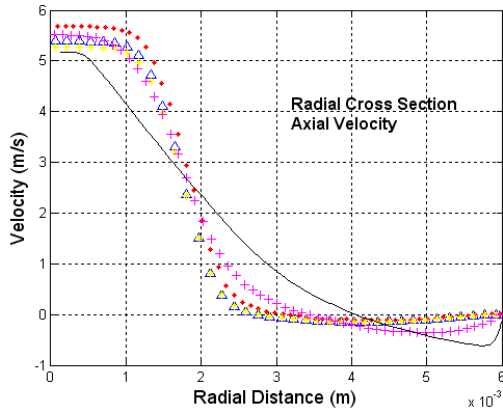


Figure 21.H. Axial velocity, SST, Re 5000, station 0.016m

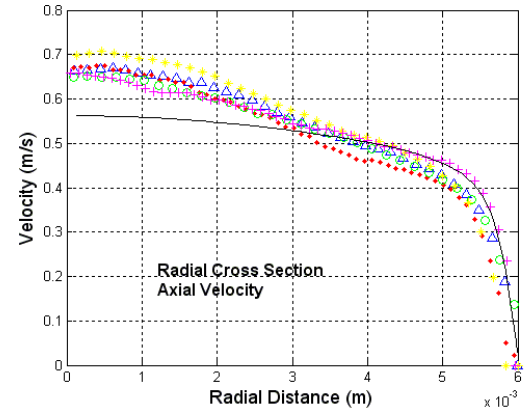


Figure 21.K. Axial velocity, SST, Re 5000, station 0.06m

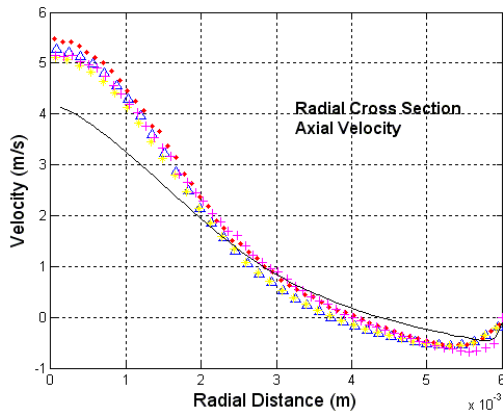


Figure 21.I. Axial velocity, SST, Re 5000, station 0.024m

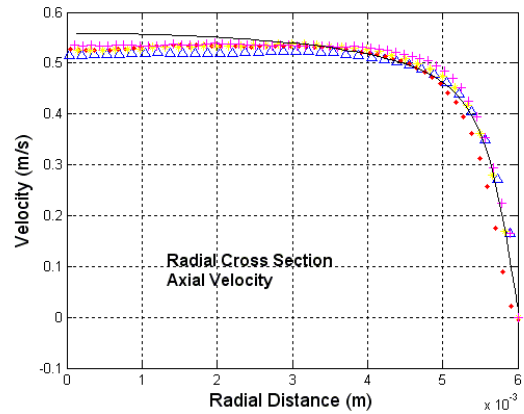


Figure 21.L. Axial velocity, SST, Re 5000, station 0.08m



Figure 21.M. Legend for figures 21.A-21.L

Figure 22 (22.A-22.L) shows the shear stress profiles of the 12 different cross sections for the 5000 Reynolds SST case.

As shown in figure 21, the alignment to the experimental data is trending to converge better to the experimental data. This can be seen through the entrance and converging section of this geometry (sections -0.088 through 0.0m or figures 22.A-22.F). This is also shown at the exit section of the converging/diverging section (sections 0.06m through 0.08m or figures 22.K-22.L) as high alignment of the experimental data is achieved with the simulation.

The four middle sections (sections 0.008m through 0.032m or figures 22.G-22.J) still persist to diverge from the experimental data. It is, however, seen that better alignment is achieved in section 0.032 (figure 22.J) than has been seen before as there is only about a 1Pa difference in the maximum at around the center of the section.

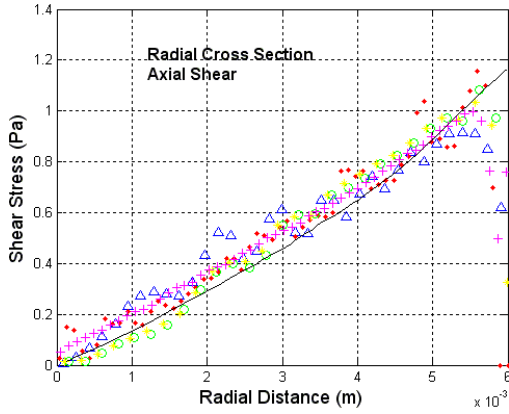


Figure 22.A. Axial shear stress, SST, Re 5000, station -0.088m

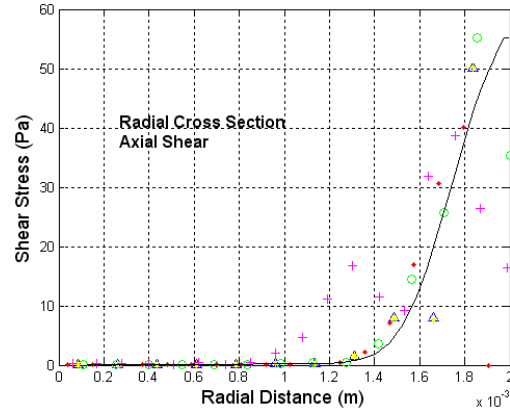


Figure 22.D. Axial shear stress, SST, Re 5000, station -0.02m

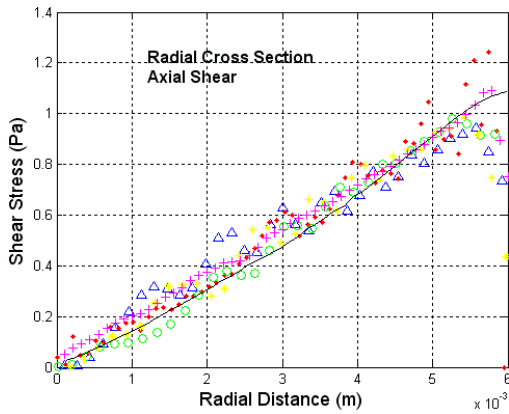


Figure 22.B. Axial shear stress, SST, Re 5000, station -0.064m

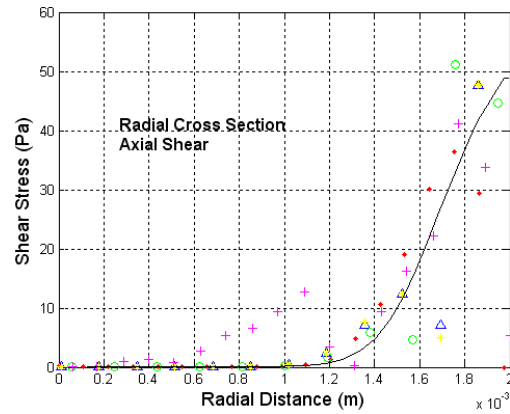


Figure 22.E. Axial shear stress, SST, Re 5000, station -0.008m

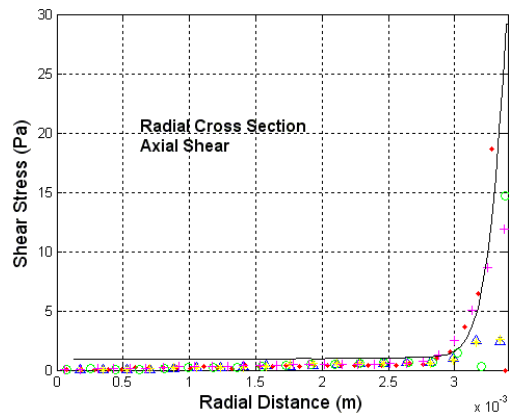


Figure 22.C. Axial shear stress, SST, Re 5000, station -0.048m

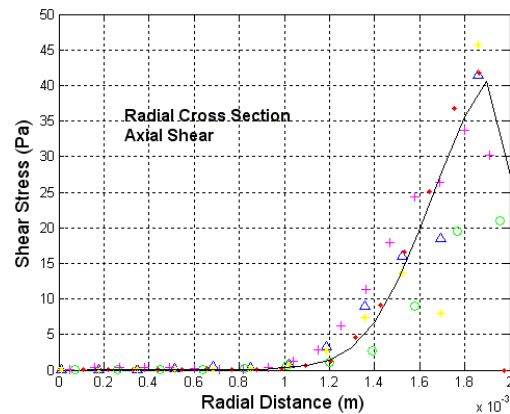


Figure 22.F. Axial shear stress, SST, Re 5000, station 0.0m

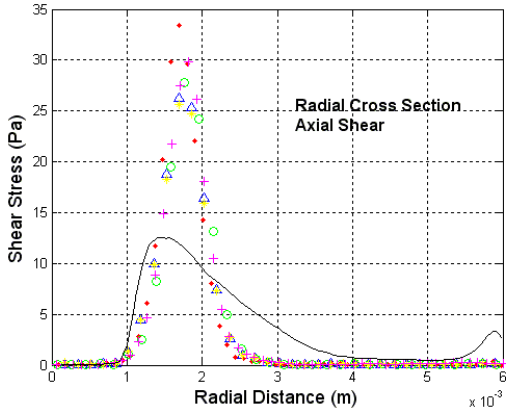


Figure 22.G. Axial shear stress, SST, Re 5000, station 0.008m

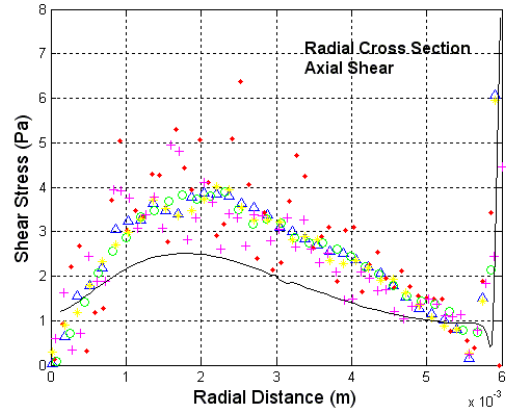


Figure 22.J. Axial shear stress, SST, Re 5000, station 0.32m

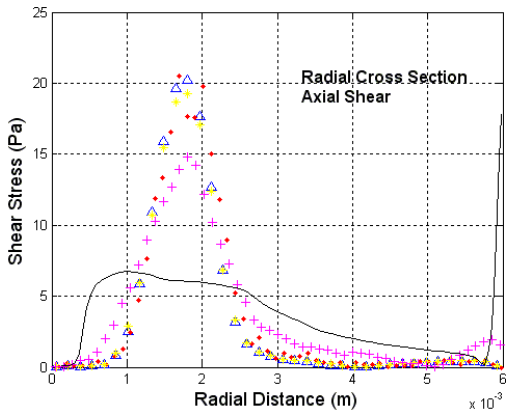


Figure 22.H. Axial shear stress, SST, Re 5000, station 0.016m

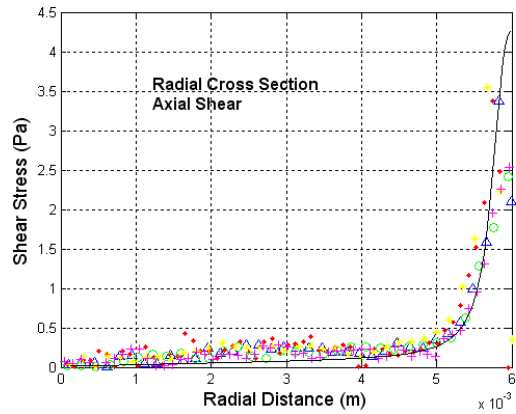


Figure 22.K. Axial shear stress, SST, Re 5000, station 0.06m

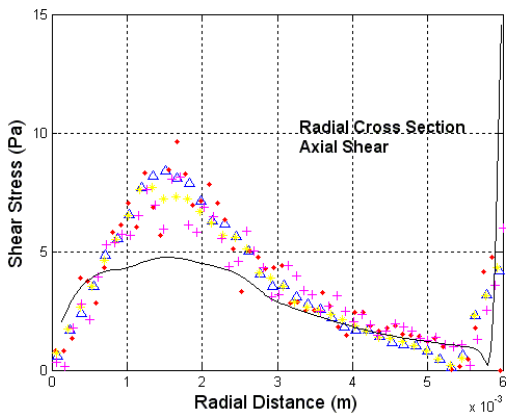


Figure 22.I. Axial shear stress, SST, Re 5000, station 0.024m

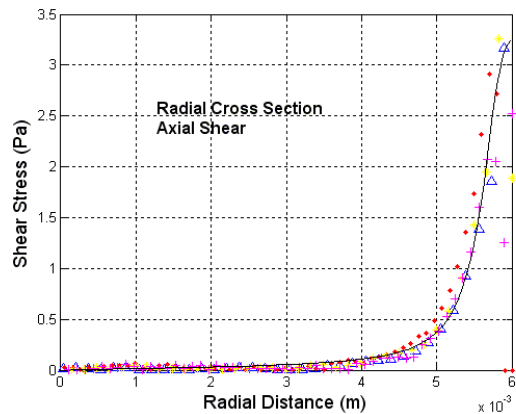


Figure 22.L. Axial shear stress, SST, Re 5000, station 0.08m



Figure 22.M. Legend for figures 22.A-22.L

Aligning better than any of the BSL results discussed yet, figure 23 (23.A-23.L) shows the 12 different axial velocity cross sections of the 6500 Reynolds BSL solution. As seen in section -0.088m through section 0.0m (figures 23.A-23.F) the simulation data falls within the error of the experimental data set.

Though not within the error of the experimental data, the section post of the sudden expansion also align better than any of the previous BSL solution sets. This can be seen in sections 0.008m through 0.08m (figures 23.G-23.L). Starting from very last sections, section 0.08m (figure 23.L) falls within the error of the experimental data and section 0.06m (figure 23.K) is just short of falling within the error of the experimental data. The sections in-between the sudden expansion (section 0.0m or figure 23.F) and the end sections (sections 0.06m & 0.08m or figures 23.K & 23.L) follow alignment that is very close to the error metric of the experimental data. The final comparison to note is section 0.032m (figure 23.J). This section also shows that the 6500 BSL velocity profiles are the best set of BSL solution sets. This section shows a maximum flow velocity difference of $\sim 1.7\text{m/s}$. This is in comparison to values $>2\text{m/s}$ in previous plots.

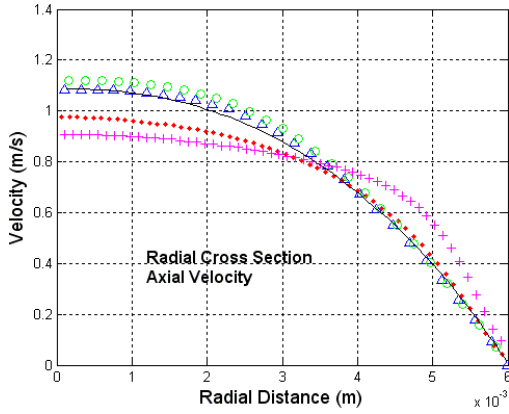


Figure 23.A. Axial velocity, BSL, Re 6500, station -0.088m

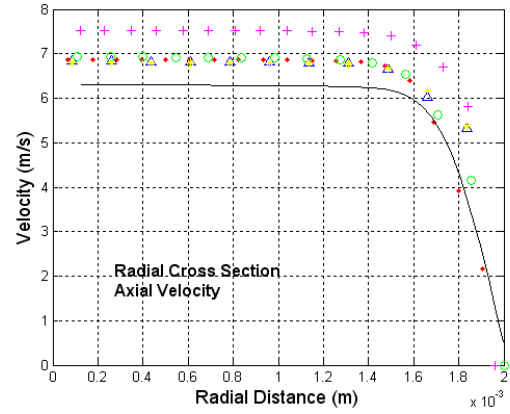


Figure 23.D. Axial velocity, BSL, Re 6500, station -0.02m

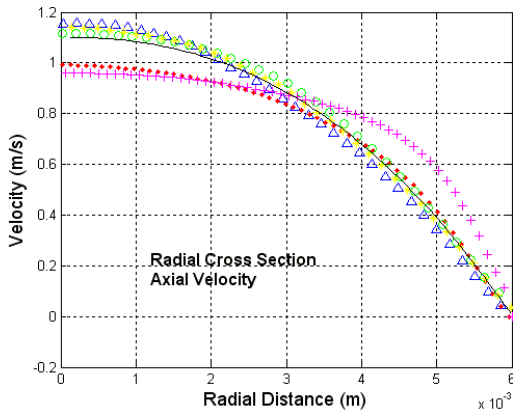


Figure 23.B. Axial velocity, BSL, Re 6500, station -0.064m

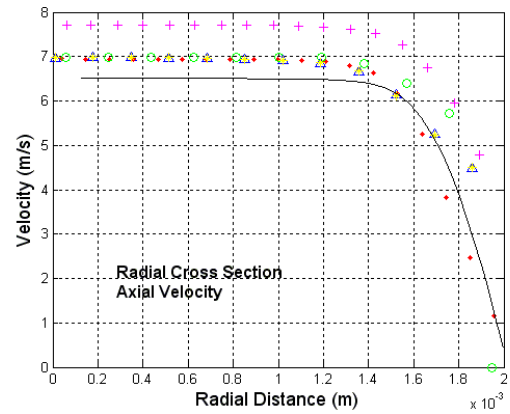


Figure 23.E. Axial velocity, BSL, Re 6500, station -0.008m

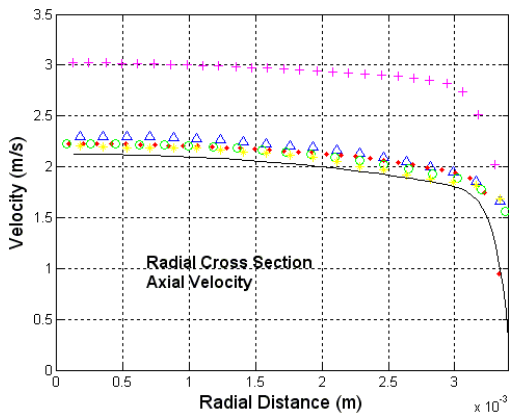


Figure 23.C. Axial velocity, BSL, Re 6500, station -0.048m

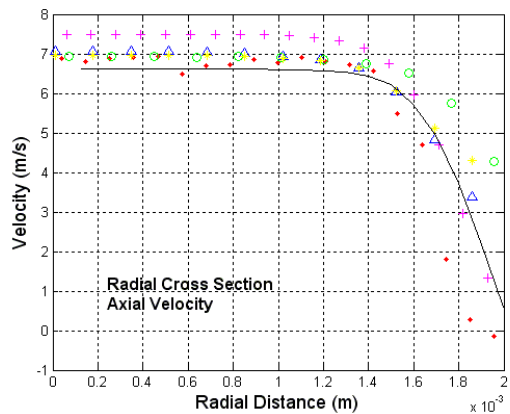


Figure 23.F. Axial velocity, BSL, Re 6500, station 0.0m

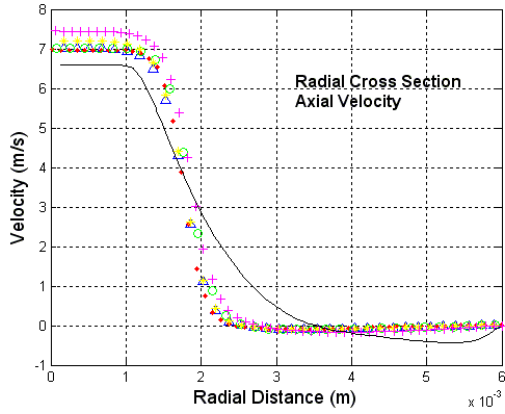


Figure 23.G. Axial velocity, BSL, Re 6500, station 0.008m

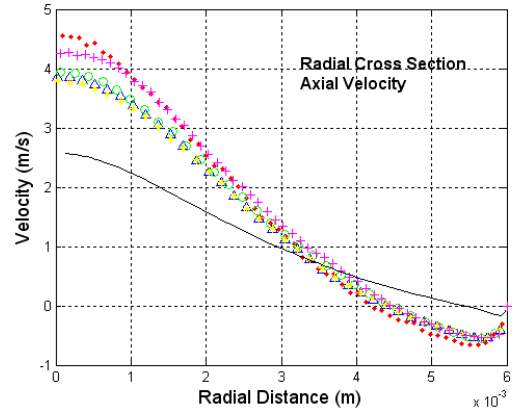


Figure 23.J. Axial velocity, BSL, Re 6500, station 0.032m

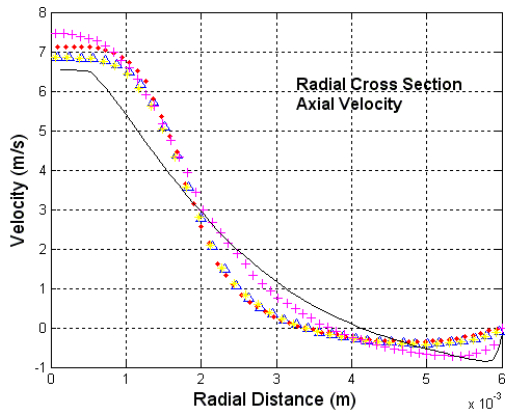


Figure 23.H. Axial velocity, BSL, Re 6500, station 0.016m

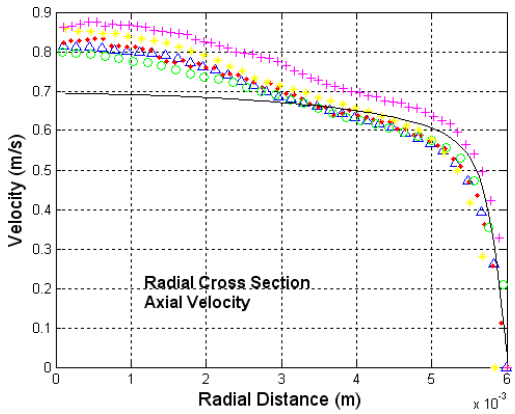


Figure 23.K. Axial velocity, BSL, Re 6500, station 0.06m

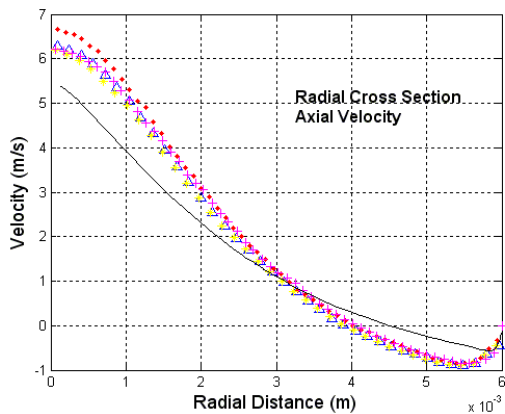


Figure 23.I. Axial velocity, BSL, Re 6500, station 0.024m

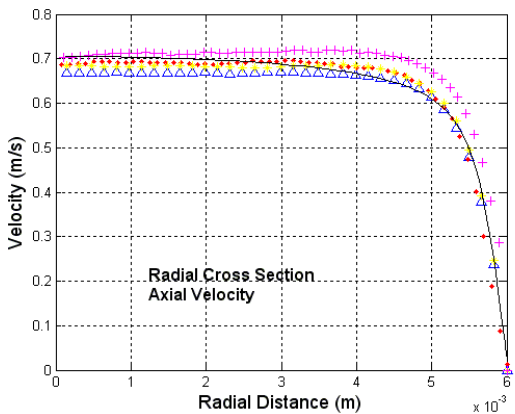


Figure 23.L. Axial velocity, BSL, Re 6500, station 0.08m



Figure 23.M. Legend for figures 23.A-23.L

Figure 24 (24.A-24.L) shows the shear stress cross sections for the 6500 Reynolds BSL solution at the 12 different cross sections. The data in this figure set also aligns with the results discussed in figure set 23. As can be seen from the entrance to the expansion sections (sections -0.088m through 0.0m or figures 24.A-24.F) high alignment of the simulation data is achieved to the experimental data; for most plots falling within the error of the experimental data.

As discussed in figure set 23, the greatest divergence to the experimental data exists within sections 0.008m through 0.032m (figures 24.G-24.J). The simulation data in these sections also back the results of its velocity profiles. The one noticeable distinction with these plots is the greater profile alignment to the experimental shear stress values. In sections 0.008m through 0.032m (figures 24.G-24.J) it can be seen that though the scaling may be off to some extent, the profile of the simulation data represents the experimental data well.

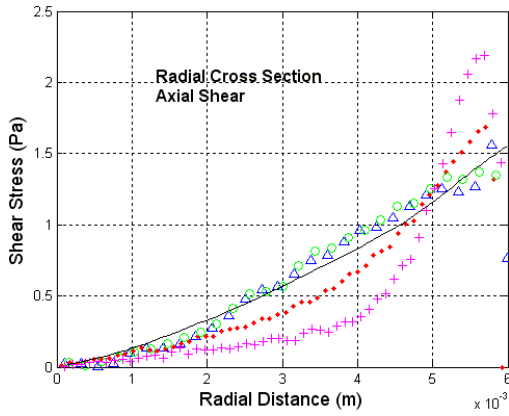


Figure 24.A. Axial shear stress, BSL, Re 6500, station -0.088m

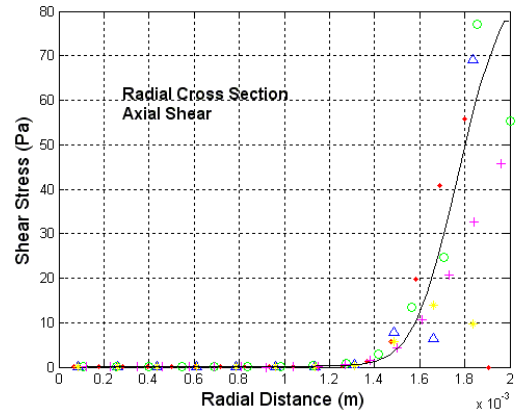


Figure 24.D. Axial shear stress, BSL, Re 6500, station -0.02m

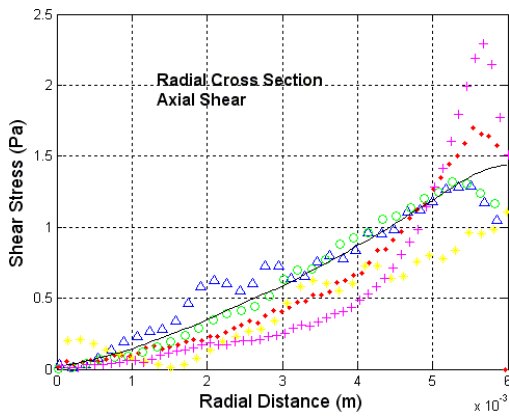


Figure 24.B. Axial shear stress, BSL, Re 6500, station -0.064m

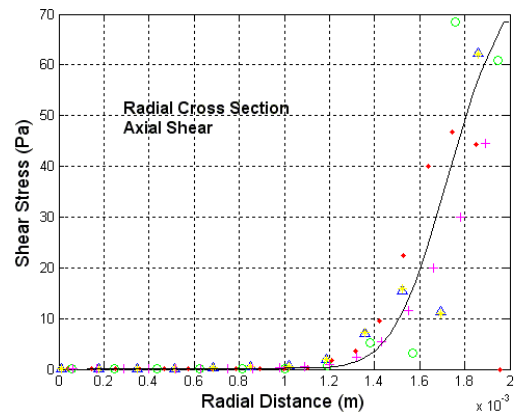


Figure 24.E. Axial shear stress, BSL, Re 6500, station -0.008m

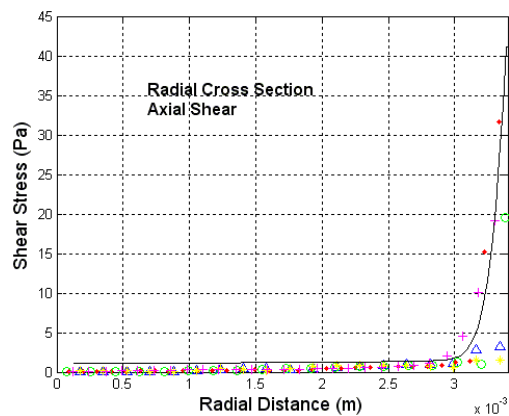


Figure 24.C. Axial shear stress, BSL, Re 6500, station -0.048m

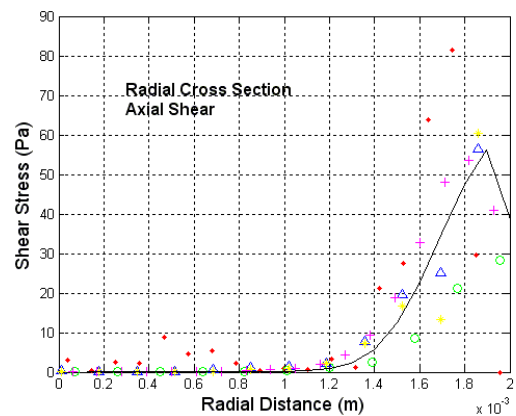


Figure 24.F. Axial shear stress, BSL, Re 6500, station 0.0m

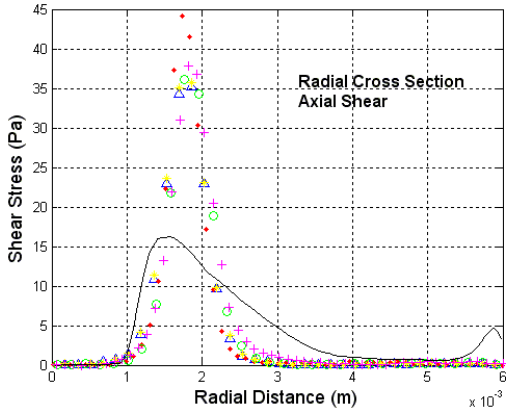


Figure 24.G. Axial shear stress, BSL, Re 6500, station 0.008m

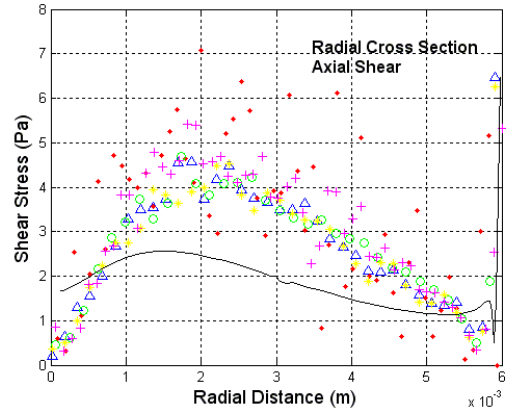


Figure 24.J. Axial shear stress, BSL, Re 6500, station 0.032m

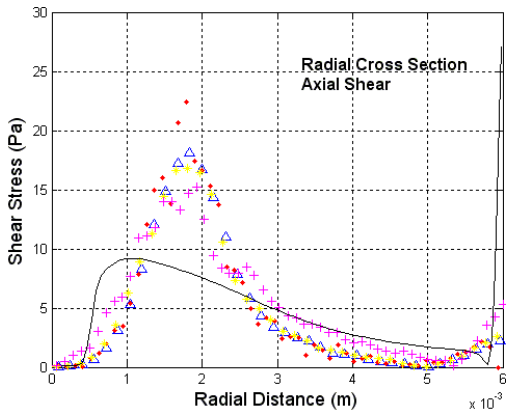


Figure 24.H. Axial shear stress, BSL, Re 6500, station 0.016m

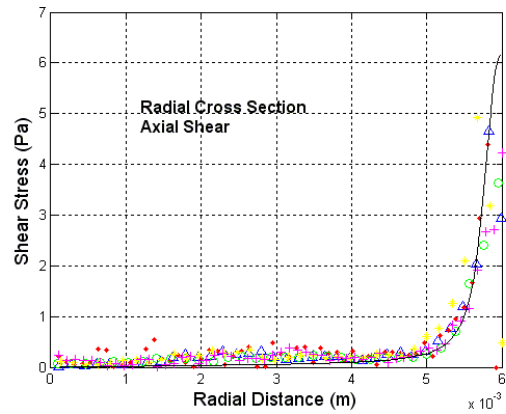


Figure 24.K. Axial shear stress, BSL, Re 6500, station 0.06m

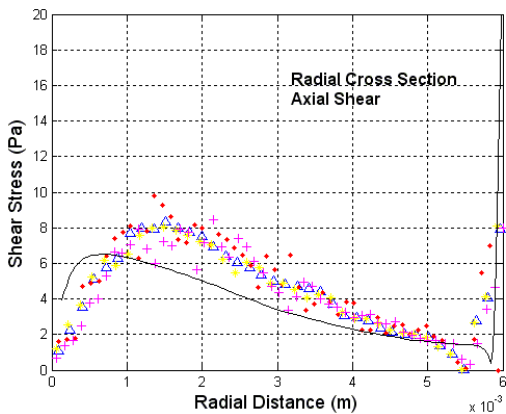


Figure 24.I. Axial shear stress, BSL, Re 6500, station 0.024m

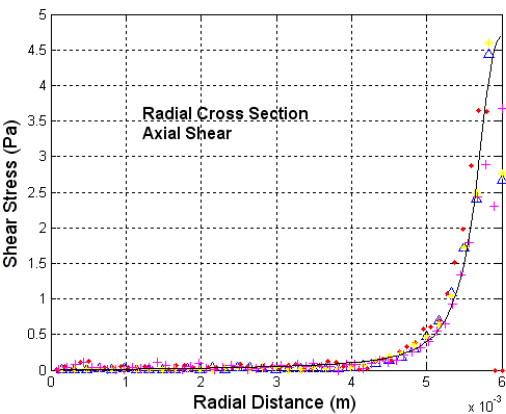


Figure 24.L. Axial shear stress, BSL, Re 6500, station 0.08m



Figure 24.M. Legend for figures 24.A-24.L

The last set of cross sectional velocity plots are shown in figure 25 (25.A-25.L). Figure 25, showing the 12 different cross sectional velocity plots for the 6500 Reynolds SST solution case, are the highest accuracy velocity plots discussed in this paper.

As noted in the previous SST velocity solution cases, very high alignment was achieved for sections -0.088m through 0.0m (figures 25.A through 25.F). In these figure sets it is noticeable that the simulation data falls within the error of the experimental data for all of these sections.

It is also noticed that the simulation data falls within the error of the experiment at sections 0.06m and 0.08m (figures 25.K-25.L). The final sections, sections 0.008 through 0.032 (figures 25.G-25.J) are also seen be very close to falling within the error of the experimental data and are the highest accuracy sets for any of the figures in this area of the BSL/SST solution sets discussed.

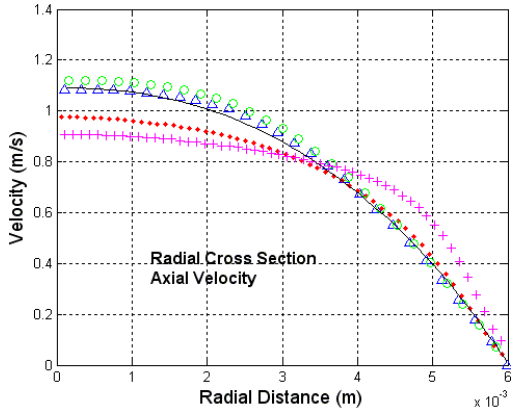


Figure 25.A. Axial velocity, SST, Re 6500, station -0.088m

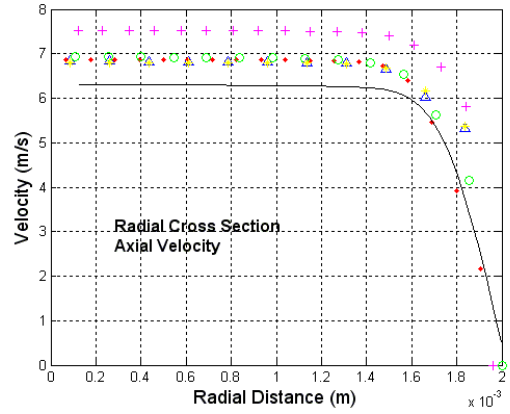


Figure 25.D. Axial velocity, SST, Re 6500, station -0.02m

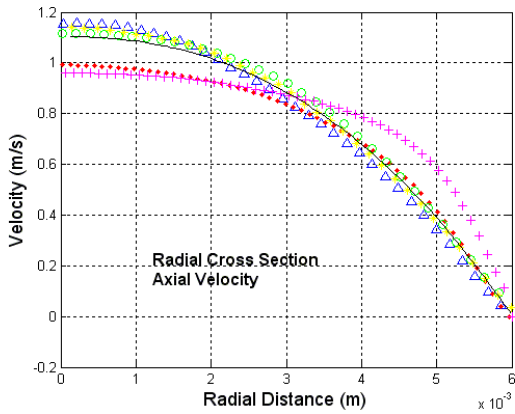


Figure 25.B. Axial velocity, SST, Re 6500, station -0.064m

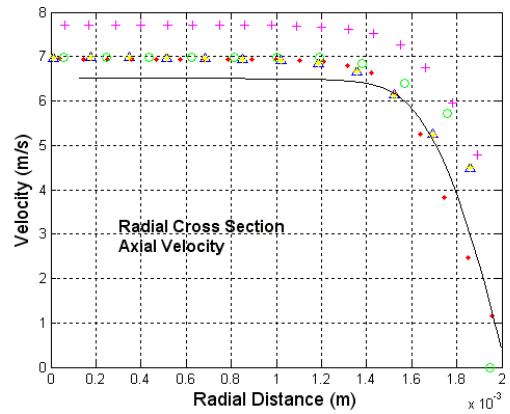


Figure 25.E. Axial velocity, SST, Re 6500, station -0.008m

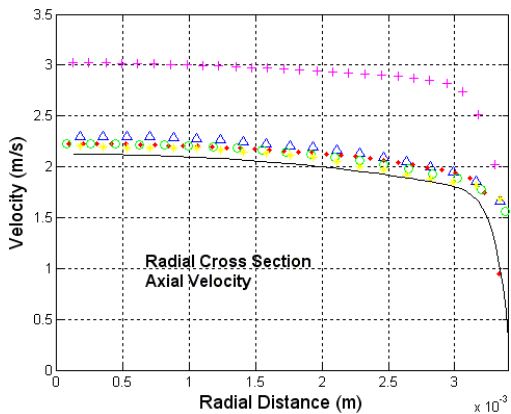


Figure 25.C. Axial velocity, SST, Re 6500, station -0.048m

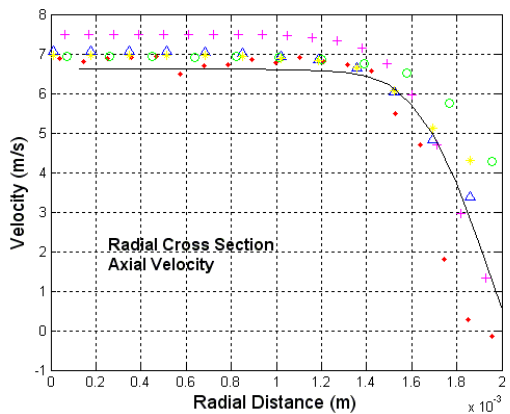


Figure 25.F. Axial velocity, SST, Re 6500, station 0.0m

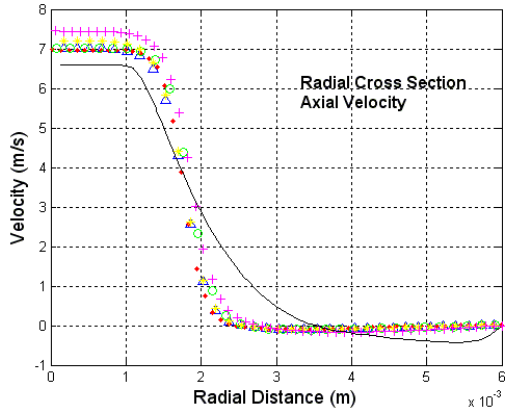


Figure 25.G. Axial velocity, SST, Re 6500, station 0.008m

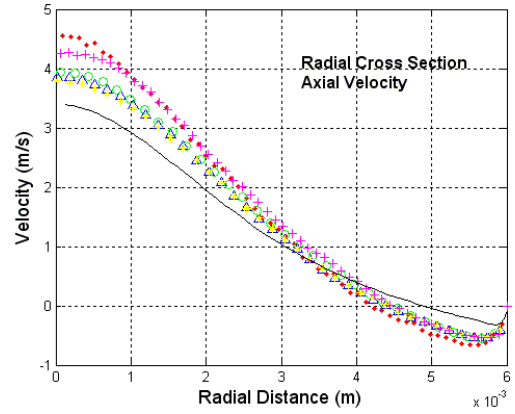


Figure 25.J. Axial velocity, SST, Re 6500, station 0.032m

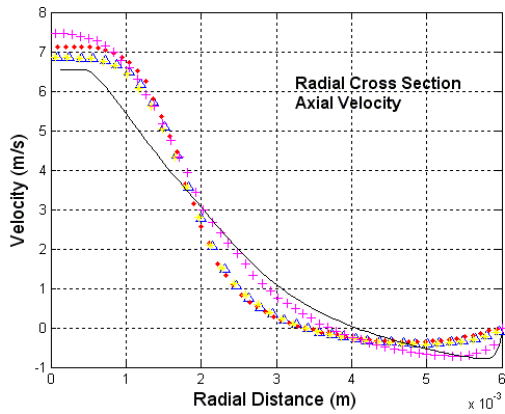


Figure 25.H. Axial velocity, SST, Re 6500, station 0.016m

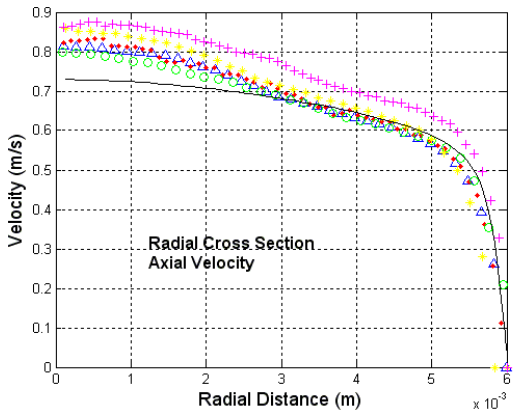


Figure 25.K. Axial velocity, SST, Re 6500, station 0.06m

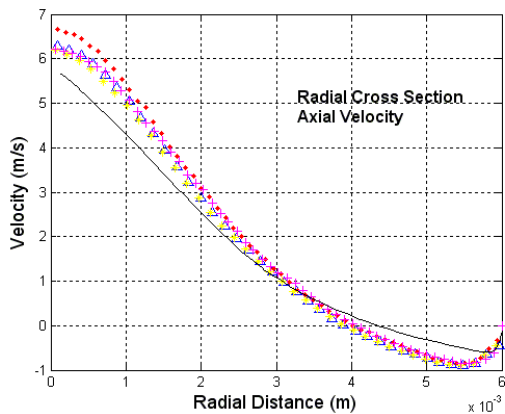


Figure 25.I. Axial velocity, SST, Re 6500, station 0.024m

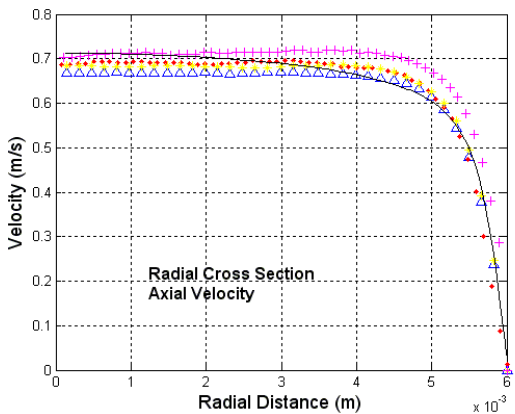


Figure 25.L. Axial velocity, SST, Re 6500, station 0.08m



Figure 25.M. Legend for figures 25.A-25.L

The very last set of cross sectional plots to discuss is figure set 26. Figure 26 (26.A-26.L) shows the shear stress cross sections for the 6500 Reynolds SST solution set at 12 different axial locations.

Figure set 26 was found to be the highest accuracy set for all of the shear stress and velocity plots discussed to this point. All of the sections (with the exception of two cross sections) data fall within the error of the experimental data set. This is partial due to some of the error that the experimental data set exhibits combined with the accuracy of the SST solver for this Reynolds case.

In sections 0.008m and 0.016m (figures 26.G & 26.H) the simulation data comes close to being within the error zone of the experimental data but is continued to be underestimated. It is also seen that the area where the shear stress is discrepant is the radial point of the sudden expansion corner ($0.2e-3m$ radial). Conclusions of the error in this section repeated over all of the BSL and SST solution sets lead to nodal element size error within the mesh. It is believed that refinement in this area would lead to better prediction of the experimental data set.

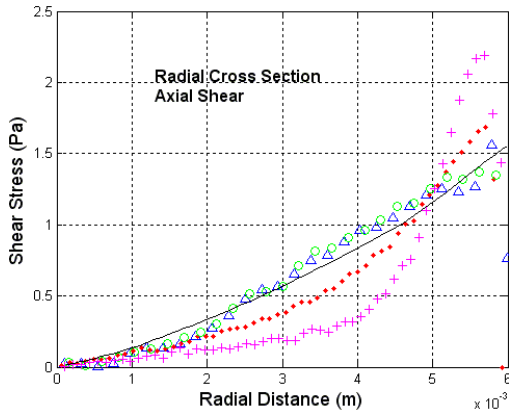


Figure 26.A. Axial shear stress, SST, Re 6500, station -0.088m

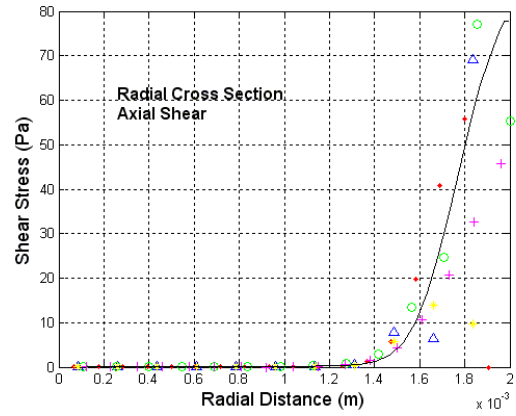


Figure 26.D. Axial shear stress, SST, Re 6500, station -0.02m

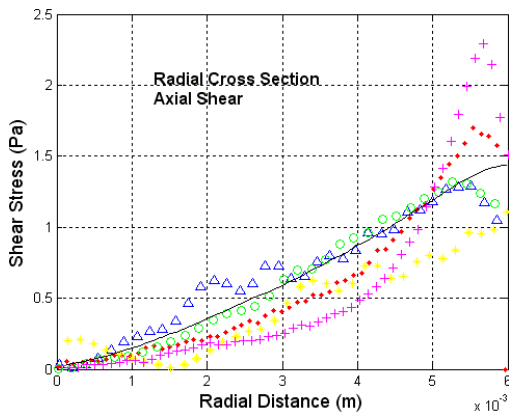


Figure 26.B. Axial shear stress, SST, Re 6500, station -0.064m

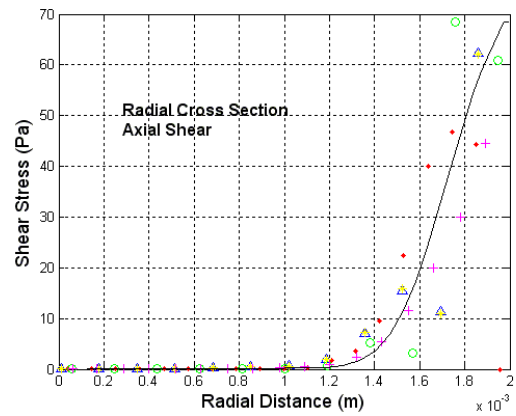


Figure 26.E. Axial shear stress, SST, Re 6500, station -0.008m

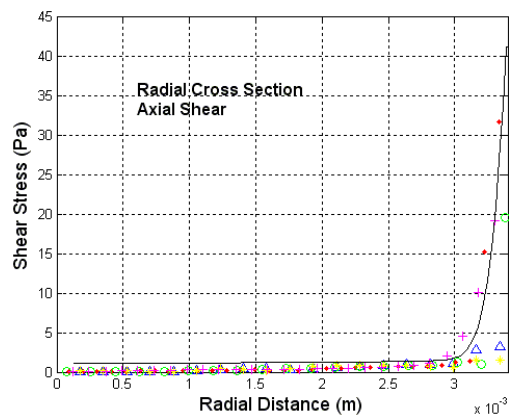


Figure 26.C. Axial shear stress, SST, Re 6500, station -0.048m

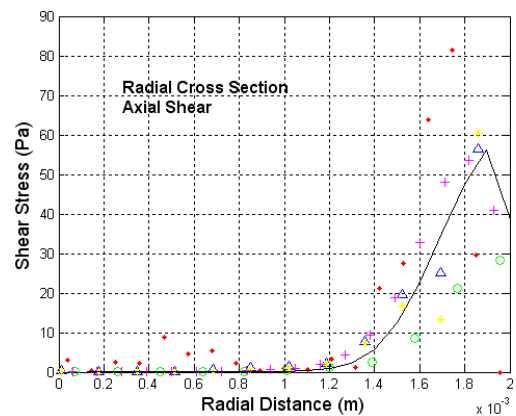


Figure 26.F. Axial shear stress, SST, Re 6500, station 0.0m

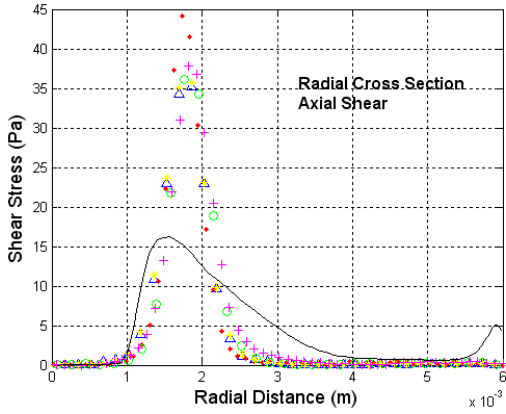


Figure 26.G. Axial shear stress, SST, Re 6500, station 0.008m

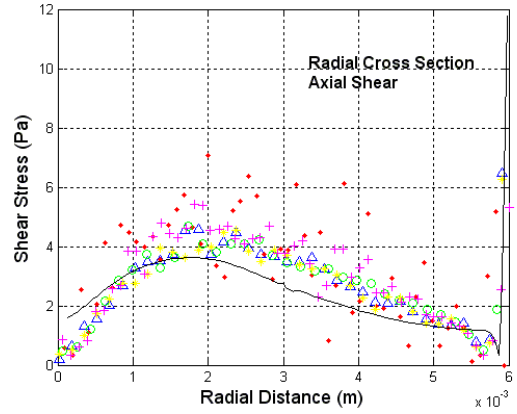


Figure 26.J. Axial shear stress, SST, Re 6500, station 0.032m

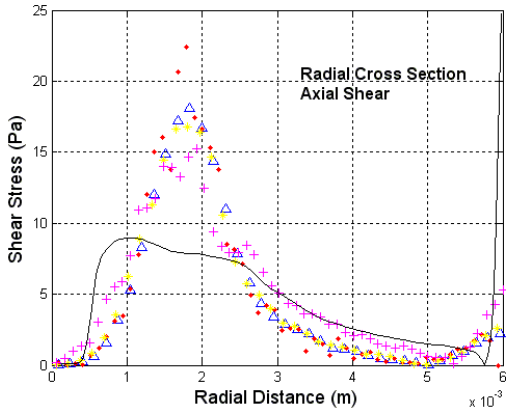


Figure 26.H. Axial shear stress, SST, Re 6500, station 0.016m

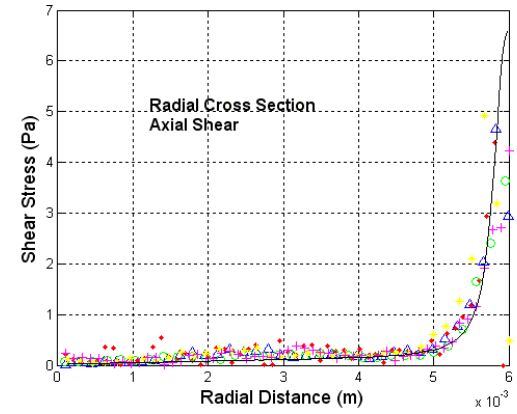


Figure 26.K. Axial shear stress, SST, Re 6500, station 0.06m

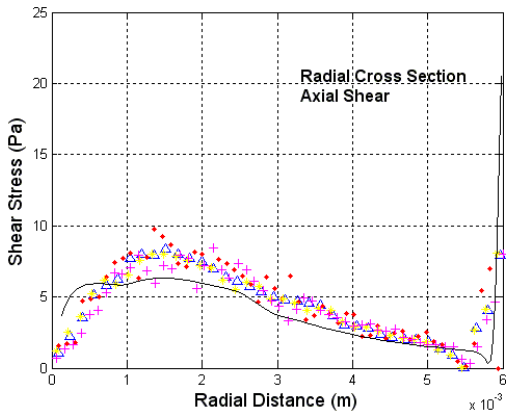


Figure 26.I. Axial shear stress, SST, Re 6500, station 0.024m

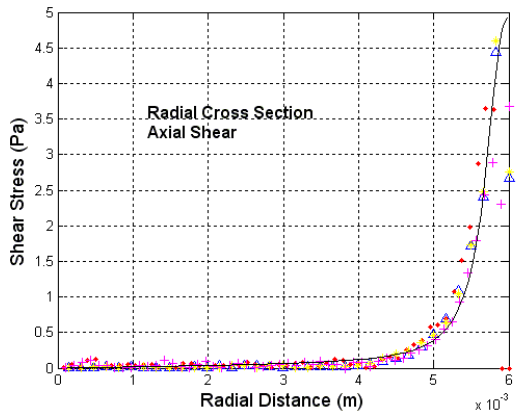


Figure 26.L. Axial shear stress, SST, Re 6500, station 0.08m



Figure 26.M. Legend for figures 26.A-26.L

Figure 27 shows the axial velocity for all of the laminar, SST, and BSL simulation cases run. As can be seen with the axial cross sections of the plots above, many of the same trends exhibit themselves in these plots. Starting with the laminar 500 Reynolds number case in figure 27.A, the simulation data matches the experimental data within the error of the experiment.

Moving to the laminar 2000 Reynolds number cases it becomes apparent that the laminar solution was the only solution to under estimate the slight turbulence of the experimental flow field. This is visible in figure 27.B as the experimental data center line velocity starts fall off at about 0.06m distance from the sudden expansion while the simulation data carries close to the maximum jet velocity through the plotted region of the flow field.

The event of estimating the turbulence in the flow is reversed upon viewing the first turbulent equation set. Figure 27.C shows the 2000 Reynolds SST solution case for the centerline velocity flow. In this plot the simulation flow velocity starts to fall off around 0.018m after the sudden expansion. In this same plot it is also seen that the simulation data does not converge back to the experimental data till around the 0.08m mark. Running the 2000 Reynolds BSL solution case, shown in figure 27.D almost the same trend is seen as from the 2000 Reynolds SST solution case. This underestimation of the centerline velocity is thought to be in part of the overestimation of the turbulence modeled for these flows.

Figure 27.E and 27.F show the 3500 Reynolds SST solution case and the BSL solution case respectively. Once again the simulation data for both of these solution sets yields very close results to one another. Upon closer inspection of these plots (figures 27.E and 27.F)

the trend of the simulation data aligning better to the experimental data for higher Reynolds number is shown once more. Comparing the results from the axial velocity of the 2000 Reynolds SST and BSL case to the 3500 Reynolds SST and BSL case, it is apparent that the 3500 Reynolds case alignment is more than twice as accurate as the 2000 Reynolds SST and BSL case for the high diverging area of the plot.

The trend for the simulation data to align better to the experimental data is then exasperated further moving to the last two sets of centerline velocity plots. Figures 27.G, 27.H, 27.I and 27.J show the centerline velocity of the 5000 Reynolds SST and BSL case along with the 6500 Reynolds SST and BSL case respectively. Comparing these plots to the lower Reynolds number centerline velocity plots along with each other brings out another trend that was noted in the radial velocity plots. In these last four plots (figures 27.G, 27.H, 27.I and 27.J) the trend to align better to the data becomes apparent along with the trend to underestimate the max centerline velocity. The trend to under estimate the max velocity is brought out in figures 27.G and 27.H by about a 3m/s drop in maximum velocity to the experimental data along with a 5m/s drop in maximum velocity for figures 27.I and 27.J.

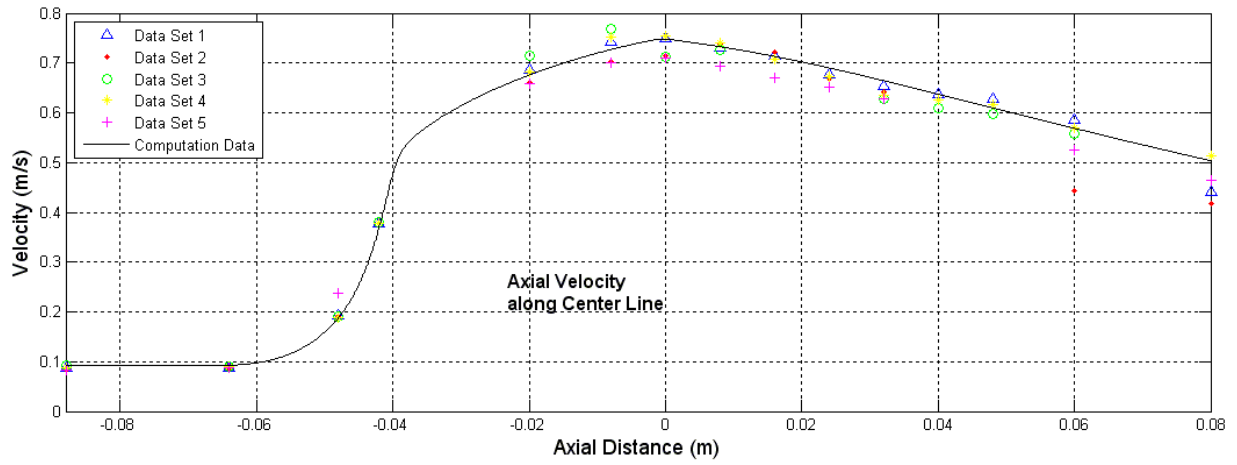


Figure 27.A. Axial velocity along axis, laminar, Re 500

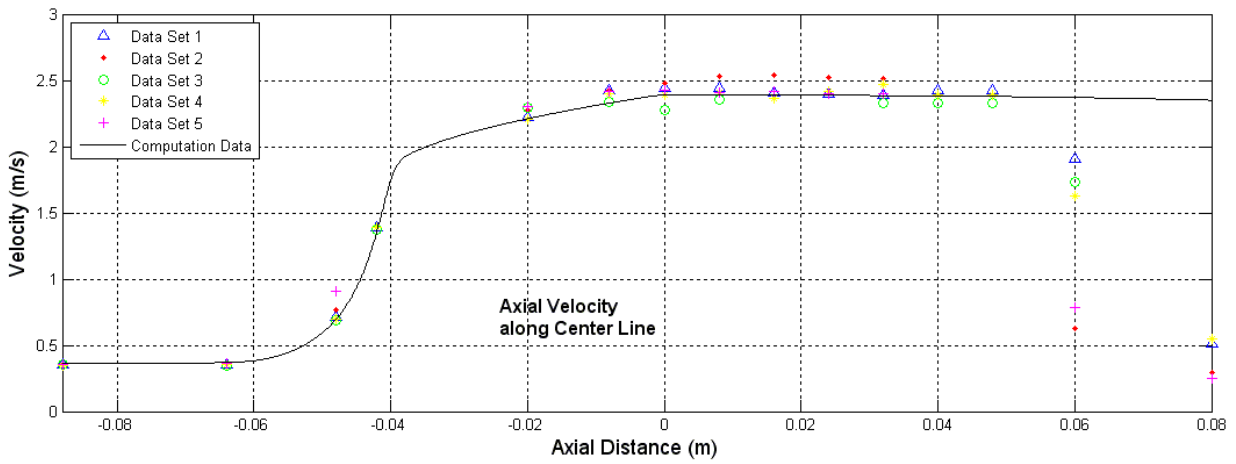


Figure 27.B. Axial velocity along axis, laminar, Re 2000

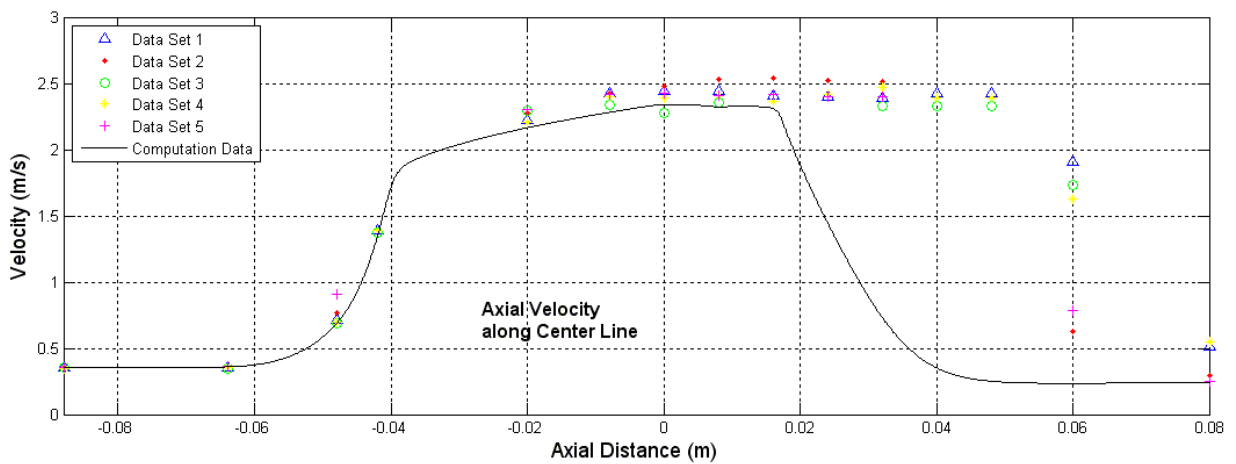


Figure 27.C. Axial velocity along axis, SST, Re 2000

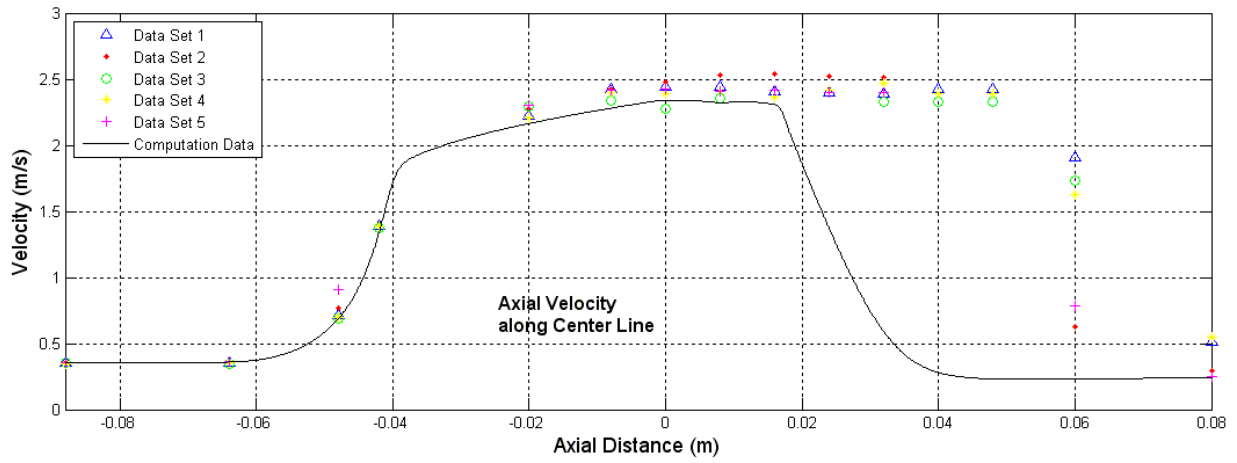


Figure 27.D. Axial velocity along axis, BSL, Re 2000

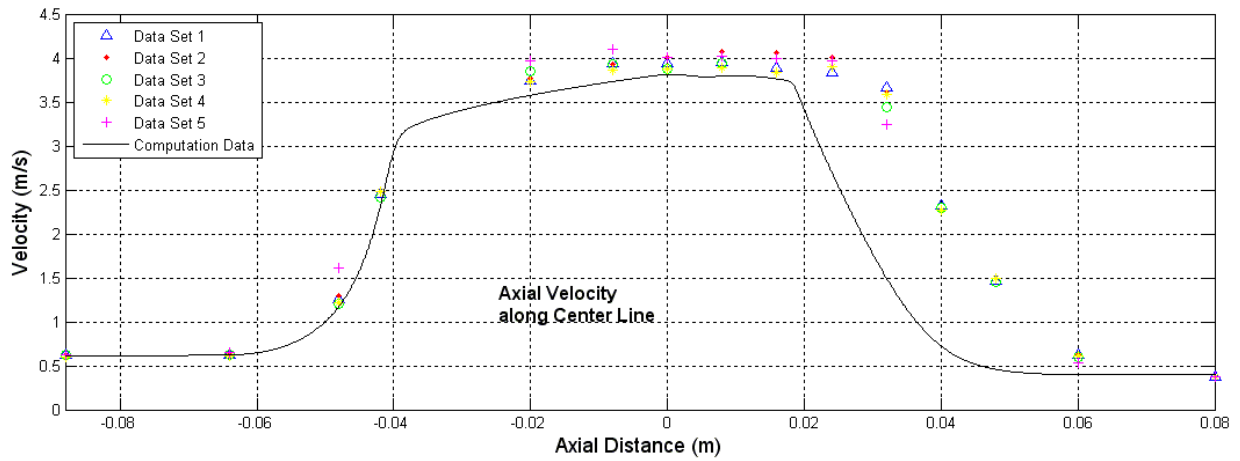


Figure 27.E. Axial velocity along axis, SST, Re 3500

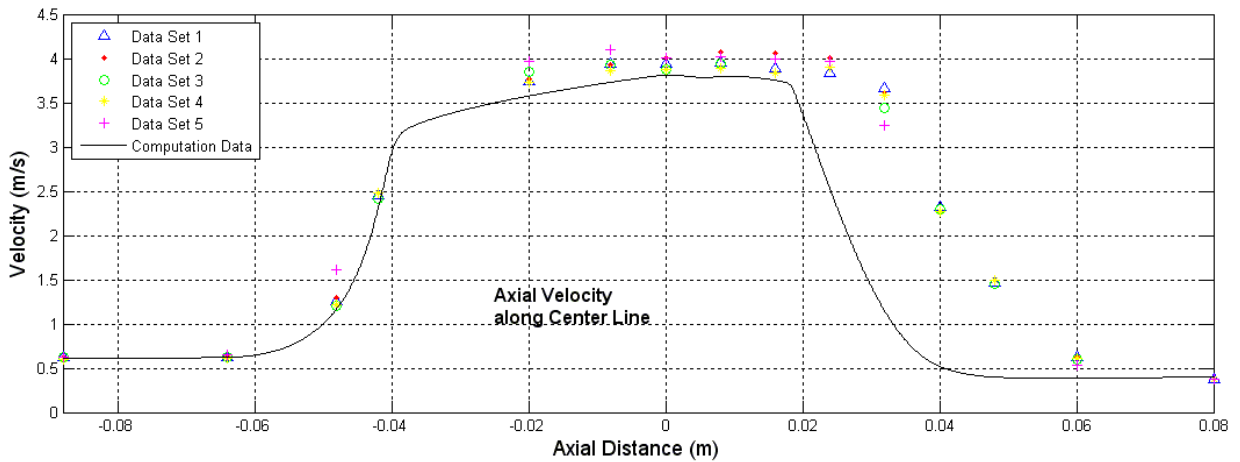


Figure 27.F. Axial velocity along axis, BSL, Re 3500

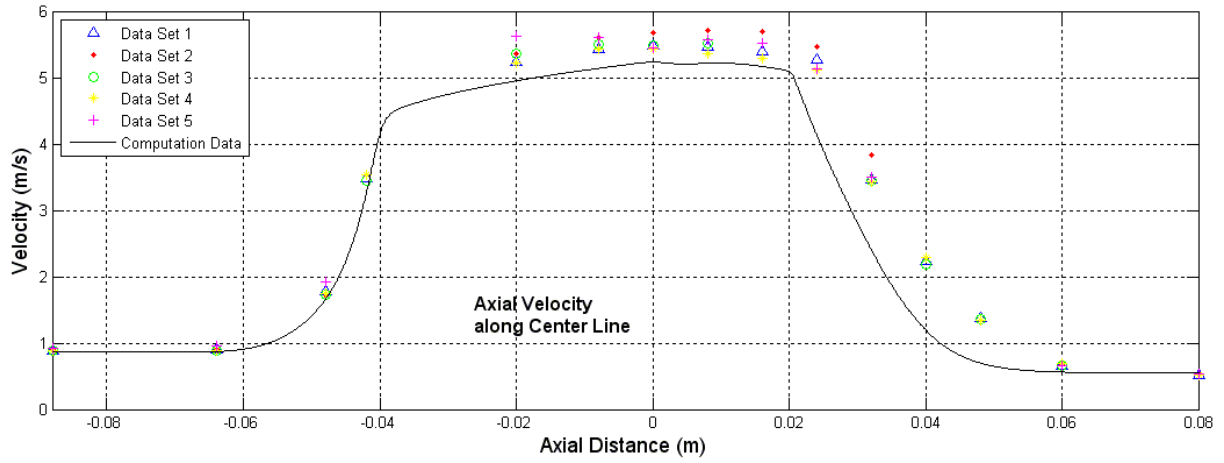


Figure 27.G. Axial velocity along axis, SST, Re 5000

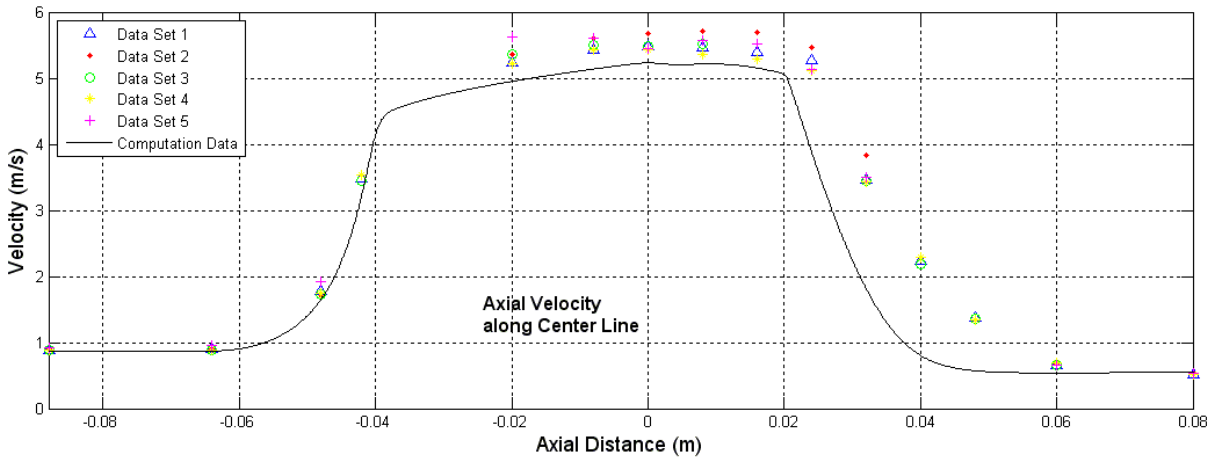


Figure 27.H. Axial velocity along axis, BSL, Re 5000

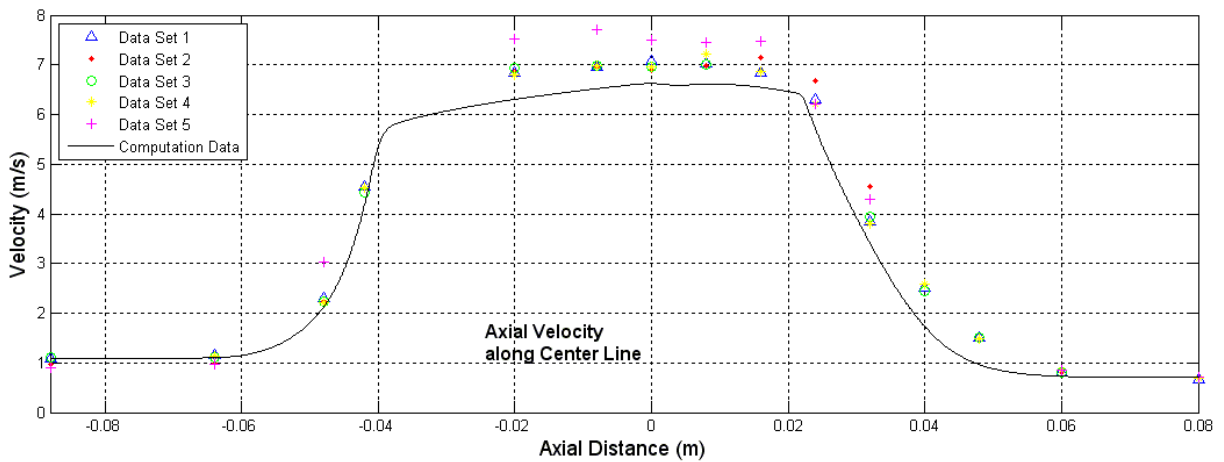


Figure 27.I. Axial velocity along axis, SST, Re 6500

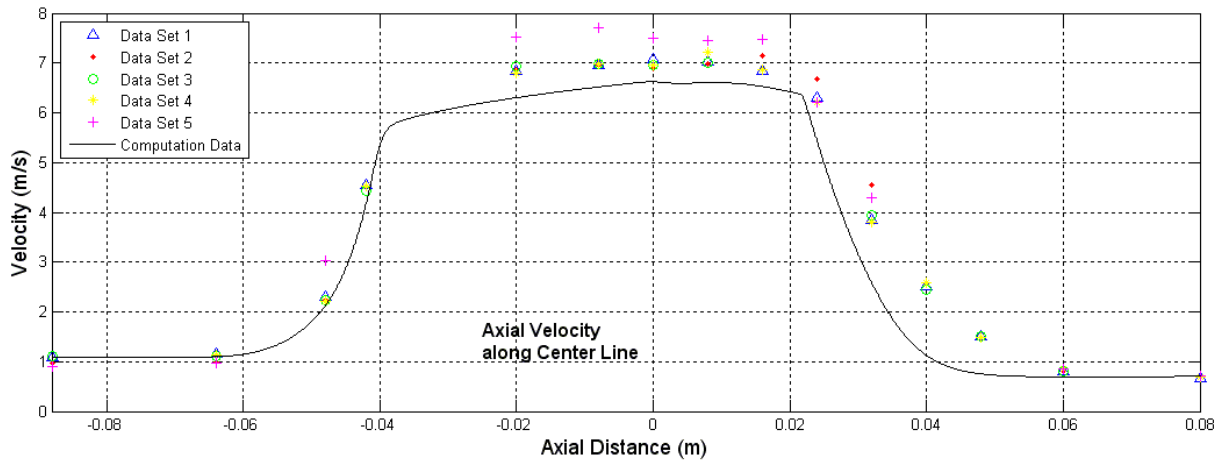


Figure 27.J. Axial velocity along axis, BSL, Re 6500

Figure set 28 shows the pressure along the wall of the converging/diverging section for each of the laminar, SST, and BSL solution cases. Reviewing these plots a few common trends become visible. The first trend that becomes apparent is the slight underestimation in the wall pressure for the -0.088m mark to the -0.04m mark for almost all of the cases. The only plot that this underestimation is not apparent in is figure 28.A showing the laminar 500 Reynolds case solution. Also noticed in the figure 28.A is the drifting wide range of the experimental data; the other plots for the wall pressure tend to have smaller ranges in the data shown. The second noticeable trend is the singularity that appears at the -0.04m mark. While not apparent in the laminar 500 Reynolds case it becomes growingly apparent as the Reynolds number is increased up to the 6500 Reynolds cases.

The third noticeable trend lightly shows up in the lower Reynolds number but becomes more apparent at the 5000 and 6500 Reynolds cases. This third trend is the non-alignment in the pressure profile around the -0.02m mark. Upon close inspection of the -0.02m mark at the higher Reynolds number it becomes apparent that the experimental data tends to hang for a little or even move up slightly in pressure. This trend to hang at the same pressure or move up slightly is contradicted with the experimental data profile.

Though the singularity in the simulation data can be explained by the mesh quality, it is not apparent why the simulation does not predict the pressure holding event that happens during the contraction of the geometry as the no turbulence cases and the fully turbulent cases do not show this kind of trend in the simulation data.

The under estimation in the entrance pressure of the converging/diverging section is believed to be in connection to the under meshed development length section.

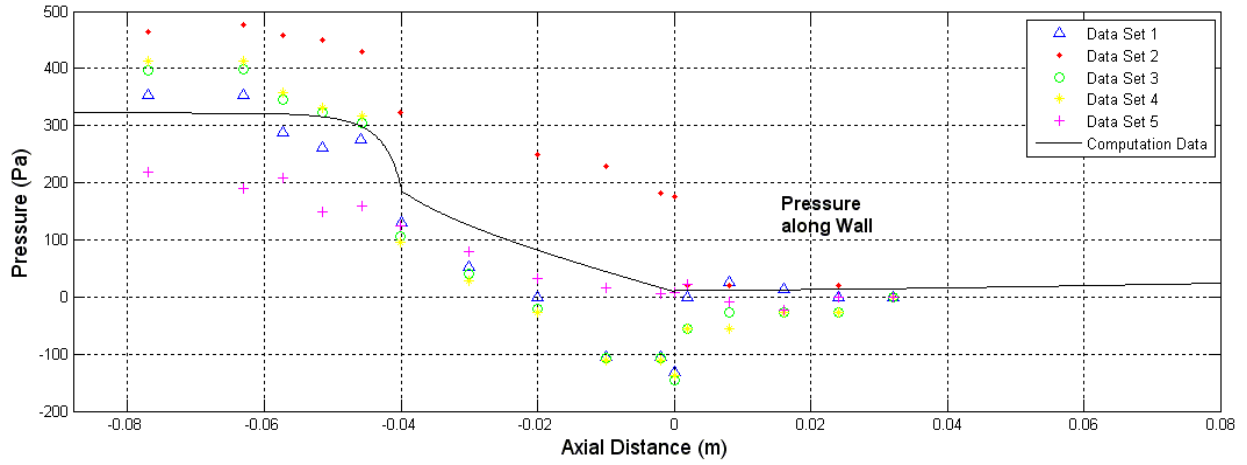


Figure 28.A. Wall pressure profile, laminar, Re 500

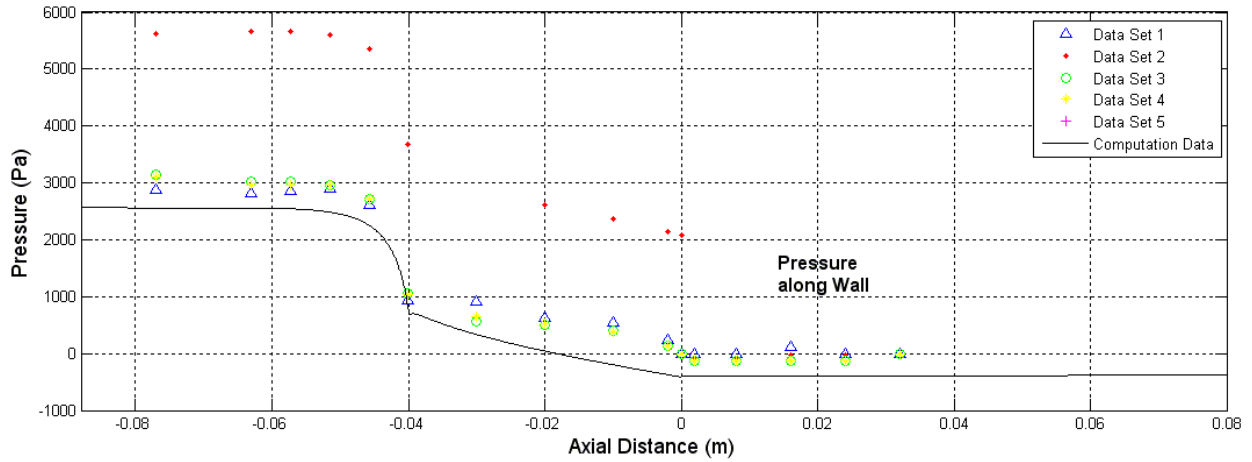


Figure 28.B. Wall pressure profile, laminar, Re 2000

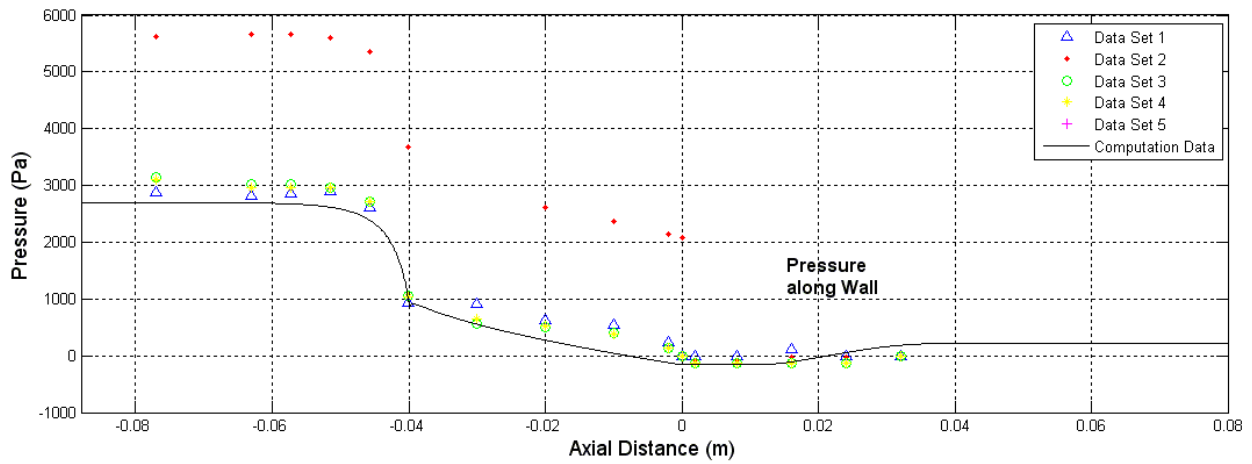


Figure 28.C. Wall pressure profile, SST, Re 2000

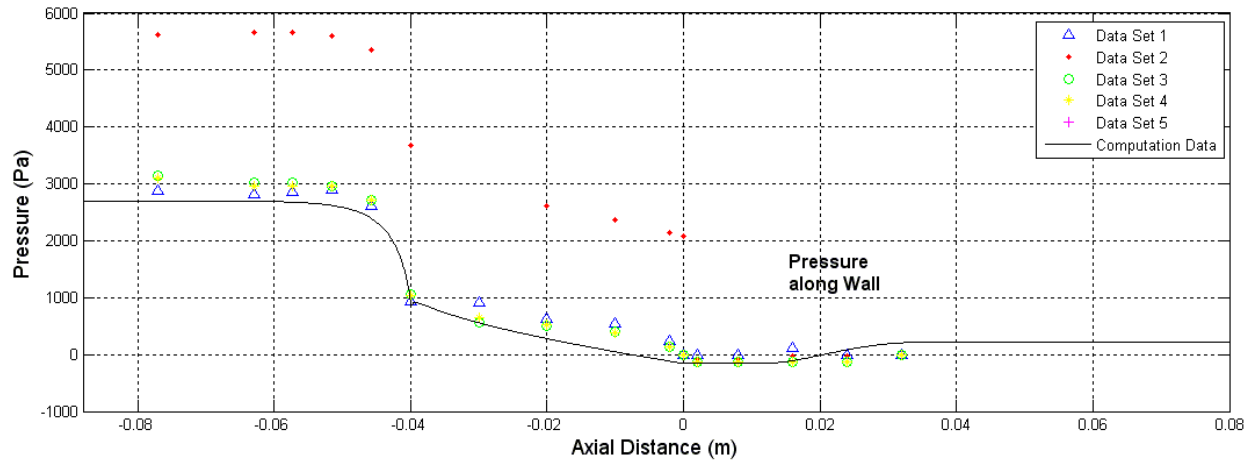


Figure 28.D. Wall pressure profile, BSL, Re 2000

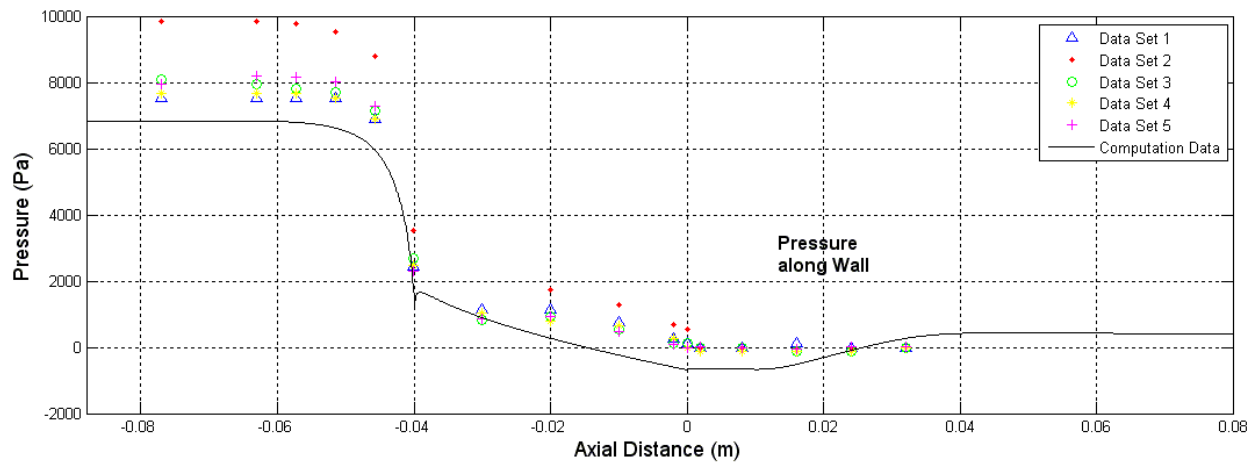


Figure 28.E. Wall pressure profile, SST, Re3500

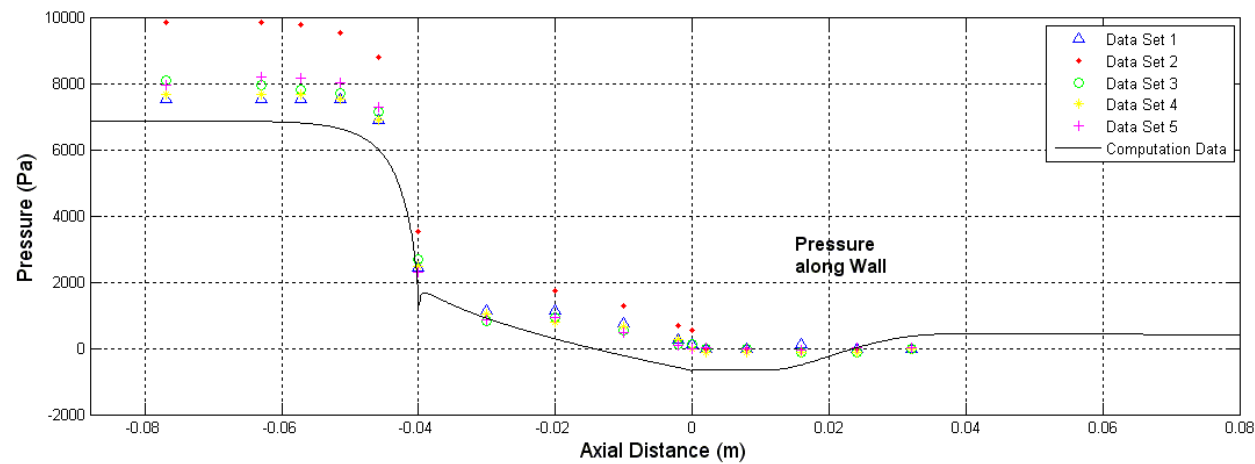


Figure 28.F. Wall pressure profile, BSL, Re 3500

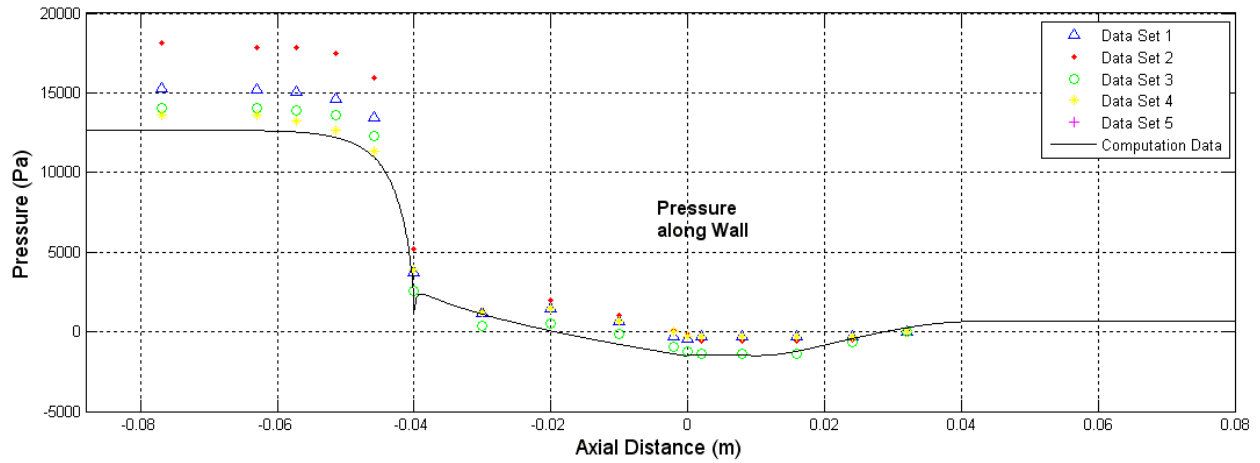


Figure 28.G. Wall pressure profile, SST, Re 5000

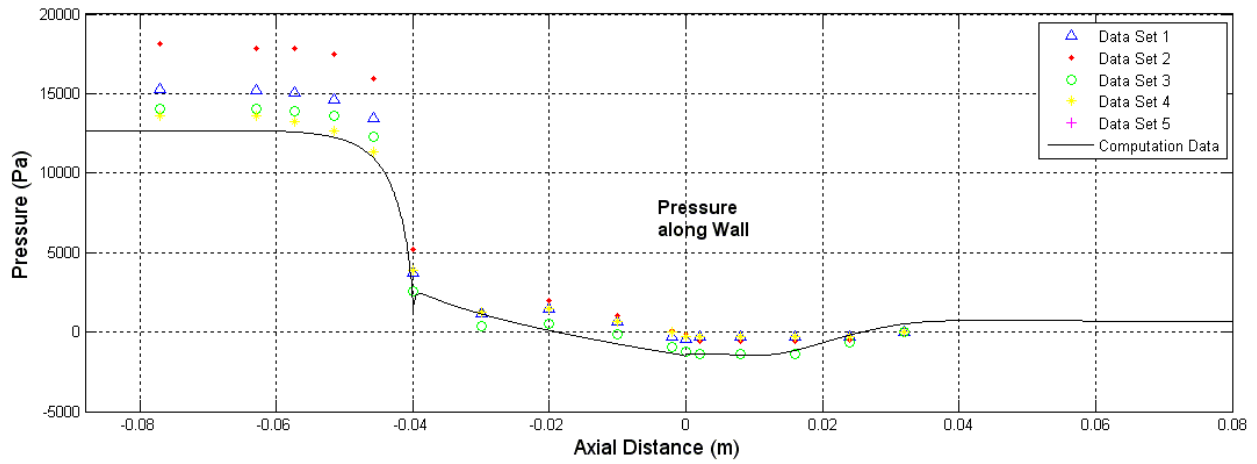


Figure 28.H. Wall pressure profile, BSL, Re 5000

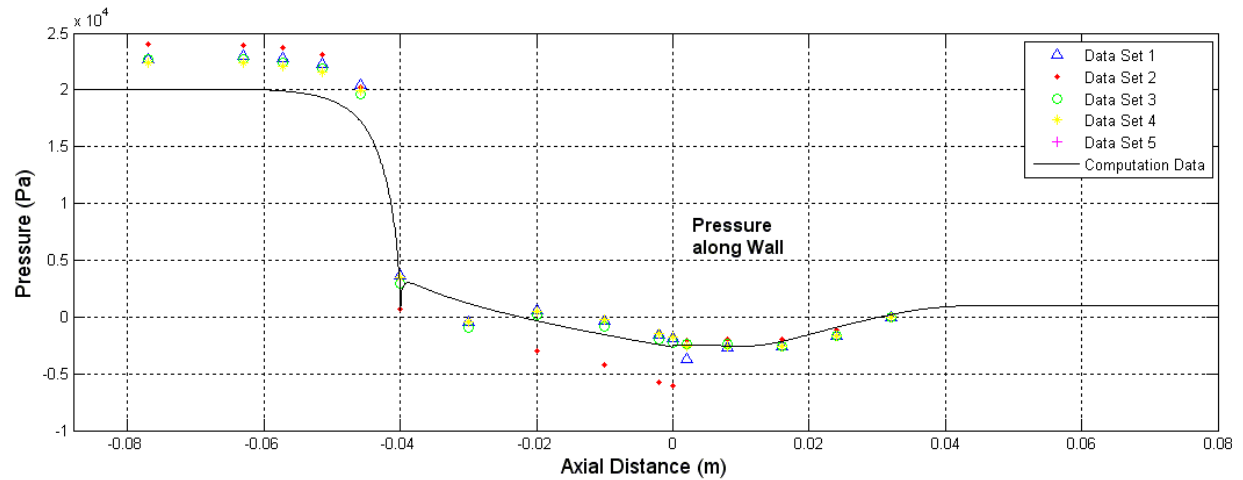


Figure 28.I. Wall pressure profile, SST, Re 6500

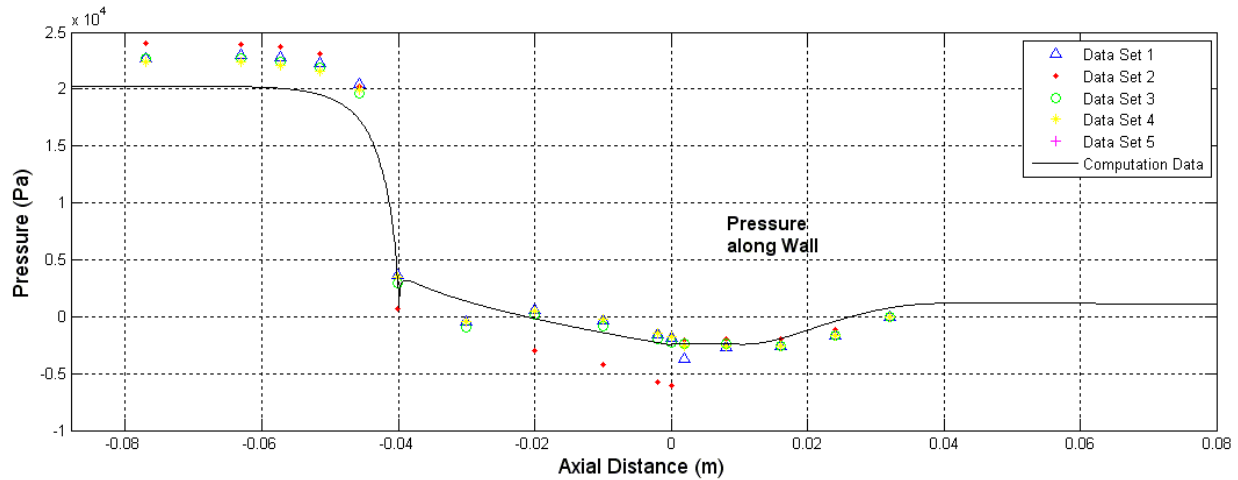


Figure 28.J. Wall pressure profile, BSL, Re 6500

Figure set 29 shows the wall shear stress for the laminar, SST, and BSL cases. As seen in all the plots within figure set 29, the first region of all the plots match the experimental data within the error of the data set. The first noticeable trend that does not line up with the experimental data can be seen at $\sim -0.052\text{m}$ mark. This trend is the overestimation in the shear stress of the simulation data to the experimental data. This non-alignment of the data is thought to be due to a firm non-slip boundary condition that was placed on the simulation.

From this point all of the simulations trends to align to the experimental data until the flow after the sudden expansion of the flow field (the 0.0m mark). For figures 29.A and 29.B, the simulation tracks the wall shear stress of the experimental data for the length of the monitored section. Introducing the turbulence solution sets to the flows brings out the recirculation areas seen in the 3500 Reynolds numbers and above. Close examination of figure 29.D reveals a re-circulation area that is evident from the experimental data mark at the $\sim -0.032\text{m}$ mark. Though the experimental data is short of providing a reattachment point it does appear that the turbulent simulations track the reattachment point marginally in the lower Reynolds numbers and very closely at the higher Reynolds numbers. The trend to overestimate the turbulence at Reynolds number around the 2000 to 3500 Reynolds

numbers and start to align better to the simulation data was also visible in the figures before. Moving to the very last two plots (figures 29.I and 29.J, showing the 6500 Reynolds cases for the SST and BSL solutions respectively), it can be seen that the reattachment point is very close to the experimental data if interpolating between the experimental data set points.

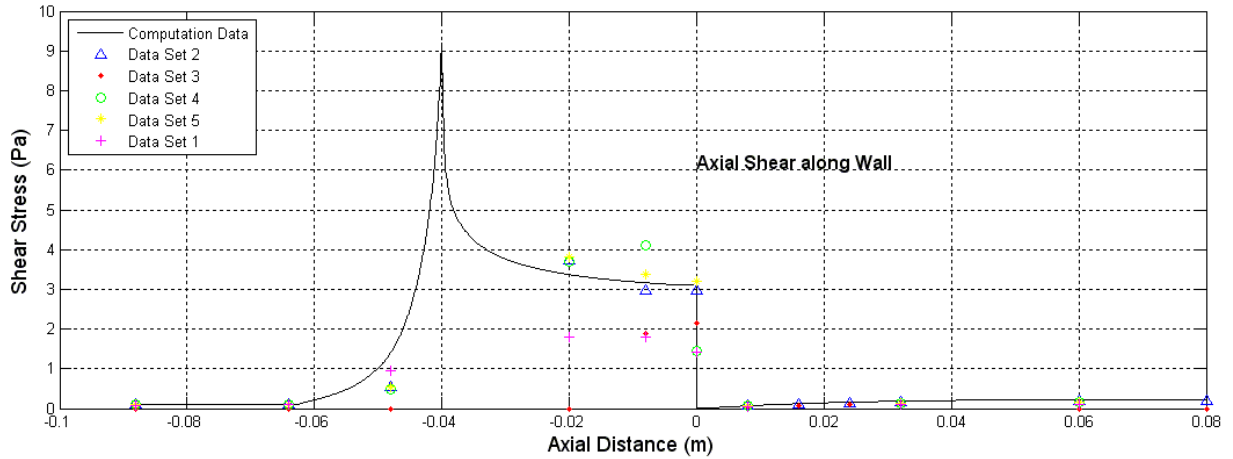


Figure 29.A. Wall shear stress profile, laminar, Re 500

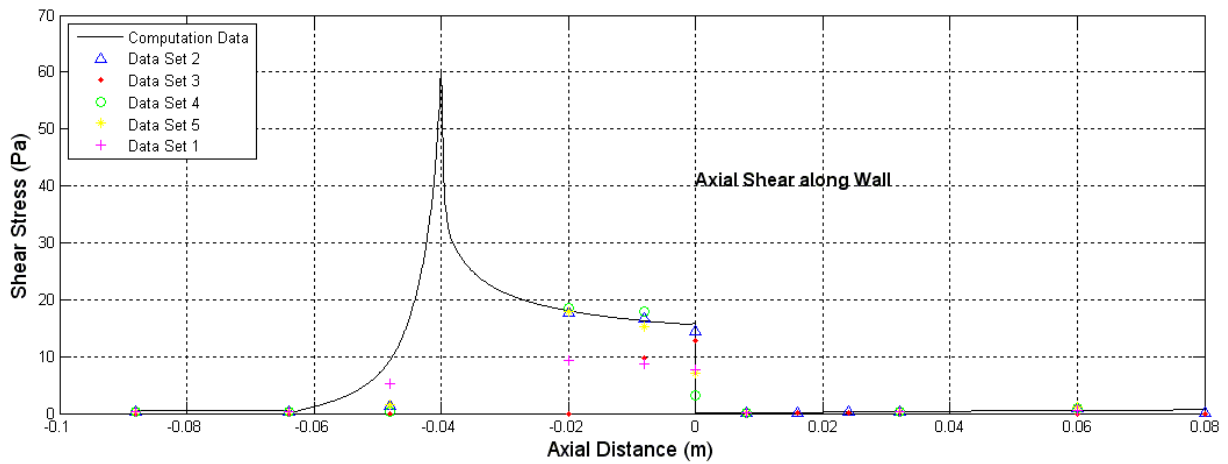


Figure 29.B. Wall shear stress profile, laminar, Re 2000

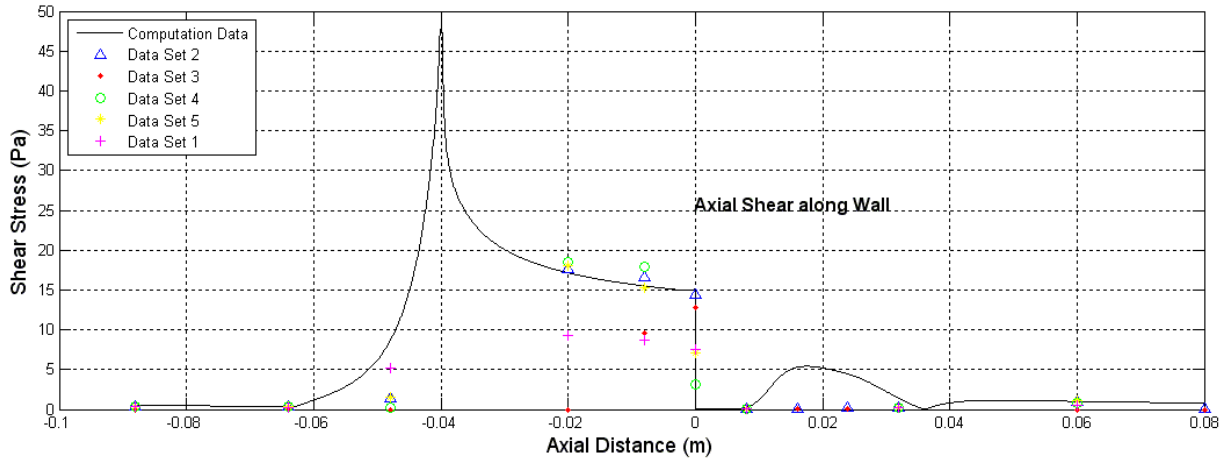


Figure 29.C. Wall shear stress profile, SST, Re 2000

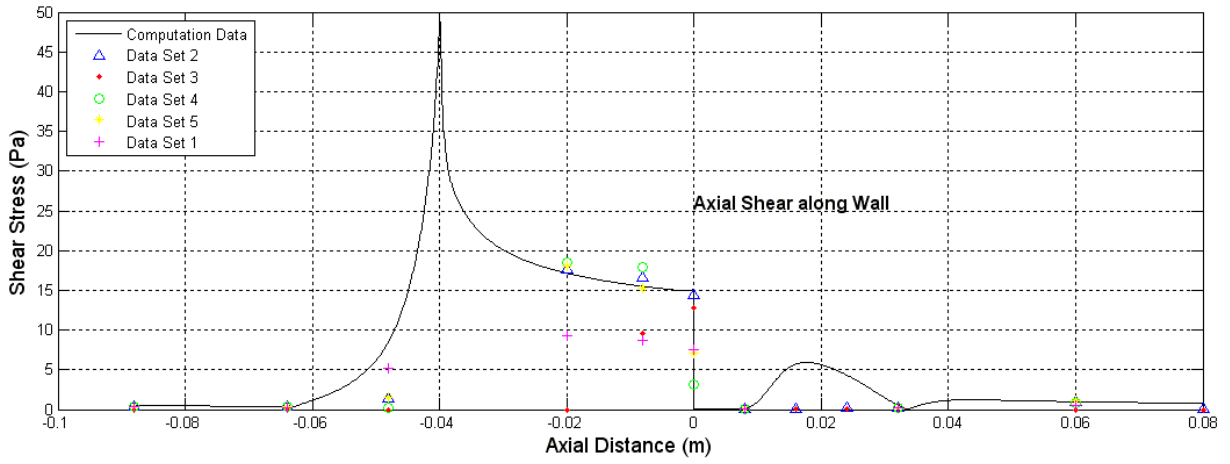


Figure 29.D. Wall shear stress profile, BSL, Re 2000

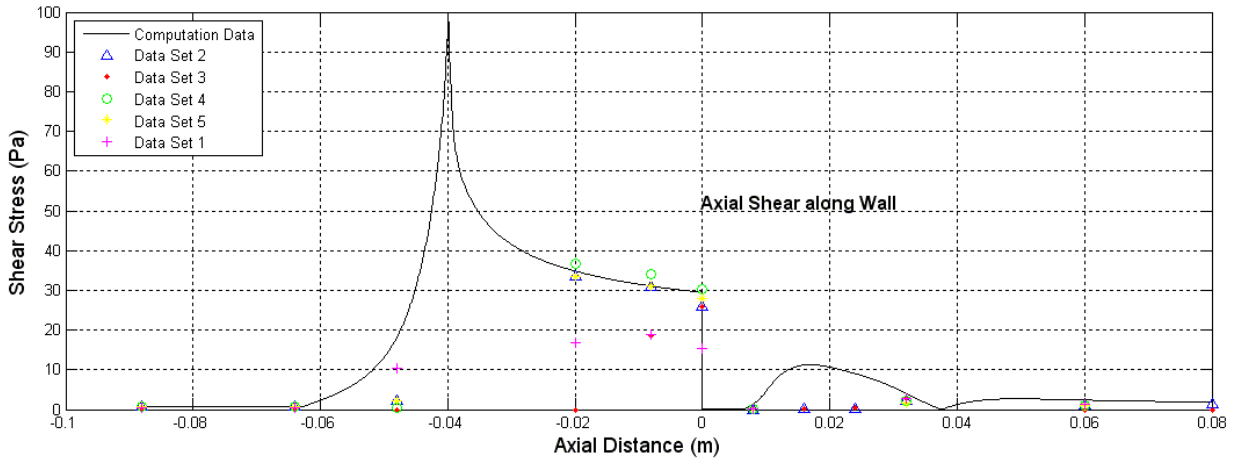


Figure 29.E. Wall shear stress profile, SST, Re 3500

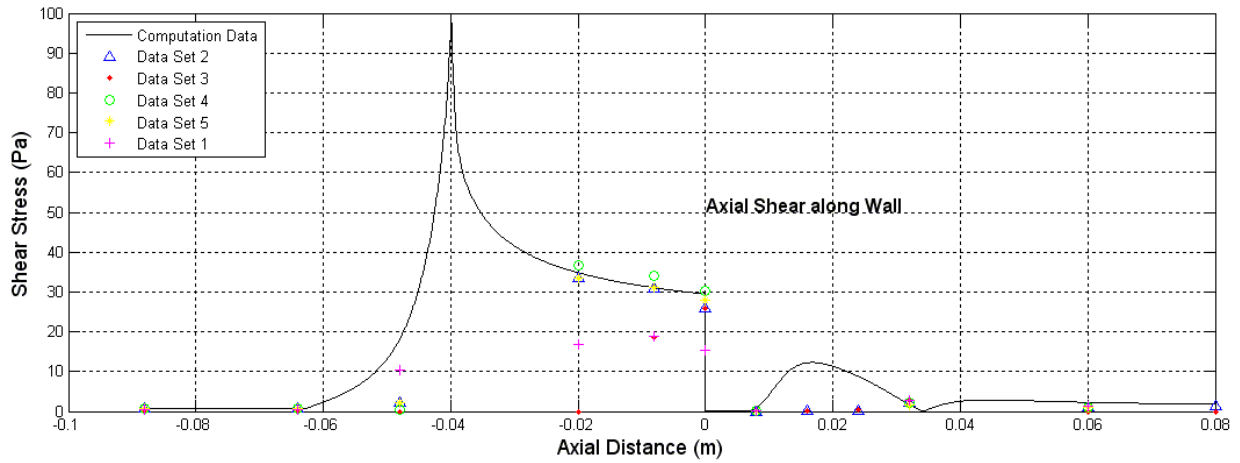


Figure 29.F. Wall shear stress profile, BSL, Re 3500

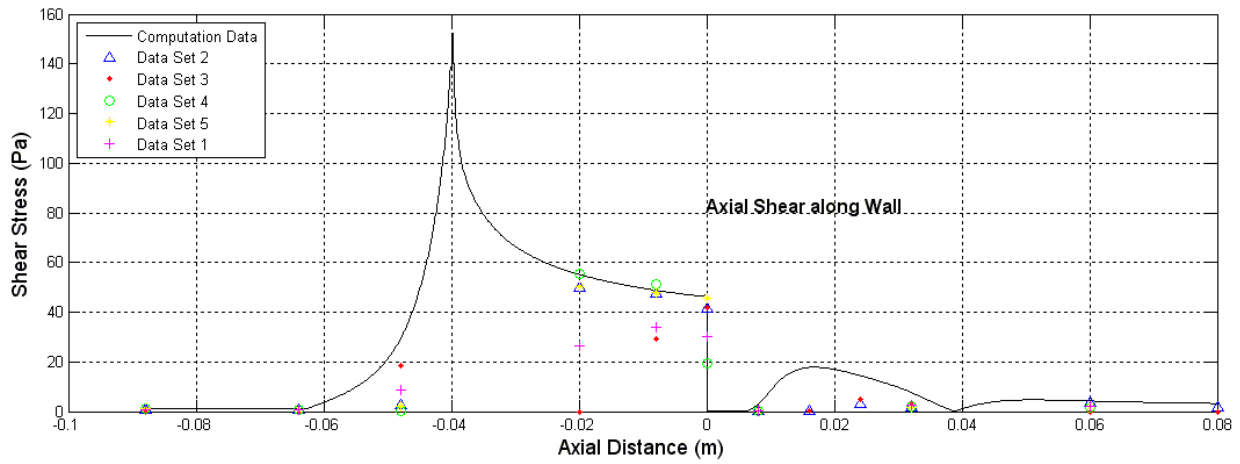


Figure 29.G. Wall shear stress profile, SST, Re 5000

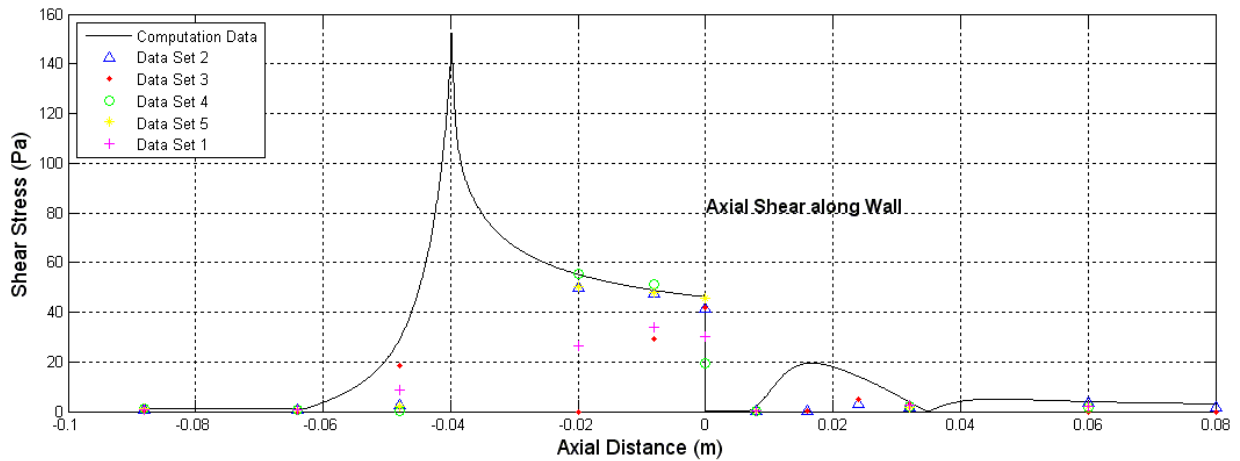


Figure 29.H. Wall shear stress profile, BSL, Re 5000

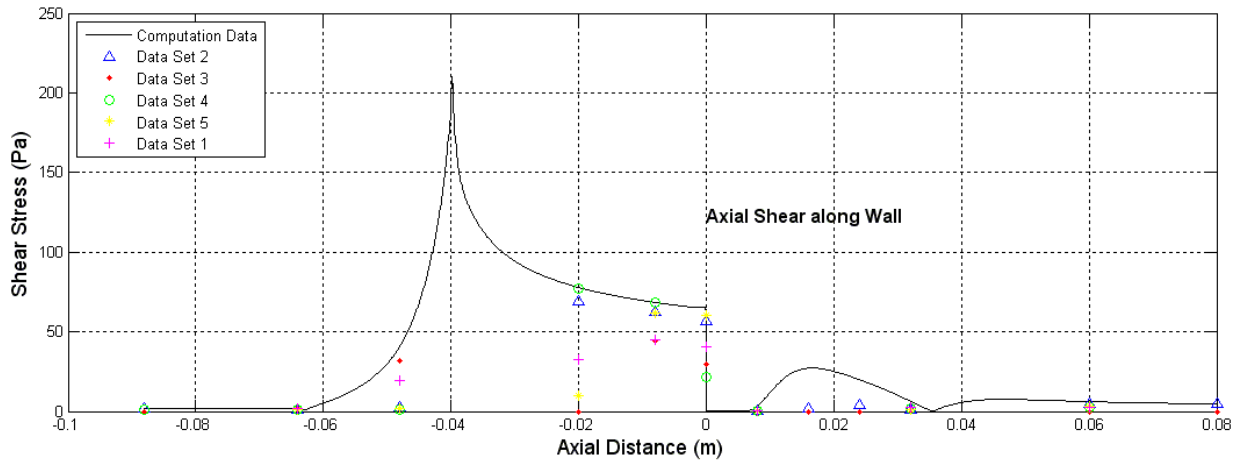


Figure 29.I. Wall shear stress profile, SST, Re 6500

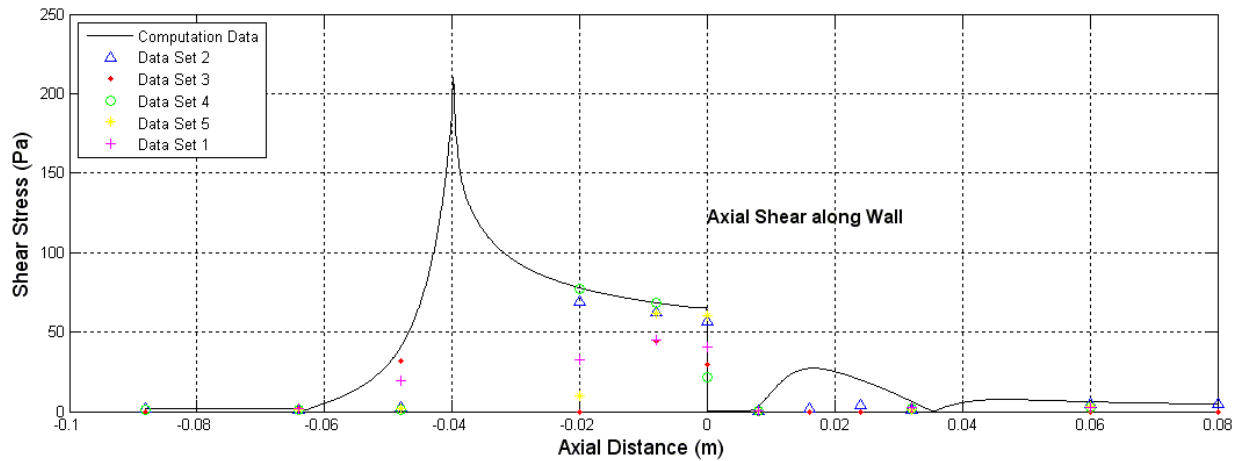


Figure 29.J. Wall shear stress profile, BSL, Re 6500

The last of the results section includes plots of the HI percentage for the simulations that were run. In figure set 30, these plots, in can be seen. The HI percentage plots detail the total as well as the HI percentage for each section of the converging/diverging geometry. A total of 11 sections can be seen for each simulation.

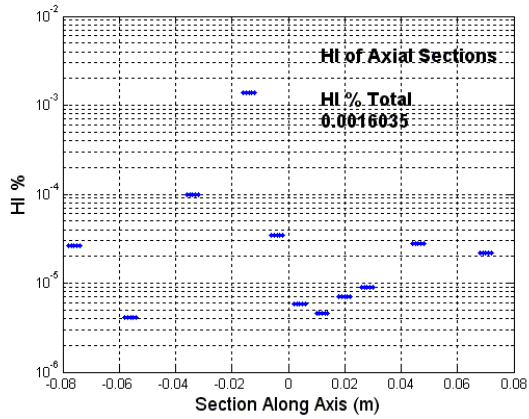


Figure 30.A. Hemolysis index, laminar, Re 500

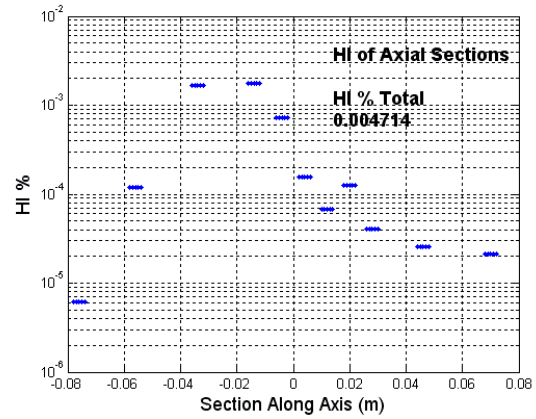


Figure 30.D. Hemolysis index, BSL, Re 2000

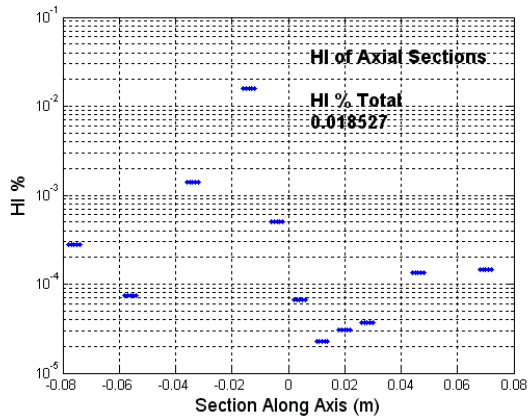


Figure 30.B. Hemolysis index, laminar, Re 2000

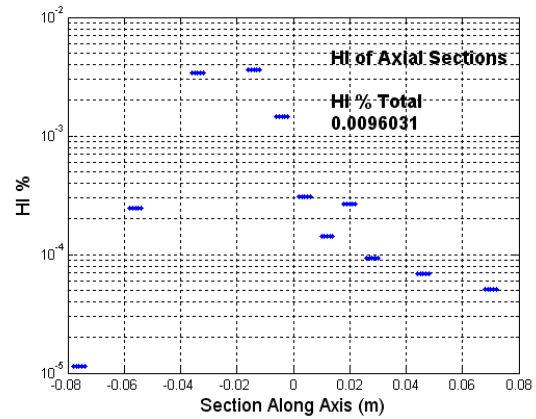


Figure 30.E. Hemolysis index, SST, Re 3500

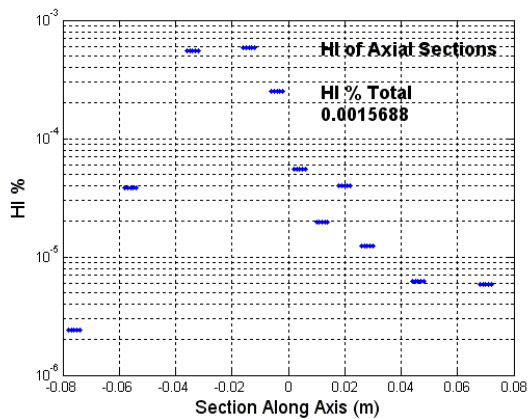


Figure 30.C. Hemolysis index, SST, Re 2000

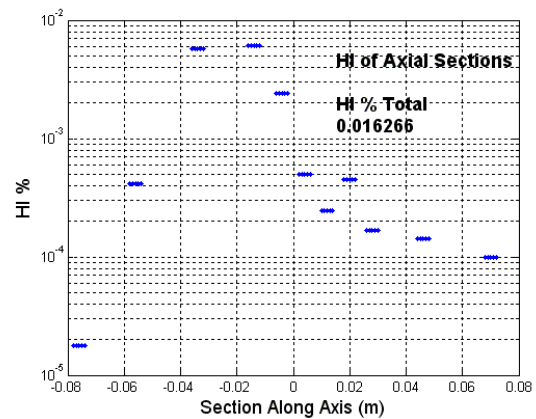


Figure 30.F. Hemolysis index, BSL, Re 3500

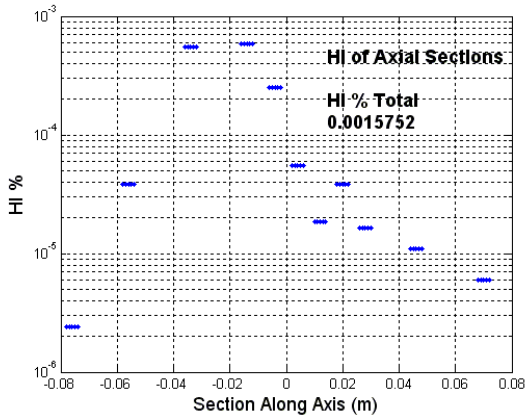


Figure 30.G. Hemolysis index, SST, Re 5000

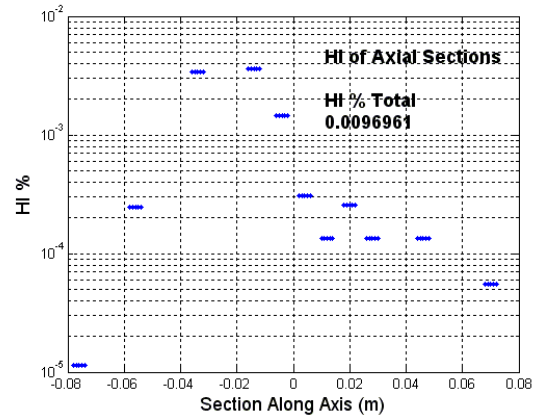


Figure 30.I. Hemolysis index, SST, Re 6500

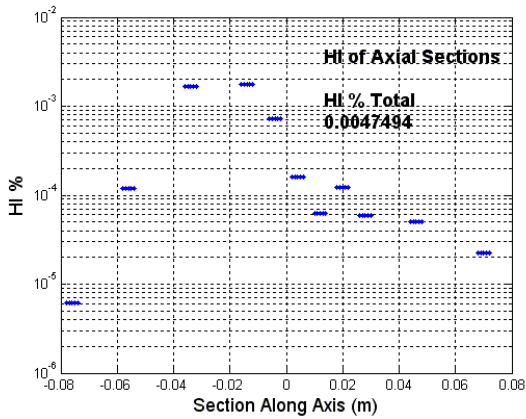


Figure 30.H. Hemolysis index, BSL, Re 5000

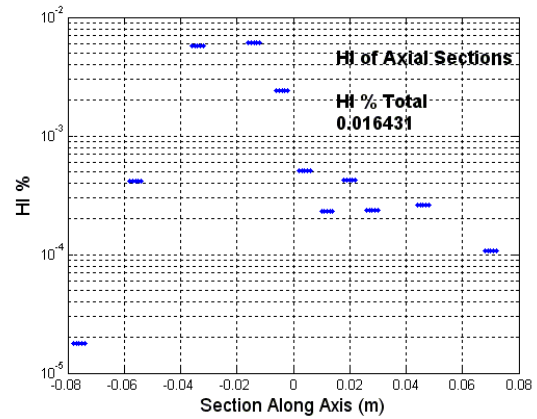


Figure 30.J. Hemolysis index, BSL, Re 6500

As can be seen from figure 30 the profile of the laminar set has a distinct difference from the profile of the BSL and SST simulation runs. In figures 30.A and 30.B, 500 and 2000 Reynolds number laminar runs, the majority of the HI % is accumulated from the contraction of the geometry. This follows what previous research has shown as the blood cells striking the external geometry contributes to the high damage profiles. Also in figures 30.A and 30.B, as the flow profile starts to develop and starts to regain high shear stress against the wall, an increase in the HI% tends to increase.

Figures 30.C-30.F detail the HI% for the BSL simulation runs. This almost exactly matches the HI% for the runs performed with the SST turbulence model; seen in figures 30.G-30.J. In these runs as within the laminar runs, as the Reynolds number increases so does the HI% for both the total HI% as well as the sectional percentages. The difference in figure 30.C-30.J is the profile of the hemolysis damage through the different sections. The profile in figure 30.C-30.J takes on a shape that one would more expect from a turbulent flow condition. This is that the HI% seems to increase even before the contraction of the geometry and then wavers after the sudden expansion. Both of these observations, increasing before the contraction and wavering after the sudden expansion, is seen as well as can be explained in the axial shear stress profiles earlier examined, figures 29.A-29.J.

5. CONCLUSION

General remarks of the simulation include good alignment of the lower Reynolds values. It was seen that the 500 Reynolds value, using laminar boundary conditions, yielded very high accuracy simulation to experimental flow predictions.

Simulation inlet and outlet flow profiles were also seen to have high alignment for almost all of the Reynolds numbers. These flow profiles were complimented by the alignment of the overall pressure drop of the differing Reynolds number simulations.

The highest aligning turbulent/transitional solver was found to be the SST for the transitional and fully turbulent flow conditions. Though both the BSL and SST solver trended to yield higher accuracies at flow conditions closer to 6500 Reynolds number, it was seen that the highest aligning turbulent simulation was using the SST solver at the 6500 Reynolds number flow conditions.

It was also noticed that refinements to the solvers could be made for both the BSL as well as the SST solutions. This was evident from the over turbulent nature both solvers caused for the transitional and turbulent cases. Looking at the transitional cases, both the SST and BLS solver greatly overestimated the turbulence in the recirculation area of the sudden expansion, as was noted in figure set 27. Moving to the Reynolds number in the full turbulent region, both the SST and BSL solver still overestimated the turbulence in the sudden expansion except for the case of the SST solver when the Reynolds number was brought up to 6500. The case where the SST solver was brought up to a Reynolds flow of 6500, the solver actually managed to capture the experimental data almost within the overall error only missing it by relatively small amounts in one very limited section of the geometry. It is by this that the SST solver was determined to be the most optimized solver (out of those examined) for the geometry shown.

Items noted that could improve the simulation accuracy include a mesh reduction/refinement at the edge of the sudden expansion and the region tracking the jet flow after the sudden expansion. Refinements in this area of the simulation is thought to bring better alignment to the jet length generated by the re-circulation area and influence the reattachment point of the simulation data. Refinements in this area also thought to eliminate the singularity happening at the edge of the sudden expansion, as was shown in the cross sectional shear stress plots at the 0.0m mark.

Another item noticed that is believed to be correctable with mesh refinements is the discrepancy of the entrance cross sectional shear stress profiles close to the wall at the entrance of the converging/diverging section. It is believed to be because of the y^+ value being just under 2 for the entrance development length that the entrance shear stress profile were not at their optimal modeled state. This can be seen in the cross sectional shear stress profiles at the -0.088m mark for most all the cases.

The last thing noted in the simulation of the flow field is the non-alignment of the pressure profile and shear stress profiles to simulate the trend of the experimental data in the convergence area of the converging/diverging section. As this non-alignment to the experimental data seems to predict a higher gradient in pressure around and after the -0.02 mark as well as an over estimated wall shear stress, it is believed that a slight slip region may be occurring just after the contraction of the converging/diverging section.

6. REFERENCES

- [1] S.F.C. Stewart, E.G. Paterson, G.W.Burgreen, P. Hariharan, M. Giarra, V. Reddy, S.W. Day, K.B. Manning, S. Deutsch, M.R. Berman, M.R. Myers, R.A. Malinauskas, Assessment of CFD Performance in Simulations of an Idealized Medical Device – Results of FDA’s First Computational Interlaboratory Study, https://fdacfd.nci.nih.gov/interlab_study_1_nozzle/
- [2] NandiniDuraismwamy, Richard T. Schoephoerster, Michael R. Moreno, James E. Moore, Stented artery flow patterns and their effects on the artery wall, *Journal of Annual Review of Fluid Mechanics* 39 (2007) 357-382.
- [3] J.P Abraham, E.M Sparrow, R.D Lovik, Unsteady three-dimensional fluid mechanic analysis of blood flow in plaque-narrowed and plaque freed arteries, *International Journal of Heat and Mass Transfer* 51 (2008) 5633-5641.
- [4] D.N Ku, *Blood Flow*, McGraw-Hill, New York, 1964.
- [5] Miguel A. Moyers-Gonzalez, Robert G. Owens, Jiannong Fang, A non-homogeneous constitutive model for human blood Part III. Oscillatory flow, *Journal of Non-Newtonian Fluid Mechanics* JNNFM-2832 (2008).
- [6] S.W. Lee, D.A. Steinmann, On the relative importance of rheology for image-based CFD models of the carotid bifurcation, *J. Biomed. Eng.-Trans. ASME* 129 (2007) 273-278.
- [7] J.F. Stoltz, M.Lucuis, Viscolasticity and thixotropy of human blood, *Bioheology* 18 (1981) 453-473.
- [8] D. Carswell, D. MacBride, T.N. Croft, A.K. Slone, M. Cross, G. Foster, A CFD model for the prediction of haemolysis in micro axial left ventricular assist devices, *Applied Mathematical Modelling* 37 (2013) 4199-4207.

- [9] S.S. Lee, K.Ahn, S.J. Lee, K. Sun, P. Goedhart, M. Hardeman, Shear induced damage of red blood cells monitored by the decrease of their deformability, Korea – Aust. Rheol. J. 16 (3) (2004) 141-146.
- [10] L. Leverett, J. Hellums, C. Alfrey, E. Lynch, Red Blood cell damage by shear, Biophys. J. 12 (1972) 257-273.
- [11] P. Lu, H. Lai, J. Liu, A re-evaluation and discussion on the threshold limit for hemolysis in a turbulent shear flow, J. Biomech. 34 (2001) 1361-1364.
- [12] R. Paul, J. Apel, S. Klaus, F. Schugner, P. Schwindke, H. Reul, Shear stress related blood damage in laminar coquette flow, Artif. Organs 27 (6) (2003) 517-529.
- [13] M. Griginoni, C. Daniele, U. Morbiducci, G. D'Avenio, G. Benedetto, V. Barbaro, The power-law mathematical model for blood damage prediction: Analytical development and physical inconsistencies, Artif. Organs 28 (5) (2004) 467-475.
- [14] P. Blackshear, F. Dorman, J. Steinbach, Some mechanical effects that influence haemolysis, Trans. Am. Soc. Artif. Int. Organs 11 (1965) 112.
- [15] X. Song, A. Throckmorton, H. Wood, J. Antaki, D. Olsen, Computational fluid dynamics prediction of blood damage in a centrifugal pump, Artif. Organs 27 (10) (2003) 938-941.
- [16] M. Giersiepen, L. Wurzinger, R. Opitz, H. Reul, Estimation of shear stress-related blood damage in heart valve prostheses – in vitro comparison of 25 aortic valves, Int. J. Artif. Organs 13 (1990) 300-306.
- [17] G. Heuser, R. Opitz, A coquette viscometer for short time shearing in blood. Biorheology 1980;17:17-24.
- [18] D. Bluestein, E. Rambod, M. Gharib, Vortex shedding as a mechanism for free emboli formation in mechanical heart valves, Journal of Biomechanical Engineering 122 (2) (2000) 125-134.

- [19] W. Yin, Y. Alemu, K. Affeld, J. Jesty, D. Bluestein, Flow induced platelet activation in bileaflet and monoaflet mechanical heart valves, *Annals of Biomedical Engineering* 32 (8) (2004) 1058-1066.
- [20] Y. Alemu, D. Bluestein, Flow induced platelet activation and damage accumulation in a mechanical heart valve: numerical studies, *Artificial Organs* 31 (9) (2007) 677-688.
- [21] K. Dumont, J. Vierendeels, R. Kaminsky, G. van Nooten, P. Verdonck, D. Bluestein, Comparison of the hemodynamic and thrombogenic performance of two bileaflet mechanical heart valves using a CFD/FSI model, *Journal of Biomechanical Engineering* 129 (4) (2007) 558-565.
- [22] M. Grigioni, U. Morbiducci, G. D'Avenio, G. Di Benedetto, C. Del Gaudio. A novel formulation for blood trauma prediction by a modified power law mathematical model, *Biomech model mechanbiol* 4 (2005) 249-260.
- [23] M. Grigioni, C. Daniele, U. Morbiducci, G. D' Avenio, G. Di Benedetto, V. Barbaro, The power-law mathematical model for blood damage prediction: analytical developments and physical inconsistencies, *Artif Organs* 28 (5) (2004) 467-475.
- [24] U. Morbiducci, R. Ponzini, M. Nobili, D. Massai, F.M. Montevecchi, D. Bluestein, A. Redaelli, Blood damage safety of prosthetic heart valves. Shear-induced platelet activation and local flow dynamics: A fluid-structure interaction approach, *Journal of Biomechanics* 42 (2009) 1952-1960.
- [25] M. Nobili, J.F. Sheriff, U. Morbiducci, A. Redaelli, J. Jesty, D. Blustein, Platelet activation due to hemodynamic shear stresses: damage accumulation model and comparison to in vitro measurements. *ASAIO Journal* 54 (2008) 64-72.
- [26] A.O. Borisyuk, Experimental study of wall pressure fluctuation in rigid and elastic pipes behind an axisymmetric narrowing, *Journal of Fluids and Structures* 26 (2010) 658-674.

- [27] M.S. Mandal, S. Mukhopadhyay, G.C. Layek, Pulsatile flow of an incompressible inhomogeneous fluid in a smoothly expanded vascular tube, *International Journal of Engineering Science* 57 (2012) 1-10.
- [28] G.C. Layel, S. Mukhopadhyay, Laminar flow separation in an axi-symmetric sudden smooth expanded circular tube, *Journal of Applied Mathematics and Computing*, 28 (2008) 235-247.
- [29] L. Goubergrits, K. Affeld, Numerical estimation of blood damage in artificial organs, *Artificial Organs*, 28 (5) (2004) 496-517.
- [30] S.F.C. Stewart, E.G. Paterson, G.W. Burgreen, P. Hariharan, M. Giarra, V. Reddy, S.W. Day, K.B. Manning, S. Deutsch, M.R. Berman, M.R. Myers, R.A. Malinauskas, Multilaboratory Particle Image Velocimetry Analysis of the FDA Benchmark Nozzle Model to Support Validation of Computational Fluid Dynamics Simulations, *Journal of Biomechanical Engineering* 133 (2011).
- [31] L. Prandtl, O.G. Tietjens, *Applied Hydro- and Aeromechanics*, Dover Publications Inc, New York – New York, Copyright 1934.
- [32] H. Yamaguchi, A. Ito, M. Kuribayashi, X.R. Zhang, H. Nishiyama, Basic flow characteristics in three dimensional branching channel with sudden expansion, *European Journal of Mechanics B/Fluids*, 25 (2006) 909-922.
- [33] S. Hyun, C. Kleinstreuer, J.P. Archie Jr. Hemodynamics analyses of arterial expansions with implications to thrombosis and restenosis, *Medical Engineering & Physics*, 22 (2000) 13-27.

APPENDIX A. AXIAL CENTERLINE VELOCITY

```
%% Plotting Script
clear,clc

%% Variables
% Reynolds
%This is the selection of the differing Reynolds Number
% data sets. Selecting 500, 2000, 3500, 5000, or 6500 will import that
% Reynolds Number data set to the variables data1 and txt1.

% Type %breakdown is as follows:
% 1 - Lam Velocity
% 2 - SST Velocity
% 3 - BSL Velocity
% 4 - k-e Velocity

%% Importing compiled data.
% This section of the program will import the 'xlsx' files appropriate to
% the user selection of the Reynolds number wanted as well as if the user
% wants to plot velocity or sheer. the variable "description" looks for the
% characters stated in the raw data of the appropriate Reynolds number
% selected.
for fig = 1:10;
    switch fig
        case 1
            reynolds = 500;
            type = 1;
        case 2
            reynolds = 2000;
            type = 1;
        case 3
            reynolds = 2000;
            type = 2;
        case 4
            reynolds = 2000;
            type = 3;
        case 5
            reynolds = 3500;
            type = 2;
        case 6
            reynolds = 3500;
            type = 3;
        case 7
            reynolds = 5000;
            type = 2;
        case 8
            reynolds = 5000;
            type = 3;
        case 9
            reynolds = 6500;
            type = 2;
        case 10
            reynolds = 6500;
            type = 3;
```

```

        otherwise
    end
switch reynolds
    case 500
        [data1,txt1] = xlsread('Sudden_Expansion_500_243.xlsx');
        [data2,txt2] = xlsread('Sudden_Expansion_500_297.xlsx');
        [data3,txt3] = xlsread('Sudden_Expansion_500_468.xlsx');
        [data4,txt4] = xlsread('Sudden_Expansion_500_763.xlsx');
        [data5,txt5] = xlsread('Sudden_Expansion_500_999.xlsx');
        switch type
            case 1
                description = char('plot-z-distribution-axial-velocity');
                [sym_data,sym_txt] = xlsread('a_vel_lam_500.xlsx');
                type_lab = '500_lam_v';
            otherwise
                disp({type;'Invalid Sym Number'})
                disp('Please enter a valid sym number')
        end
    case 2000
        [data1,txt1] = xlsread('Sudden_Expansion_2000_243.xlsx');
        [data2,txt2] = xlsread('Sudden_Expansion_2000_297.xlsx');
        [data3,txt3] = xlsread('Sudden_Expansion_2000_468.xlsx');
        [data4,txt4] = xlsread('Sudden_Expansion_2000_763.xlsx');
        [data5,txt5] = xlsread('Sudden_Expansion_2000_999.xlsx');
        switch type
            case 1
                description = char('plot-z-distribution-axial-velocity');
                [sym_data,sym_txt] = xlsread('a_vel_lam_2000.xlsx');
                type_lab = '2000_lam_v';
            case 2
                description = char('plot-z-distribution-axial-velocity');
                [sym_data,sym_txt] = xlsread('a_vel_sst_2000.xlsx');
                type_lab = '2000_sst_v';
            case 3
                description = char('plot-z-distribution-axial-velocity');
                [sym_data,sym_txt] = xlsread('a_vel_bsl_2000.xlsx');
                type_lab = '2000_bsl_v';
            case 4
                description = char('plot-z-distribution-axial-velocity');
                [sym_data,sym_txt] = xlsread('a_vel_k-e_2000.xlsx');
                type_lab = '2000_k-e_v';
            otherwise
                disp({type;'Invalid Sym Number'})
                disp('Please enter a valid sym number')
        end
    case 3500
        [data1,txt1] = xlsread('Sudden_Expansion_3500_243.xlsx');
        [data2,txt2] = xlsread('Sudden_Expansion_3500_297.xlsx');
        [data3,txt3] = xlsread('Sudden_Expansion_3500_468.xlsx');
        [data4,txt4] = xlsread('Sudden_Expansion_3500_763.xlsx');
        [data5,txt5] = xlsread('Sudden_Expansion_3500_999.xlsx');
        switch type
            case 2
                description = char('plot-z-distribution-axial-velocity');
                [sym_data,sym_txt] = xlsread('a_vel_sst_3500.xlsx');
                type_lab = '3500_sst_v';
            case 3

```

```

        description = char('plot-z-distribution-axial-velocity');
        [sym_data,sym_txt] = xlsread('a_vel_bsl_3500.xlsx');
        type_lab = '3500_bsl_v';
    case 4
        description = char('plot-z-distribution-axial-velocity');
        [sym_data,sym_txt] = xlsread('a_vel_k-e_3500.xlsx');
        type_lab = '3500_k-e_v';
    otherwise
        disp({type;'Invalid Sym Number'})
        disp('Please enter a valid sym number')
    end
case 5000
[data1,txt1] = xlsread('Sudden_Expansion_5000_243.xlsx');
[data2,txt2] = xlsread('Sudden_Expansion_5000_297.xlsx');
[data3,txt3] = xlsread('Sudden_Expansion_5000_468.xlsx');
[data4,txt4] = xlsread('Sudden_Expansion_5000_763.xlsx');
[data5,txt5] = xlsread('Sudden_Expansion_5000_999.xlsx');
switch type
    case 2
        description = char('plot-z-distribution-axial-velocity');
        [sym_data,sym_txt] = xlsread('a_vel_sst_5000.xlsx');
        type_lab = '5000_sst_v';
    case 3
        description = char('plot-z-distribution-axial-velocity');
        [sym_data,sym_txt] = xlsread('a_vel_bsl_5000.xlsx');
        type_lab = '5000_bsl_v';
    case 4
        description = char('plot-z-distribution-axial-velocity');
        [sym_data,sym_txt] = xlsread('a_vel_k-e_5000.xlsx');
        type_lab = '5000_k-e_v';
    otherwise
        disp({type;'Invalid Sym Number'})
        disp('Please enter a valid sym number')
    end
case 6500
[data1,txt1] = xlsread('Sudden_Expansion_6500_243.xlsx');
[data2,txt2] = xlsread('Sudden_Expansion_6500_297.xlsx');
[data3,txt3] = xlsread('Sudden_Expansion_6500_468.xlsx');
[data4,txt4] = xlsread('Sudden_Expansion_6500_763.xlsx');
[data5,txt5] = xlsread('Sudden_Expansion_6500_999.xlsx');
switch type
    case 2
        description = char('plot-z-distribution-axial-velocity');
        [sym_data,sym_txt] = xlsread('a_vel_sst_6500.xlsx');
        type_lab = '6500_sst_v';
    case 3
        description = char('plot-z-distribution-axial-velocity');
        [sym_data,sym_txt] = xlsread('a_vel_bsl_6500.xlsx');
        type_lab = '6500_bsl_v';
    case 4
        description = char('plot-z-distribution-axial-velocity');
        [sym_data,sym_txt] = xlsread('a_vel_k-e_6500.xlsx');
        type_lab = '6500_k-e_v';
    otherwise
        disp({type;'Invalid Sym Number'})
        disp('Please enter a valid sym number')
    end
end

```

```

        otherwise
            disp({reynolds;'Invalid Reynolds Number'})
            disp('Please enter a valid reynolds number')
        end

end

%% Program Body
% Selecting a data set from the imported data for searching
for data_set = 1:5
    switch data_set
        case 1
            data = data1;
            txt = txt1;
            mark = ('^b');
        case 2
            data = data2;
            txt = txt2;
            mark = ('.r');
        case 3
            data = data3;
            txt = txt3;
            mark = ('og');
        case 4
            data = data4;
            txt = txt4;
            mark = ('*y');
        case 5
            data = data5;
            txt = txt5;
            mark = ('+m');
        otherwise
            end
    end
    % Searching through each line of the imported data, looking for a
match
    % to the input variables.
    for n = 1:length(data)
        if length(char(txt(n,1))) == length(description)...
&& isnan(data(n,2));
            if length(description) == sum((char(txt(n,1))) ==
(description));
                break
            else
                end
        else
            end
    end
    % Plotting the section of data found based off of the input variables
    plot_data = data((n+2):(n+1+data(n+1)),1:2);
    plot(plot_data(:,1),plot_data(:,2),mark)
    clear data txt mark plot_data
    hold on
end

% Setting the labels and the title for the graph
%grid
xlabel('Axial Distance (m)',...
'FontSize',13);

```

```

ylabel('Velocity (m/s)',...
      'FontSize',13);
x_min = -0.088;
x_max = 0.08;
xlim([x_min,x_max])
clear data1 data2 data3 data4 data5 txt1 txt2 txt3 txt4 txt5
description...
      data_set n x_min x_max section sym_txt type
% Plotting the symulation data on the experimental data imported
plot(sym_data(:,1),sym_data(:,2),'k')
grid
gtext({'\bfAxial Velocity','\bfalong Center Line'],'FontSize',12)
legend('Data Set 1','Data Set 2','Data Set 3','Data Set 4','Data Set
5',...
      'Computation Data','location','NorthWest');
hold off
plot_handle = [num2str(type_lab)]
saveas(gcf,plot_handle,'bmp')
close;
end

```

APPENDIX B. RADIAL VELOCITY & SHEAR SECTIONAL PROFILES

```
%% Plotting Script
% This script will read through xlsx files (quantity 5) and search for the
% input variables of "description" (a text variable) and "section" (a
% numerical variable). In order for the program to function properly all
% xlsx files that the program calls up must be closed when running the
% program.
%
% The program is written to graph the section of interest in each
% data file compounded. In order for the text and data sections of the
% imported data to import properly, the first row of the xlsx file must
% have a matrix cell with some text and a separate matrix cell with some
% numerical value.
%
% The program is also written to function off of NaN operators for the
% simulated imported xlsx data. For this NaN operators must be recognized
% before and after the data set sought after. To add NaN values to the end
% of the xlsx data set place some character at the end of the data set
% followed by some numerical value. E.X. at the end of the data set (last
% value in A23) enter "end" in cell A24 and "1234" in cell A25.
%
% If the program errors at line 124 it means there is an error in the setup
% of the xlsx data being imported. The experimental data being imported
% must have the correct name assignment in front of the correct section.
% The second row from this must contain the length of the data set,
% followed by the data set. 2;1;1 sets have been added to missing data
% sets.
clear,clc

%% Variables
reynolds = 6500; %This is the selection of the differing Reynolds Number
% data sets. Selecting 500, 2000, 3500, 5000, or 6500 will import that
% Reynolds Number data set to the variables data1 and txt1.

type = 7; %This is the type of data that the user wishes to plot. The
% breakdown is as follows:
% 1 - Lam Velocity
% 2 - SST Velocity
% 3 - BSL Velocity
% 4 - k-e Velocity
% 5 - Lam Shear
% 6 - SST Shear
% 7 - BSL Shear
% 8 - k-e Shear

vis = 0.0035;

for plot_fig = 1:12;
    switch plot_fig
        case 1
            section = -0.088;
        case 2
            section = -0.064;
        case 3
```



```

        section = -0.048;
    case 4
        section = -0.02;
    case 5
        section = -0.008;
    case 6
        section = 0.0;
    case 7
        section = 0.008;
    case 8
        section = 0.016;
    case 9
        section = 0.024;
    case 10
        section = 0.032;
    case 11
        section = 0.06;
    case 12
        section = 0.08;
    otherwise
end

%% Importing compiled data.
% This section of the program will import the 'xlsx' files appropriate to
% the user selection of the Reynolds number wanted as well as if the user
% wants to plot velocity or sheer. the variable "description" looks for
the
% characters stated in the raw data of the appropriate Reynolds number
% selected.
switch reynolds
    case 500
        [data1,txt1] = xlsread('Sudden_Expansion_500_243.xlsx');
        [data2,txt2] = xlsread('Sudden_Expansion_500_297.xlsx');
        [data3,txt3] = xlsread('Sudden_Expansion_500_468.xlsx');
        [data4,txt4] = xlsread('Sudden_Expansion_500_763.xlsx');
        [data5,txt5] = xlsread('Sudden_Expansion_500_999.xlsx');
        switch type
            case 1
                description = char('plot-profile-axial-velocity-at-z');
                [sym_data,sym_txt] = xlsread('r_vel_lam_500.xlsx');
                type_lab = '500_lam_v';
            case 5
                description = char('plot-profile-shear-stress-at-z');
                [sym_data,sym_txt] = xlsread('r_shear_lam_500.xlsx');
                sym_data = [sym_data(:,1),vis.*sym_data(:,2)];
                type_lab = '500_lam_s';
            otherwise
                disp({type;'Invalid Sym Number'})
                disp('Please enter a valid sym number')
        end
    case 2000
        [data1,txt1] = xlsread('Sudden_Expansion_2000_243.xlsx');
        [data2,txt2] = xlsread('Sudden_Expansion_2000_297.xlsx');
        [data3,txt3] = xlsread('Sudden_Expansion_2000_468.xlsx');
        [data4,txt4] = xlsread('Sudden_Expansion_2000_763.xlsx');
        [data5,txt5] = xlsread('Sudden_Expansion_2000_999.xlsx');

```

```

switch type
    case 1
        description = char('plot-profile-axial-velocity-at-z');
        [sym_data,sym_txt] = xlsread('r_vel_lam_2000.xlsx');
        type_lab = '2000_lam_v';
    case 2
        description = char('plot-profile-axial-velocity-at-z');
        [sym_data,sym_txt] = xlsread('r_vel_sst_2000.xlsx');
        type_lab = '2000_sst_v';
    case 3
        description = char('plot-profile-axial-velocity-at-z');
        [sym_data,sym_txt] = xlsread('r_vel_bsl_2000.xlsx');
        type_lab = '2000_bsl_v';
    case 4
        description = char('plot-profile-axial-velocity-at-z');
        [sym_data,sym_txt] = xlsread('r_vel_k-e_2000.xlsx');
        type_lab = '2000_k-e_v';
    case 5
        description = char('plot-profile-shear-stress-at-z');
        [sym_data,sym_txt] = xlsread('r_shear_lam_2000.xlsx');
        sym_data = [sym_data(:,1),vis.*sym_data(:,2)];
        type_lab = '2000_lam_s';
    case 6
        description = char('plot-profile-shear-stress-at-z');
        [sym_data,sym_txt] = xlsread('r_shear_sst_2000.xlsx');
        sym_data = [sym_data(:,1),vis.*sym_data(:,2)];
        type_lab = '2000_sst_s';
    case 7
        description = char('plot-profile-shear-stress-at-z');
        [sym_data,sym_txt] = xlsread('r_shear_bsl_2000.xlsx');
        sym_data = [sym_data(:,1),vis.*sym_data(:,2)];
        type_lab = '2000_bsl_s';
    case 8
        description = char('plot-profile-shear-stress-at-z');
        [sym_data,sym_txt] = xlsread('r_shear_k-e_2000.xlsx');
        sym_data = [sym_data(:,1),vis.*sym_data(:,2)];
        type_lab = '2000_k-e_s';
    otherwise
        disp({type;'Invalid Sym Number'})
        disp('Please enter a valid sym number')
end
case 3500
[data1,txt1] = xlsread('Sudden_Expansion_3500_243.xlsx');
[data2,txt2] = xlsread('Sudden_Expansion_3500_297.xlsx');
[data3,txt3] = xlsread('Sudden_Expansion_3500_468.xlsx');
[data4,txt4] = xlsread('Sudden_Expansion_3500_763.xlsx');
[data5,txt5] = xlsread('Sudden_Expansion_3500_999.xlsx');
switch type
    case 2
        description = char('plot-profile-axial-velocity-at-z');
        [sym_data,sym_txt] = xlsread('r_vel_sst_3500.xlsx');
        type_lab = '3500_sst_v';
    case 3
        description = char('plot-profile-axial-velocity-at-z');
        [sym_data,sym_txt] = xlsread('r_vel_bsl_3500.xlsx');
        type_lab = '3500_bsl_v';
    case 4

```

```

        description = char('plot-profile-axial-velocity-at-z');
        [sym_data,sym_txt] = xlsread('r_vel_k-e_3500.xlsx');
        type_lab = '3500_k-e_v';
    case 6
        description = char('plot-profile-shear-stress-at-z');
        [sym_data,sym_txt] = xlsread('r_shear_sst_3500.xlsx');
        sym_data = [sym_data(:,1),vis.*sym_data(:,2)];
        type_lab = '3500_sst_s';
    case 7
        description = char('plot-profile-shear-stress-at-z');
        [sym_data,sym_txt] = xlsread('r_shear_bsl_3500.xlsx');
        sym_data = [sym_data(:,1),vis.*sym_data(:,2)];
        type_lab = '3500_bsl_s';
    case 8
        description = char('plot-profile-shear-stress-at-z');
        [sym_data,sym_txt] = xlsread('r_shear_k-e_3500.xlsx');
        sym_data = [sym_data(:,1),vis.*sym_data(:,2)];
        type_lab = '3500_k-e_s';
    otherwise
        disp({type;'Invalid Sym Number'})
        disp('Please enter a valid sym number')
end
case 5000
[data1,txt1] = xlsread('Sudden_Expansion_5000_243.xlsx');
[data2,txt2] = xlsread('Sudden_Expansion_5000_297.xlsx');
[data3,txt3] = xlsread('Sudden_Expansion_5000_468.xlsx');
[data4,txt4] = xlsread('Sudden_Expansion_5000_763.xlsx');
[data5,txt5] = xlsread('Sudden_Expansion_5000_999.xlsx');
switch type
    case 2
        description = char('plot-profile-axial-velocity-at-z');
        [sym_data,sym_txt] = xlsread('r_vel_sst_5000.xlsx');
        type_lab = '5000_sst_v';
    case 3
        description = char('plot-profile-axial-velocity-at-z');
        [sym_data,sym_txt] = xlsread('r_vel_bsl_5000.xlsx');
        type_lab = '5000_bsl_v';
    case 4
        description = char('plot-profile-axial-velocity-at-z');
        [sym_data,sym_txt] = xlsread('r_vel_k-e_5000.xlsx');
        type_lab = '5000_k-e_v';
    case 6
        description = char('plot-profile-shear-stress-at-z');
        [sym_data,sym_txt] = xlsread('r_shear_sst_5000.xlsx');
        sym_data = [sym_data(:,1),vis.*sym_data(:,2)];
        type_lab = '5000_sst_s';
    case 7
        description = char('plot-profile-shear-stress-at-z');
        [sym_data,sym_txt] = xlsread('r_shear_bsl_5000.xlsx');
        sym_data = [sym_data(:,1),vis.*sym_data(:,2)];
        type_lab = '5000_bsl_s';
    case 8
        description = char('plot-profile-shear-stress-at-z');
        [sym_data,sym_txt] = xlsread('r_shear_k-e_5000.xlsx');
        sym_data = [sym_data(:,1),vis.*sym_data(:,2)];
        type_lab = '5000_k-e_s';
    otherwise

```

```

        disp({type;'Invalid Sym Number'})
        disp('Please enter a valid sym number')
    end
case 6500
    [data1,txt1] = xlsread('Sudden_Expansion_6500_243.xlsx');
    [data2,txt2] = xlsread('Sudden_Expansion_6500_297.xlsx');
    [data3,txt3] = xlsread('Sudden_Expansion_6500_468.xlsx');
    [data4,txt4] = xlsread('Sudden_Expansion_6500_763.xlsx');
    [data5,txt5] = xlsread('Sudden_Expansion_6500_999.xlsx');
    switch type
        case 2
            description = char('plot-profile-axial-velocity-at-z');
            [sym_data,sym_txt] = xlsread('r_vel_sst_6500.xlsx');
            type_lab = '6500_sst_v';
        case 3
            description = char('plot-profile-axial-velocity-at-z');
            [sym_data,sym_txt] = xlsread('r_vel_bsl_6500.xlsx');
            type_lab = '6500_bsl_v';
        case 4
            description = char('plot-profile-axial-velocity-at-z');
            [sym_data,sym_txt] = xlsread('r_vel_k-e_6500.xlsx');
            type_lab = '6500_k-e_v';
        case 6
            description = char('plot-profile-shear-stress-at-z');
            [sym_data,sym_txt] = xlsread('r_shear_sst_6500.xlsx');
            sym_data = [sym_data(:,1),vis.*sym_data(:,2)];
            type_lab = '6500_sst_s';
        case 7
            description = char('plot-profile-shear-stress-at-z');
            [sym_data,sym_txt] = xlsread('r_shear_bsl_6500.xlsx');
            sym_data = [sym_data(:,1),vis.*sym_data(:,2)];
            type_lab = '6500_bsl_s';
        case 8
            description = char('plot-profile-shear-stress-at-z');
            [sym_data,sym_txt] = xlsread('r_shear_k-e_6500.xlsx');
            sym_data = [sym_data(:,1),vis.*sym_data(:,2)];
            type_lab = '6500_k-e_s';
        otherwise
            disp({type;'Invalid Sym Number'})
            disp('Please enter a valid sym number')
    end
otherwise
    disp({reynolds;'Invalid Reynolds Number'})
    disp('Please enter a valid reynolds number')
end

%% Program Body
% Setting the X scale of the plot as well as setting the simulation
section
% based off of the axial variable "section".
switch section
    case -0.088
        section_sym = char('n088 at ln088');
        x_min = 0;
        x_max = 0.006;
    case -0.064

```

```

        section_sym = char('n064 at ln064');
        x_min = 0;
        x_max = 0.006;
    case -0.048
        section_sym = char('n048 at ln048');
        x_min = 0;
        x_max = 0.0034;
    case -0.02
        section_sym = char('n020 at ln020');
        x_min = 0;
        x_max = 0.002;
    case -0.008
        section_sym = char('n008 at ln008');
        x_min = 0;
        x_max = 0.002;
    case 0
        section_sym = char('p000 at lp000');
        x_min = 0;
        x_max = 0.002;
    case 0.008
        section_sym = char('p008 at lp008');
        x_min = 0;
        x_max = 0.006;
    case 0.016
        section_sym = char('p016 at lp016');
        x_min = 0;
        x_max = 0.006;
    case 0.024
        section_sym = char('p024 at lp024');
        x_min = 0;
        x_max = 0.006;
    case 0.032
        section_sym = char('p032 at lp032');
        x_min = 0;
        x_max = 0.006;
    case 0.06
        section_sym = char('p060 at lp060');
        x_min = 0;
        x_max = 0.006;
    case 0.08
        section_sym = char('p080 at lp080');
        x_min = 0;
        x_max = 0.006;
    otherwise
        disp({section;'Invalid Cross Section'})
        disp('Please enter a valid cross section')
end

% Selecting a data set from the imported data for searching
for data_set = 1:5
    switch data_set
        case 1
            data = data1;
            txt = txt1;
            mark = ('^b');
        case 2
            data = data2;

```

```

        txt = txt2;
        mark = ('.r');
    case 3
        data = data3;
        txt = txt3;
        mark = ('og');
    case 4
        data = data4;
        txt = txt4;
        mark = ('*y');
    case 5
        data = data5;
        txt = txt5;
        mark = ('+m');
    otherwise
    end
    % Searching through each line of the imported data, looking for a
match
    % to the input variables.
    for n = 1:length(data)
        if length(char(txt(n,1))) == length(description)...
&& data(n,2) == section
            if length(description) == sum((char(txt(n,1))) ==
(description));
                break
            else
            end
        else
        end
    end
    % Plotting the section of data found based off of the input variables
figure(plot_fig)
plot_data = data((n+2):(n+1+data(n+1)),1:2);
plot(plot_data(:,1),plot_data(:,2),mark)
clear data txt mark plot_data
hold on
end

% Setting the labels and the title for the graph
%grid
xlabel('Radial Distance (m)',...
'FontSize',13)
switch type
    case {1,2,3,4}
        y_txt =char('Velocity (m/s)');
    case {5,6,7,8}
        y_txt = char('Shear Stress (Pa)');
    otherwise
    end
ylabel(y_txt,...
'FontSize',13)
xlim([x_min,x_max])
clear data1 data2 data3 data4 data5 txt1 txt2 txt3 txt4 txt5
description...
    data_set n x_min x_max section

```

```

% Searching the simulation data for the variable "section_sym"
for n = 1:length(sym_data)
    if length(char(sym_txt(n,1))) == length(section_sym)
        if length(section_sym) == sum((char(sym_txt(n,1))) ==
(section_sym));
            n = n+4;
            sym_start = n;
            break
        else
            end
    else
        end
end

% Finding the end of the symulation data set.
while isnan(sym_data(n,1)) == 0;
    n = n+1;
end
sym_end = n-1;
clear section_sym %sym_txt n

% Plotting the symulation data on the experimental data imported
plot_data = sym_data(sym_start:sym_end,1:2);
plot_data = [plot_data(:,1),(plot_data(:,2))];
plot(plot_data(:,1),plot_data(:,2),'k')
grid
switch type
    case {1,2,3,4}
        gtext({'\bfRadial Cross Section','\bfAxial
Velocity'},'FontSize',12)
    case {5,6,7,8}
        gtext({'\bfRadial Cross Section','\bfAxial Shear'},'FontSize',12)
    otherwise
end
hold off
plot_handle = [num2str(type_lab) num2str(plot_fig)]
saveas(gcf,plot_handle,'bmp')
close(plot_fig);
end

```

APPENDIX C. AXIAL WALL SHEAR

```
%% Plotting Script
clear,clc

%% Variables
% Reynolds %This is the selection of the differing Reynolds Number
% data sets. Selecting 500, 2000, 3500, 5000, or 6500 will import that
% Reynolds Number data set to the variables data1 and txt1.

% Type %breakdown is as follows:
% 1 - Lam Velocity
% 2 - SST Velocity
% 3 - BSL Velocity
% 4 - k-e Velocity

%% Importing compiled data.
% This section of the program will import the 'xlsx' files appropriate to
% the user selection of the Reynolds number wanted as well as if the user
% wants to plot velocity or sheer. the variable "description" looks for the
% characters stated in the raw data of the appropriate Reynolds number
% selected.
for fig = 1:10;
    switch fig
        case 1
reynolds = 500;
            type = 1;
        case 2
            reynolds = 2000;
            type = 1;
        case 3
            reynolds = 2000;
            type = 2;
        case 4
            reynolds = 2000;
            type = 3;
        case 5
            reynolds = 3500;
            type = 2;
        case 6
            reynolds = 3500;
            type = 3;
        case 7
            reynolds = 5000;
            type = 2;
        case 8
            reynolds = 5000;
            type = 3;
        case 9
            reynolds = 6500;
            type = 2;
        case 10
            reynolds = 6500;
            type = 3;
    otherwise
```



```

end
switch reynolds
    case 500
        [data1,txt1] = xlsread('Sudden_Expansion_500_243.xlsx');
        [data2,txt2] = xlsread('Sudden_Expansion_500_297.xlsx');
        [data3,txt3] = xlsread('Sudden_Expansion_500_468.xlsx');
        [data4,txt4] = xlsread('Sudden_Expansion_500_763.xlsx');
        [data5,txt5] = xlsread('Sudden_Expansion_500_999.xlsx');
        switch type
            case 1
                description = char('plot-wall-distribution-pressure');
                [sym_data,sym_txt] = xlsread('w_shear_lam_500.xlsx');
                type_lab = '500_lam_v';
            otherwise
                disp({type;'Invalid Sym Number'})
                disp('Please enter a valid sym number')
        end
    case 2000
        [data1,txt1] = xlsread('Sudden_Expansion_2000_243.xlsx');
        [data2,txt2] = xlsread('Sudden_Expansion_2000_297.xlsx');
        [data3,txt3] = xlsread('Sudden_Expansion_2000_468.xlsx');
        [data4,txt4] = xlsread('Sudden_Expansion_2000_763.xlsx');
        [data5,txt5] = xlsread('Sudden_Expansion_2000_999.xlsx');
        switch type
            case 1
                description = char('plot-wall-distribution-pressure');
                [sym_data,sym_txt] = xlsread('w_shear_lam_2000.xlsx');
                type_lab = '2000_lam_v';
            case 2
                description = char('plot-wall-distribution-pressure');
                [sym_data,sym_txt] = xlsread('w_shear_sst_2000.xlsx');
                type_lab = '2000_sst_v';
            case 3
                description = char('plot-wall-distribution-pressure');
                [sym_data,sym_txt] = xlsread('w_shear_bsl_2000.xlsx');
                type_lab = '2000_bsl_v';
            case 4
                description = char('plot-wall-distribution-pressure');
                [sym_data,sym_txt] = xlsread('w_shear_k-e_2000.xlsx');
                type_lab = '2000_k-e_v';
            otherwise
                disp({type;'Invalid Sym Number'})
                disp('Please enter a valid sym number')
        end
    case 3500
        [data1,txt1] = xlsread('Sudden_Expansion_3500_243.xlsx');
        [data2,txt2] = xlsread('Sudden_Expansion_3500_297.xlsx');
        [data3,txt3] = xlsread('Sudden_Expansion_3500_468.xlsx');
        [data4,txt4] = xlsread('Sudden_Expansion_3500_763.xlsx');
        [data5,txt5] = xlsread('Sudden_Expansion_3500_999.xlsx');
        switch type
            case 2
                description = char('plot-wall-distribution-pressure');
                [sym_data,sym_txt] = xlsread('w_shear_sst_3500.xlsx');
                type_lab = '3500_sst_v';
            case 3
                description = char('plot-wall-distribution-pressure');

```

```

        [sym_data,sym_txt] = xlsread('w_shear_bsl_3500.xlsx');
        type_lab = '3500_bsl_v';
    case 4
        description = char('plot-wall-distribution-pressure');
        [sym_data,sym_txt] = xlsread('w_shear_k-e_3500.xlsx');
        type_lab = '3500_k-e_v';
    otherwise
        disp({type;'Invalid Sym Number'})
        disp('Please enter a valid sym number')
    end
case 5000
[data1,txt1] = xlsread('Sudden_Expansion_5000_243.xlsx');
[data2,txt2] = xlsread('Sudden_Expansion_5000_297.xlsx');
[data3,txt3] = xlsread('Sudden_Expansion_5000_468.xlsx');
[data4,txt4] = xlsread('Sudden_Expansion_5000_763.xlsx');
[data5,txt5] = xlsread('Sudden_Expansion_5000_999.xlsx');
switch type
    case 2
        description = char('plot-wall-distribution-pressure');
        [sym_data,sym_txt] = xlsread('w_shear_sst_5000.xlsx');
        type_lab = '5000_sst_v';
    case 3
        description = char('plot-wall-distribution-pressure');
        [sym_data,sym_txt] = xlsread('w_shear_bsl_5000.xlsx');
        type_lab = '5000_bsl_v';
    case 4
        description = char('plot-wall-distribution-pressure');
        [sym_data,sym_txt] = xlsread('w_shear_k-e_5000.xlsx');
        type_lab = '5000_k-e_v';
    otherwise
        disp({type;'Invalid Sym Number'})
        disp('Please enter a valid sym number')
    end
case 6500
[data1,txt1] = xlsread('Sudden_Expansion_6500_243.xlsx');
[data2,txt2] = xlsread('Sudden_Expansion_6500_297.xlsx');
[data3,txt3] = xlsread('Sudden_Expansion_6500_468.xlsx');
[data4,txt4] = xlsread('Sudden_Expansion_6500_763.xlsx');
[data5,txt5] = xlsread('Sudden_Expansion_6500_999.xlsx');
switch type
    case 2
        description = char('plot-wall-distribution-pressure');
        [sym_data,sym_txt] = xlsread('w_shear_sst_6500.xlsx');
        type_lab = '6500_sst_v';
    case 3
        description = char('plot-wall-distribution-pressure');
        [sym_data,sym_txt] = xlsread('w_shear_bsl_6500.xlsx');
        type_lab = '6500_bsl_v';
    case 4
        description = char('plot-wall-distribution-pressure');
        [sym_data,sym_txt] = xlsread('w_shear_k-e_6500.xlsx');
        type_lab = '6500_k-e_v';
    otherwise
        disp({type;'Invalid Sym Number'})
        disp('Please enter a valid sym number')
    end
otherwise

```

```

        disp({reynolds;'Invalid Reynolds Number'})
        disp('Please enter a valid reynolds number')
    end

%% Program Body
% Selecting a data set from the imported data for searching
for data_set = 1:5
    switch data_set
        case 1
            data = data1;
            txt = txt1;
            mark = ('^b');
        case 2
            data = data2;
            txt = txt2;
            mark = ('.r');
        case 3
            data = data3;
            txt = txt3;
            mark = ('og');
        case 4
            data = data4;
            txt = txt4;
            mark = ('*y');
        case 5
            data = data5;
            txt = txt5;
            mark = ('+m');
        otherwise
            end
        % Searching through each line of the imported data, looking for a
match
        % to the input variables.
        for n = 1:length(data)
            if length(char(txt(n,1))) == length(description)...
&& isnan(data(n,2));
                if length(description) == sum((char(txt(n,1))) ==
(description));
                    break
                else
                    end
            else
                end
            end
        end
        % Plotting the section of data found based off of the input variables
        plot_data = data((n+2):(n+1+data(n+1)),1:2);
        plot(plot_data(:,1),plot_data(:,2),mark)
        clear data txt mark plot_data
        hold on
    end

% Setting the labels and the title for the graph
%grid
xlabel('Axial Distance (m)',...
    'FontSize',13);
ylabel('Shear Stress(Pa)',...

```

```

        'FontSize',13);
x_min = -0.088;
x_max = 0.08;
xlim([x_min,x_max])
clear data1 data2 data3 data4 data5 txt1 txt2 txt3 txt4 txt5
description...
    data_set n x_min x_max section sym_txt type
% Plotting the symulation data on the experimental data imported
plot(sym_data(:,1),sym_data(:,2),'k')
grid
gtext({'\bfAxial Shear','\bfalong Wall'},'FontSize',12)
legend('Data Set 1','Data Set 2','Data Set 3','Data Set 4','Data Set
5',...
    'Computation Data','location','NorthEast');
hold off
plot_handle = [num2str(type_lab)]
saveas(gcf,plot_handle,'bmp')
close;
end

```

APPENDIX D. WALL PRESSURE

```
%% Plotting Script
clear,clc

%% Variables
% Reynolds %This is the selection of the differing Reynolds Number
% data sets. Seselecting 500, 2000, 3500, 5000, or 6500 will import that
% Reynolds Number data set to the variables data1 and txt1.

% Type %breakdown is as follows:
% 1 - Lam Velocity
% 2 - SST Velocity
% 3 - BSL Velocity
% 4 - k-e Velocity

%% Importing compiled data.
% This section of the program will import the 'xlsx' files appropriat to
% the user selection of the reynolds number wanted as well as if the user
% wants to plot velocity or sheer. the variable "description" looks for the
% characters stated in the raw data of the appropriate reynolds number
% selected.
for fig = 1:10;
    switch fig
        case 1
            reynolds = 500;
            type = 1;
        case 2
            reynolds = 2000;
            type = 1;
        case 3
            reynolds = 2000;
            type = 2;
        case 4
            reynolds = 2000;
            type = 3;
        case 5
            reynolds = 3500;
            type = 2;
        case 6
            reynolds = 3500;
            type = 3;
        case 7
            reynolds = 5000;
            type = 2;
        case 8
            reynolds = 5000;
            type = 3;
        case 9
            reynolds = 6500;
            type = 2;
        case 10
            reynolds = 6500;
            type = 3;
        otherwise
```

```

end
switch reynolds
    case 500
        [data1,txt1] = xlsread('Sudden_Expansion_500_243.xlsx');
        [data2,txt2] = xlsread('Sudden_Expansion_500_297.xlsx');
        [data3,txt3] = xlsread('Sudden_Expansion_500_468.xlsx');
        [data4,txt4] = xlsread('Sudden_Expansion_500_763.xlsx');
        [data5,txt5] = xlsread('Sudden_Expansion_500_999.xlsx');
        switch type
            case 1
                description = char('plot-wall-distribution-pressure');
                [sym_data,sym_txt] = xlsread('w_pres_lam_500.xlsx');
                type_lab = '500_lam_v';
            otherwise
                disp({type;'Invalid Sym Number'})
                disp('Please enter a valid sym number')
        end
    case 2000
        [data1,txt1] = xlsread('Sudden_Expansion_2000_243.xlsx');
        [data2,txt2] = xlsread('Sudden_Expansion_2000_297.xlsx');
        [data3,txt3] = xlsread('Sudden_Expansion_2000_468.xlsx');
        [data4,txt4] = xlsread('Sudden_Expansion_2000_763.xlsx');
        [data5,txt5] = xlsread('Sudden_Expansion_2000_999.xlsx');
        switch type
            case 1
                description = char('plot-wall-distribution-pressure');
                [sym_data,sym_txt] = xlsread('w_pres_lam_2000.xlsx');
                type_lab = '2000_lam_v';
            case 2
                description = char('plot-wall-distribution-pressure');
                [sym_data,sym_txt] = xlsread('w_pres_sst_2000.xlsx');
                type_lab = '2000_sst_v';
            case 3
                description = char('plot-wall-distribution-pressure');
                [sym_data,sym_txt] = xlsread('w_pres_bsl_2000.xlsx');
                type_lab = '2000_bsl_v';
            case 4
                description = char('plot-wall-distribution-pressure');
                [sym_data,sym_txt] = xlsread('w_pres_k-e_2000.xlsx');
                type_lab = '2000_k-e_v';
            otherwise
                disp({type;'Invalid Sym Number'})
                disp('Please enter a valid sym number')
        end
    case 3500
        [data1,txt1] = xlsread('Sudden_Expansion_3500_243.xlsx');
        [data2,txt2] = xlsread('Sudden_Expansion_3500_297.xlsx');
        [data3,txt3] = xlsread('Sudden_Expansion_3500_468.xlsx');
        [data4,txt4] = xlsread('Sudden_Expansion_3500_763.xlsx');
        [data5,txt5] = xlsread('Sudden_Expansion_3500_999.xlsx');
        switch type
            case 2
                description = char('plot-wall-distribution-pressure');
                [sym_data,sym_txt] = xlsread('w_pres_sst_3500.xlsx');
                type_lab = '3500_sst_v';
            case 3
                description = char('plot-wall-distribution-pressure');

```

```

        [sym_data,sym_txt] = xlsread('w_pres_bsl_3500.xlsx');
        type_lab = '3500_bsl_v';
    case 4
        description = char('plot-wall-distribution-pressure');
        [sym_data,sym_txt] = xlsread('w_pres_k-e_3500.xlsx');
        type_lab = '3500_k-e_v';
    otherwise
        disp({type;'Invalid Sym Number'})
        disp('Please enter a valid sym number')
    end
case 5000
[data1,txt1] = xlsread('Sudden_Expansion_5000_243.xlsx');
[data2,txt2] = xlsread('Sudden_Expansion_5000_297.xlsx');
[data3,txt3] = xlsread('Sudden_Expansion_5000_468.xlsx');
[data4,txt4] = xlsread('Sudden_Expansion_5000_763.xlsx');
[data5,txt5] = xlsread('Sudden_Expansion_5000_999.xlsx');
switch type
    case 2
        description = char('plot-wall-distribution-pressure');
        [sym_data,sym_txt] = xlsread('w_pres_sst_5000.xlsx');
        type_lab = '5000_sst_v';
    case 3
        description = char('plot-wall-distribution-pressure');
        [sym_data,sym_txt] = xlsread('w_pres_bsl_5000.xlsx');
        type_lab = '5000_bsl_v';
    case 4
        description = char('plot-wall-distribution-pressure');
        [sym_data,sym_txt] = xlsread('w_pres_k-e_5000.xlsx');
        type_lab = '5000_k-e_v';
    otherwise
        disp({type;'Invalid Sym Number'})
        disp('Please enter a valid sym number')
    end
case 6500
[data1,txt1] = xlsread('Sudden_Expansion_6500_243.xlsx');
[data2,txt2] = xlsread('Sudden_Expansion_6500_297.xlsx');
[data3,txt3] = xlsread('Sudden_Expansion_6500_468.xlsx');
[data4,txt4] = xlsread('Sudden_Expansion_6500_763.xlsx');
[data5,txt5] = xlsread('Sudden_Expansion_6500_999.xlsx');
switch type
    case 2
        description = char('plot-wall-distribution-pressure');
        [sym_data,sym_txt] = xlsread('w_pres_sst_6500.xlsx');
        type_lab = '6500_sst_v';
    case 3
        description = char('plot-wall-distribution-pressure');
        [sym_data,sym_txt] = xlsread('w_pres_bsl_6500.xlsx');
        type_lab = '6500_bsl_v';
    case 4
        description = char('plot-wall-distribution-pressure');
        [sym_data,sym_txt] = xlsread('w_pres_k-e_6500.xlsx');
        type_lab = '6500_k-e_v';
    otherwise
        disp({type;'Invalid Sym Number'})
        disp('Please enter a valid sym number')
    end
otherwise

```

```

        disp({reynolds;'Invalid Reynolds Number'})
        disp('Please enter a valid reynolds number')
    end

%% Program Body
% Selecting a data set from the imported data for searching
for data_set = 1:5
    switch data_set
        case 1
            data = data1;
            txt = txt1;
            mark = ('^b');
        case 2
            data = data2;
            txt = txt2;
            mark = ('.r');
        case 3
            data = data3;
            txt = txt3;
            mark = ('og');
        case 4
            data = data4;
            txt = txt4;
            mark = ('*y');
        case 5
            data = data5;
            txt = txt5;
            mark = ('+m');
        otherwise
            end
        % Searching through each line of the imported data, looking for a
match
        % to the input variables.
        for n = 1:length(data)
            if length(char(txt(n,1))) == length(description)...
&& isnan(data(n,2));
                if length(description) == sum((char(txt(n,1))) ==
(description));
                    break
                else
                    end
            else
                end
        end
        % Plotting the section of data found based off of the input variables
        plot_data = data((n+2):(n+1+data(n+1)),1:2);
        plot(plot_data(:,1),plot_data(:,2),mark)
        clear data txt mark plot_data
        hold on
    end

% Setting the labels and the title for the graph
%grid
xlabel('Axial Distance (m)',...
    'FontSize',13);
ylabel('Pressure (Pa)',...

```



```

        'FontSize',13);
    x_min = -0.088;
    x_max = 0.08;
    xlim([x_min,x_max])
    clear data1 data2 data3 data4 data5 txt1 txt2 txt3 txt4 txt5
description...
    data_set n x_min x_max section sym_txt type
    % Plotting the symulation data on the experimental data imported
    plot(sym_data(:,1),sym_data(:,2),'k')
    grid
    gtext({'\bfPressure','\bfalong Wall'},'FontSize',12)
    legend('Data Set 1','Data Set 2','Data Set 3','Data Set 4','Data Set
5',...
        'Computation Data','location','NorthEast');
    hold off
    plot_handle = [num2str(type_lab)]
    saveas(gcf,plot_handle,'bmp')
    close;
end

```

APPENDIX E. HI SECTIONAL % & TOTAL PERCENTAGE

```
%% HI Estimation Calculator.
% This program is written to automatically load the radial velocity and shear
% data from a simulation and compute the hemolysis index (HI) from the
% data. The program looks at the radial velocity data and first and fits a
% curve to the data for each radial position that data is taken for. From
% this it subdivides the fitted curve into a set number of section
% (radially). The second part is the same operation as the first but for the
% shear stress instead of the velocity. Data for the geometry sections
% (length data) is then loaded into the program so a time value for each
% axial section can be calculated. Each section and each subdivided
% "stream" is then placed into the approximation for hemolysis.
clear,clc;

vis = 0.0035;

%% Importing the simulation data

% Type selection key:
% 1 = Lam 500 Reynolds case
% 2 = Lam 2000 Reynolds case
% 3 = BSL 2000 Reynolds case
% 4 = BSL 3500 Reynolds case
% 5 = BSL 5000 Reynolds case
% 6 = BSL 6500 Reynolds case
% 7 = SST 2000 Reynolds case
% 8 = SST 3500 Reynolds case
% 9 = SST 5000 Reynolds case
% 10 = SST 6500 Reynolds case
type = 10;

switch type
case 1
    [sym_data_v,sym_txt_v] = xlsread('r_vel_lam_500.xlsx');
    [sym_data_s,sym_txt_s] = xlsread('r_shear_lam_500.xlsx');
case 2
    [sym_data_v,sym_txt_v] = xlsread('r_vel_lam_2000.xlsx');
    [sym_data_s,sym_txt_s] = xlsread('r_shear_lam_2000.xlsx');
case 3
    [sym_data_v,sym_txt_v] = xlsread('r_vel_bsl_2000.xlsx');
    [sym_data_s,sym_txt_s] = xlsread('r_shear_bsl_2000.xlsx');
case 4
    [sym_data_v,sym_txt_v] = xlsread('r_vel_bsl_3500.xlsx');
    [sym_data_s,sym_txt_s] = xlsread('r_shear_bsl_3500.xlsx');
case 5
    [sym_data_v,sym_txt_v] = xlsread('r_vel_bsl_5000.xlsx');
    [sym_data_s,sym_txt_s] = xlsread('r_shear_bsl_5000.xlsx');
case 6
    [sym_data_v,sym_txt_v] = xlsread('r_vel_bsl_6500.xlsx');
    [sym_data_s,sym_txt_s] = xlsread('r_shear_bsl_6500.xlsx');
case 7
    [sym_data_v,sym_txt_v] = xlsread('r_vel_sst_2000.xlsx');
    [sym_data_s,sym_txt_s] = xlsread('r_shear_sst_2000.xlsx');
```

```

case 8
    [sym_data_v,sym_txt_v] = xlsread('r_vel_sst_3500.xlsx');
    [sym_data_s,sym_txt_s] = xlsread('r_shear_sst_3500.xlsx');
case 9
    [sym_data_v,sym_txt_v] = xlsread('r_vel_sst_5000.xlsx');
    [sym_data_s,sym_txt_s] = xlsread('r_shear_sst_5000.xlsx');
case 10
    [sym_data_v,sym_txt_v] = xlsread('r_vel_sst_6500.xlsx');
    [sym_data_s,sym_txt_s] = xlsread('r_shear_sst_6500.xlsx');
otherwise
    disp('!!!INPUT ERROR!!! Wrong type input.');
```

break
end

```
%% Radial section location & Data interpolation
```

```
% Selecting a section to compute
```

```
for section = 1:12;
```

```
switch section
```

```
case 1
```

```
    section_sym = char('n088 at ln088');
    x_min = 0;
    x_max = 0.006;
```

```
case 2
```

```
    section_sym = char('n064 at ln064');
    x_min = 0;
    x_max = 0.006;
```

```
case 3
```

```
    section_sym = char('n048 at ln048');
    x_min = 0;
    x_max = 0.0034;
```

```
case 4
```

```
    section_sym = char('n020 at ln020');
    x_min = 0;
    x_max = 0.002;
```

```
case 5
```

```
    section_sym = char('n008 at ln008');
    x_min = 0;
    x_max = 0.002;
```

```
case 6
```

```
    section_sym = char('p000 at lp000');
    x_min = 0;
    x_max = 0.002;
```

```
case 7
```

```
    section_sym = char('p008 at lp008');
    x_min = 0;
    x_max = 0.006;
```

```
case 8
```

```
    section_sym = char('p016 at lp016');
    x_min = 0;
    x_max = 0.006;
```

```
case 9
```

```
    section_sym = char('p024 at lp024');
    x_min = 0;
```

```

        x_max = 0.006;
case 10
    section_sym = char('p032 at lp032');
    x_min = 0;
    x_max = 0.006;
case 11
    section_sym = char('p060 at lp060');
    x_min = 0;
    x_max = 0.006;
case 12
    section_sym = char('p080 at lp080');
    x_min = 0;
    x_max = 0.006;
otherwise
    disp('!!!!INPUT ERROR!!! Wrong axial section input.');
```

```

break
end

% Finding the data related to the section selected (Shear)
for n = 1:length(sym_data_s)
if length(char(sym_txt_s(n,1))) == length(section_sym)
if length(section_sym) == sum((char(sym_txt_s(n,1))) == (section_sym));
    n = n+4;
    sym_start_s = n;
break
else
end
else
end
end

% Finding the end of the simulation data set.
while isnan(sym_data_s(n,1)) == 0;
    n = n+1;
end
    sym_end_s = n-1;

% Finding the data related to the section selected (Velocity)
for n = 1:length(sym_data_v)
if length(char(sym_txt_v(n,1))) == length(section_sym)
if length(section_sym) == sum((char(sym_txt_v(n,1))) == (section_sym));
    n = n+4;
    sym_start_v = n;
break
else
end
else
end
end

% Finding the end of the simulation data set.
while isnan(sym_data_v(n,1)) == 0;
    n = n+1;
end
    sym_end_v = n-1;

```

```

% Dividing the radial sections into 30 equally spaced sections
data_section_s = sym_data_s(sym_start_s:sym_end_s,:);
data_section_v = sym_data_v(sym_start_v:sym_end_v,:);

x = linspace(x_min,x_max,30);
for m = 1:length(x);
    p = 1;
while x(m) > data_section_s(p)
    p = p+1;
end
    p = p-1;
if p == 0
    p = 1;
else
end
    shear_p(m) = data_section_s(p,2);
    p = 1;
while x(m) > data_section_v(p)
    p = p+1;
end
    p = p-1;
if p == 0
    p = 1;
else
end
    velocity_p(m) =data_section_v(p,2);
end
    x = x';
    shear_p = shear_p';
    velocity_p = velocity_p';
    fin_x = x;
    fin_s(:,section) = abs(shear_p).*vis;
    fin_v(:,section) = abs(velocity_p);
    clear xmpshear_pvelocity_pdata_section_sdata_section_v
end
clear nsectionsym_data_ssym_data_vsym_end_ssym_end_vsym_start_s...
sym_start_vsym_txt_ssym_txt_vtypex_maxx_minsection_symvis

%% Radial measurement to sectional averages
% This section converts the radial measurements to sectional averages for
% each of the 11 sections the 12 radial measurements break up.
section = size(fin_s);
for n = 1:(section(:,2)-1);
    sec_shear(:,n) = (fin_s(:,n)+fin_s(:,n+1))./2;
    sec_vel(:,n) = (fin_v(:,n)+fin_v(:,n+1))./2;
end
clear fin_sfin_vnsection

%% Section velocity to section time
% This section converts the sectional velocity into a sectional time using
% the spacing of each section
sec_pos = [-0.088, -0.064, -0.048, -0.020, -0.008, 0.0, 0.008, 0.016,...
    0.024, 0.032, 0.060, 0.080];

for n = 1:(length(sec_pos)-1);
    sec_length(n) = sec_pos(n+1)-sec_pos(n);

```

```

end
for n = 1:(length(sec_pos)-1);
    sec_time(:,n) = sec_length(n)./sec_vel(:,n);
end
clear sec_velsec_lengthn

%% Hemolysis Index (HI) of each section
% This section calculates the HI index for each subdivision and each
% section.
rc = size(sec_shear);
for n = 1:rc(2);
    for m = 1:rc(1);
        HI(m,n) = 3.62e-5*(sec_time(m,n)^0.785)*(sec_shear(m,n)^2.416);
    end
end
clear nmsec_timercsec_shear

%% Fraction value
% This section calculates the area of each divisional section and creates a
% fractional scaling factor for each section.

area = pi*(0.006^2);
fin_x = linspace(0,0.006,31);
for n = 1:(length(fin_x)-1);
    sec_frac(n) = (pi*((fin_x(n+1)^2)-(fin_x(n)^2)))/area;
end
clear nfin_xarea

%% Fractionalizing HI
% This section applies the fraction section to the HI the application of the
% fractionalization is applied in two different ways. The first is a column
% representation for histogram plots of each section. The section is for a
% total HI index.
rc = size(HI);
for n = 1:rc(2);
    for m = 1:rc(1);
        HI_histo(m,n) = HI(m,n)*sec_frac(m);
    end
end
HI_histo = sum(HI_histo);
clear nm

HI_tot = (sum(HI_histo));
clear HIincsec_frac

%% Plotting.
% Plotting the histogram as well as the total HI for the computation.
HI_pos = (diff(sec_pos)/2)+sec_pos(1,1:(length(sec_pos)-1));
sp_dot = 1e-3;
for n = 1:length(HI_pos);
    HI_pos_l(n,1) = HI_pos(n)-(2*sp_dot);
    HI_pos_l(n,2) = HI_pos(n)-(1*sp_dot);
    HI_pos_l(n,3) = HI_pos(n);
    HI_pos_l(n,4) = HI_pos(n)+(1*sp_dot);
    HI_pos_l(n,5) = HI_pos(n)+(2*sp_dot);
end

```

```

end
for n = 1:length(HI_pos);

semilogy(HI_pos_1(n,1),HI_histo(n),'b.',HI_pos_1(n,2),HI_histo(n),'b.',...
          HI_pos_1(n,3),HI_histo(n),'b.',HI_pos_1(n,4),HI_histo(n),'b.',...
          HI_pos_1(n,5),HI_histo(n),'b.')
    hold on
end
grid
xlabel('Section Along Axis (m)',...
       'FontSize',13)
ylabel('HI %',...
       'FontSize',13)
gtext({'\bfHI of Axial Sections','\bf  ','\bfHI %
Total',num2str(HI_tot)},'FontSize',13)

```